NASA
UARL H910461-38

THIRD ANNUAL PROGRESS REPORT

ANALYTICAL STUDY OF CATALYTIC REACTORS FOR HYDRAZINE DECOMPOSITION

by
Arthur S. Kesten

prepared for
NATIONAL AERONAUTICS AND SPACE ADMINISTRATION

May, 1969

CONTRACT NAS 7-458

United Aircraft Research Laboratories
UNITED AIRCRAFT CORPORATION
EAST HARTFORD, CONNECTICUT

Copy #3

NASA
UARL H910461-38

THIRD ANNUAL PROGRESS REPORT

ANALYTICAL STUDY OF CATALYTIC REACTORS FOR HYDRAZINE DECOMPOSITION

by
Arthur S. Kesten

prepared for
NATIONAL AERONAUTICS AND SPACE ADMINISTRATION

May, 1969

CONTRACT NAS 7-458

United Aircraft Research Laboratories
UNITED AIRCRAFT CORPORATION
EAST HARTFORD, CONNECTICUT

Report H910461-38

Analytical Study of Catalytic Reactors for Hydrazine Decomposition

Third Annual Progress Report

April 15, 1968 - April 14, 1969

Contract NAS 7-458

TABLE OF CONTENTS

ABSTRACT

Analytical studies of catalyzed hydrazine decomposition reaction chambers were performed in order to establish procedures capable of predicting the effects of pulse operation of the reactor for an arbitrary duty cycle on the transient behavior of the system. These studies included an extension of a computer program previously developed to calculate temperature and reactant concentrations as functions of time and axial position in typical reaction chamber configurations. The extended program includes consideration of the effects of heat conduction and diffusion when flow is stopped. In addition, reaction chamber fluid dynamics are taken into account by allowing for feed pressure and mass flow rate changes with time. The effects of these changes on thermal and catalytic decomposition of reactants, along with heat and mass transfer between the free-gas phase and the gas within the pores of the catalyst pellets, are considered.

A series of caluclations was made using the computer program to evaluate the effects of duty cycle, nominal chamber pressure, bed loading, and catalyst bed configuration on the transient temperature, pressure, and reactant concentration distributions in the reactor system. The results of these calculations are illustrated in the report.

FOREWORD

This work was performed by United Aircraft Research Laboratories for the National Aeronautics and Space Administration under Contract NAS 7-458 initiated April 15, 1966.

Included among those who cooperated in performance of the work under Contract NAS 7-458 were Dr. A. S. Kesten, Program Manager, Dr. W. G. Burwell, Chief, Kinetics and Thermal Sciences Section, Mr. D. B. Smith, and Mrs. E. Smith of UARL.

This work was conducted under program management of the NASA Chief, Liquid Propulsion Experimental Engineering Systems, NASA Headquarters, Washington, D. C., and the Technical Manager was Mr. T. W. Price, Jet Propulsion Laboratory, Pasadena, California.

Report H910461-38

Analytical Study of Catalytic Reactors for Hydrazine Decomposition

Third Annual Progress Report

April 15, 1968 - April 14, 1969

Contract No. NAS 7-458

SUMMARY

The Research Laboratories of United Aircraft Corporation under Contract NAS 7-458 with the National Aeronautics and Space Administration have been performing an analytical study of catalytic reactors for hydrazine decomposition. This third annual technical report summarizes work performed under this contract from April 15, 1968 to April 14, 1969. Work during this period has included the development of a computer program representing a transient model of a distributed-feed catalyzed hydrazine decomposition reaction chamber. The model describes the behavior of reactors operated under conditions of continuous flow as well as pulsed flow for an arbitrary duty cycle. Both thermal and catalytic decomposition of reactants are considered along with simultaneous heat and mass transfer between the free-gas phase and the gas within the pores of the catalyst pellets. The effects of heat conduction and diffusion when flow is stopped are included in the model. In addition, reaction chamber fluid dynamics are taken into account in order to allow consideration of chamber pressure and mass flow rate changes with time. Calculations have been made of temperature and species concentration distributions as functions of time and axial position in typical hydrazine reaction chambers for a number of pulse duty cycles, mass flow rate distributions, and catalyst bed configurations.

Calculated transient temperature profiles in a continuous flow reactor have been compared with temperatures measured as a function of time in a small scale engine run at Jet Propulsion Laboratory. Generally good agreement between theoretical and experimental results was found.

The computer programs representing both the steady-state and transient models of a catalyzed hydrazine reactor have been described in detail in two computer manuals. These manuals contain operating instructions for these programs as well as descriptions of input and output formats.

INTRODUCTION

Under Contract NAS 7-458, the Research Laboratories of United Aircraft Corporation are performing analytical studies of the behavior of distributed-feed catalytic reactors for hydrazine decomposition. The specific objectives of this program are (a) to develop computer programs for predicting the temperature and concentration distributions in monopropellant hydrazine catalytic reactors in which hydrazine can be injected at arbitrary locations in the reaction chamber and (b) to perform calculations using these computer programs to demonstrate the effects of various system parameters on the performance of the reactor.

Progress previously reported in the first annual report (Ref. 1) included the development of computer programs which describe the steady-state and transient behavior of a hydrazine reactor operated under conditions of constant, continuous flow, in which complete radial mixing in the free-gas (or liquid) phase was assumed. Progress previously reported in the second annual report (Ref. 2) included an extension of the steady-state program to include radial as well as axial variations in temperature and concentrations in order to permit an analysis of various injection schemes and catalyst bed configurations which exhibit radial nonuniformities. These programs had been used to calculate temperature and reactant concentration distributions as functions of initial bed temperature, feed temperature, chamber pressure, mass flow rate distribution, catalyst size distribution, and axial injector locations.

During the third year of contract effort attention has been focused on extending the transient model of the reactor system to take the effects of reaction chamber fluid dynamics on transient response into account, and to permit consideration of pulse operation of the reactor for an arbitrary duty cycle. In addition, computer manuals have been prepared describing to potential users the operation of both the steady-state and transient computer programs (Refs. 3 and 4). Included in suceeding sections of this report are detailed descriptions of (a) the development of the equations representing the transient model of the reactor system, (b) the use of the computer program representing the transient model to compute transient temperature profiles in a typical continuous flow reactor in order to test the validity of the model by comparing the calculated results with measured temperature profiles, and (c) the use of the transient computer program to calculate the effects on transient temperature and reactant concentration distributions of initial bed temperature, chamber pressure, mass flow rate distribution, catalyst size distribution, and pulse duty cycle.

DESCRIPTION OF THE TRANSIENT MODEL

The analysis of a hydrazine engine reaction system pertains to a reaction chamber packed with catalyst particles into which liquid hydrazine is injected at arbitrarily selected axial locations. Catalyst particles are represented as "equivalent" spheres with a diameter taken as a function of the particle size and shape. Both thermal and catalytic vapor phase decomposition of hydrazine and ammonia are considered in developing equations describing the concentration distributions of these reactants. Diffusion of reactants from the free-gas phase to the outside surface of the catalyst pellets is taken into account. Since the catalyst material is impregnated on the interior and exterior surfaces of porous particles, the diffusion of reactants into the porous structure must also be considered. In addition, the conduction of heat within the porous particles must be taken into account since the decomposition reactions are accompanied by the evolution or absorption of heat.

In generalizing the transient model described in Ref. 1 to consider reactor shutdown as well as start-up, the temperature and the concentration of reactants in the interstitial (free-gas) phase are still assumed to vary only with time and axial distance along the bed. In this system film coefficients are used to describe heat and mass transfer between the interstitial phase and the outside surface of the catalyst pellets. The reactant concentrations, c_p, and the temperature, T_p, are taken as uniform within the interior of the porous particles. Heat and mass diffusion within the particles are taken into account by multiplying the reaction rates computed on the basis of uniform c_p and T_p by a utilization factor determined by analogy with the steady-state system (see Ref. 1). In addition, it is assumed that during reactor operation liquid velocities are sufficiently low relative to other rate processes so that, for all practical purposes, steady-state in the liquid and liquid-vapor regions is achieved as soon as the liquid reaches a given axial location in the reactor. No consideration is given to regression of the liquid-vapor interface as the chamber pressure builds up since the overall length of the liquid region in typical reactors is very small compared to the length of the vapor region (Ref. 1). When flow into the reactor is stopped it is easily shown that the residual liquid hydrazine in the reactor vaporizes in just a few milliseconds due to the very rapid decomposition of hydrazine in the liquid region. Therefore, even during reactor shutdown, the liquid regions plays a very small role in determing the transient behavior of the reactor system.

The transient model is concerned then with the vapor region only. The general equations describing the rates of change of enthalpy and reactant concentrations with time and axial distance in the interstitial phase are

$$\delta \frac{\partial}{\partial t}\left[\rho_i h_i\right] = -\frac{\partial}{\partial z}\left[G h_i\right] - H^{N_2H_4} r_{hom}\delta + F h_F - h_c A_P (T_i - T_P) - \frac{4h_w}{d_c}(T_i - T_w) - h_i \sum_J A_P k_c^J (c_i^J - c_P^J) \quad (1)$$

$$\delta \frac{\partial c_i^{N_2H_4}}{\partial t} = -G\frac{\partial w_i^{N_2H_4}}{\partial z} - w_i^{N_2H_4}\frac{\partial G}{\partial z} + F - r_{hom}\delta - A_P k_c^{N_2H_4}(c_i^{N_2H_4} - c_P^{N_2H_4}) \quad (2)$$

$$\delta \frac{\partial c_i^{NH_3}}{\partial t} = -G\frac{\partial w_i^{NH_3}}{\partial z} - w_i^{NH_3}\frac{\partial G}{\partial z} + r_{hom}\delta \frac{M^{NH_3}}{M^{N_2H_4}} - A_P k_c^{NH_3}(c_i^{NH_3} - c_P^{NH_3}) \quad (3)$$

$$\delta \frac{\partial c_i^{N_2}}{\partial t} = -G\frac{\partial w_i^{N_2}}{\partial z} - w_i^{N_2}\frac{\partial G}{\partial z} + r_{hom}\delta \frac{M^{N_2}}{2M^{N_2H_4}} - A_P k_c^{N_2}(c_i^{N_2} - c_P^{N_2}) \quad (4)$$

$$\delta \frac{\partial c_i^{H_2}}{\partial t} = -G\frac{\partial w_i^{H_2}}{\partial z} - w_i^{H_2}\frac{\partial G}{\partial z} + r_{hom}\delta \frac{M^{H_2}}{2M^{N_2H_4}} - A_P k_c^{H_2}(c_i^{H_2} - c_P^{H_2}) \quad (5)$$

where

$$w_i^J = \frac{c_i^J}{\rho_i} = \frac{c_i^J}{\sum_J c_i^J} \quad (6)$$

Equations (1) through (5) can be reduced to a somewhat simpler form with the aid of an overall equation of continuity which can be written as

$$\delta \frac{\partial \rho_i}{\partial t} = F - \frac{\partial G}{\partial z} - \sum_J A_P k_c^J (c_i^J - c_P^J) \quad (7)$$

Equations (1) through (5) can now be written as

$$\delta\rho_i \frac{\partial h_i}{\partial t} = -G\frac{\partial h_i}{\partial z} - h_c A_P (T_i - T_P) - H^{N_2H_4} r_{hom}\delta - F(h_i - h_F) - 4\frac{h_w}{d_c}(T_i - T_w) \quad (8)$$

$$\delta\rho_i \frac{\partial w_i^{N_2H_4}}{\partial t} + G\frac{\partial w_i^{N_2H_4}}{\partial z} = F - r_{hom}\delta - A_P k_c^{N_2H_4}(c_i^{N_2H_4} - c_P^{N_2H_4}) - w_i^{N_2H_4} F + w_i^{N_2H_4}\sum_J A_P k_c^J (c_i^J - c_P^J) \quad (9)$$

$$\delta\rho_i \frac{\partial w_i^{NH_3}}{\partial t} + G\frac{\partial w_i^{NH_3}}{\partial z} = r_{hom}\delta\frac{M^{NH_3}}{M^{N_2H_4}} - A_P k_c^{NH_3}(c_i^{NH_3} - c_P^{NH_3}) - w_i^{NH_3} F + w_i^{NH_3}\sum_J A_P k_c^J (c_i^J - c_P^J) \quad (10)$$

$$\delta\rho_i \frac{\partial w_i^{N_2}}{\partial t} + G\frac{\partial w_i^{N_2}}{\partial z} = r_{hom}\delta\frac{M^{N_2}}{2M^{N_2H_4}} - A_P k_c^{N_2}(c_i^{N_2} - c_P^{N_2}) - w_i^{N_2} F + w_i^{N_2}\sum_J A_P k_c^J (c_i^J - c_P^J) \quad (11)$$

$$\delta\rho_i \frac{\partial w_i^{H_2}}{\partial t} + G\frac{\partial w_i^{H_2}}{\partial z} = r_{hom}\delta\frac{M^{H_2}}{2M^{N_2H_4}} - A_P k_c^{H_2}(c_i^{H_2} - c_P^{H_2}) - w_i^{H_2} F + w_i^{H_2}\sum_J A_P k_c^J (c_i^J - c_P^J) \quad (12)$$

The last term on the right side of Eq. (8) represents the heat loss from the bulk vapor to the wall of the reactor. Taking the reactor wall temperature as uniform, the rate of change of wall temperature with time is

$$m_w C_w \frac{dT_w}{dt} = \pi d_c \int_0^L h_w (T_i - T_w)\, dz - h_a A_w (T_w - T_a) \quad (13)$$

where the last term on the right side of Eq. (13) represents the heat loss by forced convection from the reactor to the surrounding atmosphere. Heat loss by natural convection or radiation can be represented in Eq. (13) by adding a term of the form $h_a' A_w (T_w - T_a)^{1.25}$ or $h_a'' A_w (T_w^4 - T_a^4)$, respectively.

The mass flow rate, G, may be calculated as a function of time and axial position from the inlet mass flow rate, which is a function of pressure, and from Eq. (7). The inlet mass flow rate at any time may be calculated in terms of the steady-state (SS) inlet mass flow rate using

$$\frac{(G)_{z=0}}{[(G)_{z=0}]_{ss}} = \frac{\sqrt{P_F - P}}{\sqrt{P_F - P_{ss}}} \tag{14}$$

For choked nozzle and for a rate of change of vapor density with time which is approximately uniform throughout the reactor, Eq. (7) reduces to

$$\frac{\partial G}{\partial z} = F - \sum_J A_p k_c^J (c_i^J - c_p^J) - \frac{A_c \delta}{V_c} \left\{ G - \left(P\sqrt{\bar{M}/T_i} \right) \left(\frac{G}{P\sqrt{\bar{M}/T_i}} \right)_{ss} \right\}_{z=L} \tag{15}$$

Taking the chamber pressure to be uniform throughout the reactor, the corresponding rate of change of chamber pressure with time can be approximated by

$$\frac{dP}{dt} \sim R \left(\frac{T_i}{\bar{M}} \right)_{z=L} \frac{A_c}{V_c} \left\{ G - \left(P\sqrt{\bar{M}/T_i} \right) \left(\frac{G}{P\sqrt{\bar{M}/T_i}} \right)_{ss} \right\}_{z=L} \tag{16}$$

At a given axial location the rates of change of temperature and reactant concentrations in the catalyst particles with time are given by

$$\frac{dT_p}{dt} = -\frac{1}{\rho_s C_s} \left[(H r_{het})^{N_2H_4} + (H r_{het})^{NH_3} \right] + \frac{3 h_c}{a \rho_s C_s} (T_i - T_p) \tag{17}$$

$$\frac{dc_p^{N_2H_4}}{dt} = -\frac{1}{\alpha_p} r_{het}^{N_2H_4} + \frac{3 k_c^{N_2H_4}}{\alpha_p a} \left(c_i^{N_2H_4} - c_p^{N_2H_4} \right) \tag{18}$$

$$\frac{dc_p^{NH_3}}{dt} = \frac{1}{\alpha_p} \left[r_{het}^{N_2H_4} \frac{M^{NH_3}}{M^{N_2H_4}} - r_{het}^{NH_3} \right] + \frac{3 k_c^{NH_3}}{\alpha_p a} \left(c_i^{NH_3} - c_p^{NH_3} \right) \tag{19}$$

$$\frac{dc_p^{N_2}}{dt} = \frac{1}{a_p}\left[r_{het}^{N_2H_4}\frac{M^{N_2}}{2M^{N_2H_4}} + r_{het}^{NH_3}\frac{M^{N_2}}{2M^{NH_3}}\right] + \frac{3k_c^{N_2}}{a_p a}\left(c_i^{N_2} - c_p^{N_2}\right) \tag{20}$$

$$\frac{dc_p^{H_2}}{dt} = \frac{1}{a_p}\left[r_{het}^{N_2H_4}\frac{M^{H_2}}{2M^{N_2H_4}} + r_{het}^{NH_3}\frac{3M^{H_2}}{2M^{NH_3}}\right] + \frac{3k_c^{H_2}}{a_p a}\left(c_i^{H_2} - c_p^{H_2}\right) \tag{21}$$

where the film coefficients, h_c, h_w, and k_c, may be estimated from (Ref. 5)

$$h_w = h_c = 0.74\left(\frac{G}{A_p\mu}\right)^{-0.41}(\bar{C}_F G) + \frac{K_i}{a} \tag{22}$$

and

$$k_c^J = \left(\frac{0.61\,G}{\rho_i}\right)\left(\frac{\mu}{\rho_i D_i^J}\right)^{-0.667}\left(\frac{G}{A_p\mu}\right)^{-0.41} + \frac{D_i^J}{a} \tag{23}$$

It should be noted that the thermal conduction term in Eq. (22) and the simple diffusion term in Eq. (23) become significant only when the mass flow rate is quite small, as it is during reactor shutdown.

Recalling that the reaction of hydrazine on the catalyst surfaces is extremely fast, so that the reaction rate is controlled by the rate of transport of hydrazine to the catalyst surfaces, Eq. (18) can be used to define $r_{het}^{N_2H_4}$ by noting that $(dc_p^{N_2H_4}/dt)$ and $c_p^{N_2H_4}$ are both approximately equal to zero. The reaction rate is then given by

$$r_{het}^{N_2H_4} = \frac{3k_c^{N_2H_4}}{a}\,c_i^{N_2H_4} \tag{24}$$

The reaction rate of ammonia on the catalyst surfaces, $r_{het}^{NH_3}$, can be computed by multiplying the rate of reaction calculated on the basis of uniform T_p and c_p by the utilization factor determined by analogy with the steady-state system (see Refs. 1, 6 and 7).

This general system of equations is applicable to both normal reactor operation and reactor shutdown. Partial differential equations may be simplified considerably by noting first that, during the "on" portion of a pulse duty cycle (or during continuous reactor operation), gas velocities are so great that the time lag from the entrance to the vapor region to any axial position for the fluid is negligible compared with other transient effects. Here Eqs. (8) through (12) may be approximated by

$$\frac{\partial h_i}{\partial z} = -\frac{H^{N_2H_4}}{G} r_{hom}\,\delta - \frac{A_P}{G}\left[h_c(T_i - T_P)\right] - \frac{F}{G}(h_i - h_F) - \frac{4h_w}{Gd_c}(T_i - T_w) \qquad (25)$$

$$G\frac{\partial w_i^{N_2H_4}}{\partial z} = F - r_{hom}\delta - A_P k_c^{N_2H_4}\left(c_i^{N_2H_4} - c_P^{N_2H_4}\right) - w_i^{N_2H_4} F + w_i^{N_2H_4}\sum_J A_P k_c^J (c_i^J - c_P^J) \qquad (26)$$

$$G\frac{\partial w_i^{NH_3}}{\partial z} = r_{hom}\,\delta\,\frac{M^{NH_3}}{M^{N_2H_4}} - A_P k_c^{NH_3}(c_i^{NH_3} - c_P^{NH_3}) - w_i^{NH_3} F + w_i^{NH_3}\sum_J A_P k_c^J (c_i^J - c_P^J) \qquad (27)$$

$$G\frac{\partial w_i^{N_2}}{\partial z} = r_{hom}\,\delta\,\frac{M^{N_2}}{2M^{N_2H_4}} - A_P k_c^{N_2}(c_i^{N_2} - c_P^{N_2}) - w_i^{N_2} F + w_i^{N_2}\sum_J A_P k_c^J (c_i^J - c_P^J) \qquad (28)$$

$$G\frac{\partial w_i^{H_2}}{\partial z} = r_{hom}\,\delta\,\frac{M^{H_2}}{2M^{N_2H_4}} - A_P k_c^{H_2}(c_i^{H_2} - c_P^{H_2}) - w_i^{H_2} F + w_i^{H_2}\sum_J A_P k_c^J (c_i^J - c_P^J) \qquad (29)$$

Some simplification of the partial differential equations may be achieved in describing reactor operation during the "off" portion of a duty cycle by noting that, here, gas velocities are sufficiently low so that the terms in Eqs. (8) through (12) involving $G\frac{\partial}{\partial z}$ may be approximated when integrating these equations over small time intervals without introducing any significant error into the calculations.

Finite difference methods have been used to program for digital computation the differential equations describing the changes in temperature and concentrations in the reactor system. These methods are similar to those discussed in Ref. 1, where each of the differential equations is treated as an ordinary differential equation (by integrating with respect to time at a fixed position or vice versa). Each equation is rearranged in the form

$$\frac{dg}{ds} = \alpha - \beta g \tag{30}$$

where the quantities α and β are taken as constant while integrating the equations from s_{k-1} to s_k (corresponding to Δt or Δz). Equation (30) can be integrated to obtain

$$g_k = g_{k-1} e^{-\beta(s_k - s_{k-1})} + \frac{\alpha}{\beta}\left[1 - e^{-\beta(s_k - s_{k-1})}\right] \tag{31}$$

where g_k is the value of g at s_k, and g_{k-1} is the value of g at s_{k-1}. An alternative form of Eq. (31) is

$$g_k = g_{k-1} + \left(\frac{dg}{ds}\right)_{k-1}\left[\frac{1 - e^{-\beta(s_k - s_{k-1})}}{\beta}\right] \tag{32}$$

It is convenient to use equations of the form of Eq. (31) to compute particle concentrations and temperatures, and to use equations of the form of Eq. (32) to compute interstitial concentrations and temperatures.

The equations representing the transient model of a hydrazine catalytic reactor have been programmed using FØRTRAN IV source language for the UNIVAC 1108 digital computer. This computer program is discussed in detail in a computer manual (Ref. 4). The manual includes input and output descriptions and a description of possible operational problems associated with the program.

RESULTS OF CALCULATIONS

A series of calculations of the transient behavior of a typical continuous flow reactor for which experimental information is available (Ref. 8) was made in order to examine the effectiveness of the transient model. The calculations pertain to a 50 lb_f nominal thrust hydrazine reactor 2.4 in. in diameter into which liquid hydrazine is injected at the upstream end of the reactor only. The catalyst bed packing was taken to consist of 25-30 mesh catalyst particles for the first 0.25 in. and 1/8 in. x 1/8 in. cylindrical pellets for the remainder of the bed. This configuration is referred to in the figures as "mixed bed #1". The steady-state chamber pressure was taken as 200 psia, the steady-state mass flow rate as 6.5 lb/ft^2-sec, and the initial chamber pressure as 14.7 psia. The results of these calculations are shown in Figs. 1 through 4. Gas temperatures are plotted as function of time at each of four axial positions in Fig. 1* for a case in which the initial bed temperature was taken as 530 deg R. Measured gas temperature profiles (Ref. 8) are also shown in Fig. 1 for purposes of comparison. Generally good agreement between theoretical and experimental results may be noted, particularly during the early stages of the transient. While the differences between measured and calculated rates of response are in part due to the thermocouple response time, the use of steady-state utilization factors to describe heat and mass diffusion within catalyst particles under transient conditions results in calculated response rates which are a little too high. The calculated mole-fraction profiles for hydrazine and ammonia, corresponding to the temperature profiles shown in Fig. 1, are illustrated in Fig. 2, and the corresponding mole-fraction profiles for nitrogen and hydrogen are illustrated in Fig. 3. Here, the mole-fractions are plotted as functions of axial position at various times.

Temperatures are plotted as functions of time at a fixed axial position in Fig. 4 for cases in which the initial bed temperatures were taken as 530, 950, and 1420 deg R respectively. The comparison between calculated and measured temperature profiles is similar for low and elevated initial bed temperature cases.

Additional calculations were made for the reactor configuration noted above in order to examine the effect of pulsed flow on initial transient response. The calculated results illustrated in Figs. 5 through 11 refer to a reactor operated under pulsed flow conditions at a steady-state chamber pressure of 260 psia, a steady-state mass flow rate of 5.8 lb/ft^2-sec, an initial chamber pressure of 14.7 psia, and an initial bed temperature af 530 deg R. Calculations were made for the first two pulses of a duty cycle consisting of alternate on and off times of 50 msec and 100 msec respectively.

*A plot similar to Fig. 1 was included in Ref. 8; the calculated temperature profiles illustrated in that plot were slightly in error.

The temperature in the interstitial phase is plotted in Fig. 5 as a function of time at various axial locations in the reaction chamber. The temperature rises rapidly after reactor startup, particularly in the upstream portion of the chamber. When flow into the reactor is turned off, the gas temperature in the upstream section of the reactor rises extremely rapidly at first because of thermal decomposition of residual hydrazine in this region. In the regions of the reactor downstream of the small catalyst particles, where the gas temperature is too low after 50 msec to permit significant thermal decomposition of hydrazine, the temperature falls due to heat transfer from the gas to the colder catalyst pellets and to the chamber walls. The heat gained by the catalyst pellets in these regions results in a very small temperature change because of the large mass of the particles. This is illustrated in Fig. 6 where catalyst particle temperature is plotted as a function of time at the same axial locations chosen for Fig. 5.

The rapid pressure buildup and decay resulting from pulse operation of the reactor for this case is shown in Fig. 7. The species mole-fraction profiles associated with this pressure variation and the temperature distributions illustrated in Figs. 5 and 6 and shown in Figs. 8 through 11. The variation of mole-fraction of hydrazine with time at various axial locations is plotted in Fig. 8. This plot illustrates the very rapid thermal decomposition of residual hydrazine in the hotter upstream regions of the reaction chamber during reactor shutdown as well as the somewhat slower catalytic decomposition in the cooler downstream regions of the reactor. The variation of mole-fraction of ammonia with time is illustrated at various axial locations in Fig. 9. Following reactor shutdown the residual ammonia near the upstream end of the reactor decomposes catalytically in the hot catalyst particles. In the cooler downstream regions, ammonia is displaced gradually by the nitrogen and hydrogen formed from hydrazine and ammonia decomposition upstream. These decomposition products flow downstream during shutdown as the chamber pressure decays. These processes lead to the ammonia mole-fraction profiles shown in Fig. 9 and the mole-fraction profiles of nitrogen and hydrogen shown in Figs. 10 and 11 respectively.

The effects of various reactor operating conditions on the transient behavior of typical hydrazine reactors are illustrated in Figs. 12 through 38. The calculated results refer to a 23 lb_f nominal thrust engine 1.4 in. in diameter with a packed length of 1.2 in. into which liquid hydrazine is injected at a temperature of 530 deg R. A reference case was chosen in which hydrazine injection was taken at the reactor inlet only and in which the steady-state mass flow rate was taken as 5.76 lb/ft^2-sec (0.04 lb/in^2-sec), the injector pressure as 150 psia, the initial chamber pressure as 14.7 psia,

the initial bed temperature as 530 deg R, the pulse duty cycle as alternating 60 msec on and 60 msec off, and the catalyst bed configuration as 0.2 in. of 25-30 mesh catalyst particles followed by 1.0 in. of 14-18 mesh catalyst particles. This bed configuration is referred to in the figures as "mixed bed #2". Injector pressure, mass flow rate, axial injection profile, catalyst bed configuration, and pulse duty cycle were then varied in turn and the calculated interstitial temperatures at two axial positions in the bed were then plotted as a function of time. The transient behavior of the reference case is illustrated in Figs. 12 through 22. Transient interstitial temperature profiles are plotted in Fig. 12 for two axial positions, one at the end of the bed and one at approximately the midpoint of the bed. Also plotted in Fig. 12 are the temperature profiles computed at these same points for the reactor operating under conditions of continuous rather than pulsed flow. The transient particle temperature profiles associated with the interstitial temperatures shown in Fig. 12 are plotted in Fig. 13, while the chamber pressure is plotted as a function of time in Fig. 14. The associated mole-fraction profiles for hydrazine are plotted in Figs. 15 and 16, for ammonia in Figs. 17 and 18, for nitrogen in Figs. 19 and 20, and for hydrogen in Figs. 21 and 22.

In Fig. 23, transient interstitial temperature profiles are plotted for an injector pressure of 500 psia with all other conditions taken as those of the reference case. The very slight effect of pressure on transient response may be noted by comparing Figs. 12 and 23. A direct comparison of exit gas temperature profiles associated with the two different pressures is shown in Fig. 24 for the reactor operating under conditions of continuous flow.

Transient interstitial temperature profiles are plotted for steady-state mass flow rates of 1.44 lb/ft^2-sec (0.01 $lb/in.^2$-sec) in Fig. 25 and 14.4 lb/ft^2-sec (0.10 $lb/in.^2$-sec) in Fig. 26 with all other conditions taken the same as those of the reference case.* The marked effect of mass flow rate on transient response is further illustrated in Fig. 27 for a continuous flow system. Here, exit gas temperatures are plotted versus time for the three different steady-state mass flow rates.

The effects of distributed injectors on transient temperature profiles are illustrated in Figs. 28 through 30. Temperature are plotted as functions of time at the midpoint and at the end of the bed in Figs. 28 and 29 respectively for a case in which 1/4 of the hydrazine is injected at the inlet and the remaining 3/4 is injected uniformly over the first 1/2 in. of the reactor.

*An injector pressure of 500 psia was used in calculations for the high mass flow rate case since the high pressure drop associated with this flow rate precludes use of the reference injector pressure.

The exit gas temperature profiles for this case and for the reference case of all inlet injection are compared in Fig. 30 under conditions of continuous flow.

Transient interstitial temperature profiles are plotted for different catalyst bed configurations in Figs. 31 through 35. Temperature profiles associated with beds packed with all 25-30 mesh particles are shown in Fig. 31, all 14-18 mesh particles in Fig. 32, and the mixture of 25-30 mesh particles and 1/8 in. x 1/8 in. cylindrical pellets in Figs. 33 and 34. Exit gas temperature profiles for these cases are compared in Fig. 35 under conditions of continuous flow.

The transient temperature profiles at two axial positions for a pulse duty cycle consisting of alternate on and off times of 60 msec and 120 msec respectively are illustrated in Fig. 36. The temperature profiles associated with a 60 msec/240 msec pulse duty cycle are shown in Fig. 37. The effects of duty cycle on the transient response of the exit gas temperature are summarized in Fig. 38.

Additional calculations were made to illustrate the transient behavior of a high thrust hydrazine engine. The calculations pertain to a 600 lb_f nominal thrust hydrazine reactor 4.2 in. in diameter with a packed length of 1.0 in. into which liquid hydrazine is injected at the upstream end of the reactor only. The catalyst bed packing was taken to consist of all 25-30 mesh catalyst particles; the steady-state mass flow rate was taken as 40.3 lb/ft^2-sec, the injector pressure as 1405 psia, the initial chamber pressure as 0.1 psia, the initial bed temperature as 530 deg R, and the pulse duty cycle as alternating 50 msec on and 250 msec off. For this case, interstitial temperature, particle temperature, chamber pressure, and the mole-fractions of hydrazine, ammonia, nitrogen and hydrogen are plotted as functions of time at the end of the bed in Figs. 39, 40, 41, 42, 43, 44 and 45 respectively. These figures illustrate the very rapid transient response associated with this high flow rate system.

REFERENCES

1. Kesten, A. S.: Analytical Study of Catalytic Reactors for Hydrazine Decomposition. United Aircraft Research Laboratories Report F910461-12, First Annual Progress Report, Contract NAS 7-458, May 1967.

2. Kesten, A. S.: Analytical Study of Catalytic Reactors for Hydrazine Decomposition. United Aircraft Research Laboratories Report G910461-24, Second Annual Progress Report, Contract NAS 7-458, May 1968.

3. Smith, E. J., D. B. Smith, and A. S. Kesten: Analytical Study of Catalytic Reactors for Hydrazine Decomposition. United Aircraft Research Laboratories Report G910461-30, Computer Program Manual - One- and Two-Dimensional Steady-State Models, Contract NAS 7-458, August 1968.

4. Smith, D. B., E. J. Smith, and A. S. Kesten: Analytical Study of Catalytic Reactors for Hydrazine Decomposition. United Aircraft Research Laboratories Report H910461-37, Computer Programs Manual - Transient Model, Contract NAS 7-458, May 1969.

5. Bird, R. B., W. E. Stewart, and E. N. Lightfoot: Transport Phenomena. John Wiley & Sons, Inc., New York, 1960.

6. Kesten, A. S.: Analytical Study of Catalytic Reactors for Hydrazine Decomposition - Part I: Steady-State Behavior of Hydrazine Reactors. Proceedings of the Hydrazine Monopropellant Technology Symposium, The Johns Hopkins University Applied Physics Laboratory, Silver Spring, Maryland, November 1967.

7. Kesten, A. S.: Analytical Study of Catalytic Reactors for Hydrazine Decomposition - Part II: Transient Behavior of Hydrazine Reactors. Proceedings of the Hydrazine Monopropellant Technology Symposium, The Johns Hopkins University Applied Physics Laboratory, Silver Spring, Maryland, November 1967.

8. Kesten, A. S. and T. W. Price: Analytical and Experimental Studies of the Transient Behavior of Catalytic Reactors for Hydrazine Decomposition. Proceedings of the CPIA 10th Liquid Propulsion Symposium, Las Vegas, Nevada, November 1968.

LIST OF SYMBOLS

a	Radius of spherical particle, ft
A_c	Cross-sectional area of reaction chamber, ft^2
A_p	Total external surface of catalyst particle per unit volume of bed, ft^{-1}
A_w	Total surface area of chamber walls, ft^2
c_i	Reactant concentration in interstitial fluid, lb/ft^3
c_p	Reactant concentration in gas phase within the porous particle, lb/ft^3
C_F	Specific heat of fluid in the interstitial phase, Btu/lb- deg R
$\overline{C_F}$	Average specific heat of fluid in the interstitial phase, Btu/lb- deg R
C_s	Specific heat of catalyst particle, Btu/lb - deg R
C_w	Specific heat of chamber walls, Btu/lb - deg R
d_c	Diameter of reaction chamber, ft
D_i	Diffusion coefficient of reactant gas in the interstitial fluid, ft^2/sec
D_p	Diffusion coefficient of reactant gas in the porous particle, ft^2/sec
F	Rate of feed of hydrazine from distributed injectors into the system, lb/ft^3-sec
G	Mass flow rate, lb/ft^2-sec
h	Enthalpy, Btu/lb
h_a	Heat transfer coefficient for forced convection between chamber and surrounding atmosphere, Btu/ft^2-sec-deg R
h_a'	Heat transfer coefficient for natural convection between chamber and surrounding atmosphere, Btu/ft^2-sec-deg $R^{1.25}$
h_a''	Radiation heat transfer coefficient between chamber and surrounding atmosphere, Btu/ft^2-sec-deg R^4
h_c	Heat transfer coefficient between bulk fluid and particles, Btu/ft^2-sec-deg R

h_w	Heat transfer coefficient between bulk fluid and chamber walls, Btu/ft^2-sec-deg R
H	Heat of reaction (negative for exothermic reaction), Btu/lb
k_c	Mass transfer coefficient, ft/sec
K_i	Thermal conductivity of interstitial fluid, Btu/ft-sec-deg R
K_p	Thermal conductivity of the porous catalyst particle, Btu/ft-sec-deg R
L	Length of reaction chamber, ft
m_w	Thermal mass of chamber walls, lb
M	Molecular weight, lb/lb mole
$\bar{M}$	Average molecular weight, lb/lb mole
P	Chamber pressure, psia
r_{het}	Rate of (heterogeneous) chemical reaction on the catalyst surfaces, lb/ft^3-sec
r_{hom}	Rate of (homogeneous) chemical reaction in the interstitial phase, lb/ft^3-sec
R	Gas constant, equals 10.73 psia - ft^3/lb mole - deg R
t	Time, sec
T	Temperature, deg R
V_c	Volume of reactor up to nozzle throat exclusive of volume occupied by catalyst particles, ft^3
w_i	Weight fraction of reactant in interstitial phase
z	Axial distance, ft
α_p	Intraparticle void fraction
δ	Interparticle void fraction
μ	Viscosity of interstitial fluid, lb/ft-sec

ρ_i Density of interstitial fluid, lb/ft^3

ρ_s Bulk density of catalyst particle, lb/ft^3

Subscripts

a Refers to surrounding atmosphere

F Refers to feed

i Refers to interstitial phase

p Refers to gas within the porous catalyst particle

s Refers to surface of catalyst particle

SS Refers to steady-state

w Refers to chamber wall

Superscripts

J Refers to chemical species

APPENDIX I

DISTRIBUTION LIST FOR THIRD ANNUAL PROGRESS REPORT

G910461-24

Addressee	Copies
National Aeronautics & Space Administration Washington, D. C. 20546 Attn: Chief, Liq. Prop. Res. & Tech., RPL	1
National Aeronautics & Space Administration Washington, D. C. 20546 Attn: Chief, Liq. Prop. Exp. Systems, RPX	10
National Aeronautics & Space Administration Washington, D. C. 20546 Attn: Dir., Launch Vehicles & Prop., SV	1
National Aeronautics & Space Administration Washington, D. C. 20546 Attn: Dir., Advanced Manned Missions, MT	1
Air Force Rocket Propulsion Laboratory Research and Technology Division Air Force System Command Edwards, California 93523 Attn: Mr. K. Rimer	1
Air Force Rocket Propulsion Laboratory Research and Technology Division Air Force System Command Edwards, California 93523 Attn: Capt. Noyce/32725	1
U. S. Naval Ordnance Test Station China Lake, California 93553 Attn: Mr. Duane Williams	1
U. S. Naval Ordnance Test Station China Lake, California 93553 Attn: Mr. James Dake	1
U. S. Naval Ordnance Test Station China Lake, California 93553 Attn: Mr. David Oliver	1
Jet Propulsion Laboratory 4800 Oak Grove Drive Pasadena, California 91103 Attn: Mr. Theodore W. Price	10
NASA Pasadena Office 4800 Oak Grove Drive Pasadena, California 91103 Attn: Contracting Officer	1
NASA Pasadena Office 4800 Oak Grove Drive Pasadena, California 91103 Attn: Office of Tech. Information & Patent Matters	1
Scientific & Technical Information Facility P. O. Box 5700 Bethesda, Maryland 20014 Attn: NASA Rep., Code CRT	2
NASA Lewis Research Center 21000 Brookpark Road Cleveland, Ohio 44135 Attn: Mr. Paul N. Herr	3
NASA Lewis Research Center 21000 Brookpark Road Cleveland, Ohio 44135 Attn: Mr. I. A. Johnsen	1
Marshall Space Flight Center Huntsville, Alabama 35812 Attn: Mr. Kieth Coates	1
Department of Chemical Engineering University of British Columbia Vancouver 8, Canada Attn: Dr. J. Lielmezs	1
NASA Ames Research Center Moffett Field, California 94035 Attn: Technical Librarian	2
NASA Ames Research Center Moffett Field, California 94035 Attn: Mr. Harold Hornby Mission Analysis Division	Ltr. Only
NASA Ames Research Center Moffett Field, California 94035 Attn: Mr. Clarence A. Syvertson	Ltr. Only
NASA Goddard Space Flight Center Greenbelt, Maryland 20771 Attn: Technical Librarian	2
NASA Goddard Space Flight Center Greenbelt, Maryland 20771 Attn: Mr. Merland L. Moseson, Code 620	Ltr. Only
NASA Goddard Space Flight Center Greenbelt, Maryland 20771 Attn: Mr. D. Grant	Ltr. Only
Jet Propulsion Laboratory California Institute of Technology 4800 Oak Grove Drive Pasadena, California 91103 Attn: Technical Librarian	2
Jet Propulsion Laboratory California Institute of Technology 4800 Oak Grove Drive Pasadena, California 91103 Attn: Mr. Henry Burlage, Jr. Propulsion Div., 38	Ltr. Only
NASA Langley Research Center Langley Station Hampton, Virginia 23365 Attn: Technical Librarian	2
NASA Langley Research Center Langley Station Hampton, Virginia 23365 Attn: Mr. David Carter	1
NASA Langley Research Center Langley Station Hampton, Virginia 23365 Attn: Dr. Floyd L. Thompson, Dir.	Ltr. Only

Addressee	Copies
NASA Langley Research Center Langley Station Hampton, Virginia 23365 Attn: Mr. R. Hook	Ltr. Only
NASA Lewis Research Center 21000 Brookpark Road Cleveland, Ohio 44135 Attn: Technical Librarian	2
NASA Lewis Research Center 21000 Brookpark Road Cleveland, Ohio 44135 Attn: Dr. Abe Silverstein, Dir.	Ltr. Only
NASA Lewis Research Center 21000 Brookpark Road Cleveland, Ohio 44135 Attn: Mr. Steve Cohen	Ltr. Only
NASA Marshall Space Flight Center Huntsville, Alabama 35812 Attn: Technical Librarian	2
NASA Marshall Space Flight Center Huntsville, Alabama 35812 Attn: Mr. Hans G. Paul, Code R-P+VED	Ltr. Only
NASA Marshall Space Flight Center Huntsville, Alabama 35812 Attn: Mr. Werner Voss, R-P&VE-PM	Ltr. Only
NASA Manned Spacecraft Center Houston, Texas 77001 Attn: Technical Librarian	2
NASA Manned Spacecraft Center Houston, Texas 77001 Attn: Dr. Robert R. Gilruth, Dir.	Ltr. Only
NASA Manned Spacecraft Center Houston, Texas 77001 Attn: Mr. H. Pohl	Ltr. Only
NASA John F. Kennedy Space Center Cocoa Beach, Florida 32931 Attn: Technical Librarian	2
NASA John F. Kennedy Space Center Cocoa Beach, Florida 32931 Attn: Dr. Kurt H. Debus	Ltr. Only
NASA Test Facility Propulsion Engineering Office White Sands, New Mexico Attn: Technical Librarian	1
NASA Test Facility Propulsion Engineering Office White Sands, New Mexico Attn: Mr. I. D. Smith, Staff Chemist	Ltr. Only
Aeronautical Systems Division Air Force Systems Command Wright-Patterson Air Force Base Dayton, Ohio 45433 Attn: Technical Librarian	1
Aeronautical Systems Division Air Force Systems Command Wright-Patterson Air Force Base Dayton, Ohio 45433 Attn: Mr. D. L. Schmidt, Code ASRCNC-2	Ltr. Only
Air Force Missile Development Center Holloman Air Force Base, New Mexico 88330 Attn: Technical Librarian	1
Air Force Missile Development Center Holloman Air Force Base, New Mexico 88330 Attn: Maj. R. E. Bracken, Code MDGRT	Ltr. Only
Air Force Missile Test Center Patrick Air Force Base, Florida Attn: Technical Librarian	1
Air Force Missile Test Center Patrick Air Force Base, Florida Attn: Mr. L. J. Ullian	Ltr. Only
Air Force Systems Division Air Force Unit Post Office Los Angeles 45, California 90045 Attn: Technical Librarian	1
Air Force Systems Division Air Force Unit Post Office Los Angeles 45, California 90045 Attn: Col. Clark, Tech. Data Center	Ltr. Only
Technical Library AFFTC (FTBPP-2) Edwards AFB, California 93523 Attn: Technical Librarian	2
Arnold Engineering Development Center Arnold Air Force Station Tullahoma, Tennessee 37388 Attn: Technical Librarian	1
Arnold Engineering Development Center Arnold Air Force Station Tullahoma, Tennessee 37388 Attn: Dr. H. K. Doetsch	Ltr. Only
Bureau of Naval Weapons Department of the Navy Washington, D. C. 20546 Attn: Technical Librarian	1
Bureau of Naval Weapons Department of the Navy Washington, D. C. 20546 Attn: Mr. J. Kay, RTMS-41	Ltr. Only
Defense Documentation Center Headquarters Cameron Station, Building 5 5010 Duke Street Alexandria, Virginia 22314 Attn: Technical Librarian	1
Defense Documentation Center Headquarters Cameron Station, Building 5 5010 Duke Street Alexandria, Virginia 22314 Attn: TISIA	Ltr. Only
Headquarters, U. S. Air Force Washington, D. C. 20546 Attn: Technical Librarian	1
Headquarters, U. S. Air Force Washington, D. C. 20546 Attn: Col. C. K. Stambaugh, AFRST	Ltr. Only
Picatinny Arsenal Dover, New Jersey 07801 Attn: Technical Librarian	1
Picatinny Arsenal Dover, New Jersey 07801 Attn: Mr. I. Forsten, Chief Liquid Propulsion Lab., SMUPA-DL	Ltr. Only

Addressee	Copies
Air Force Rocket Propulsion Laboratory Research and Technology Division Air Force Systems Command Edwards, California 93523 Attn: Technical Librarian	1
Air Force Rocket Propulsion Laboratory Research and Technology Division Air Force Systems Command Edwards, California 93523 Attn: Mr. H. Main, RPRR	Ltr. Only
U. S. Atomic Energy Commission Technical Information Services Box 62 Oak Ridge, Tennessee 37830 Attn: Technical Librarian	1
U. S. Atomic Energy Commission Technical Information Services Box 62 Oak Ridge, Tennessee 37830 Attn: Mr. A. P. Huber Oak Ridge Gaseous Diffusion Plant (ORGDP) P. O. Box P	Ltr. Only
U. S. Army Missile Command Redstone Arsenal, Alabama 35809 Attn: Technical Librarian	1
U. S. Army Missile Command Redstone Arsenal, Alabama 35809 Attn: Dr. Walter Wharton	Ltr. Only
U. S. Naval Ordnance Test Station China Lake, California 93557 Attn: Technical Librarian	1
U. S. Naval Ordnance Test Station China Lake, California 93557 Attn: Code 4562 Chief, Missile Propulsion Division	Ltr. Only
Chemical Propulsion CPIA Information Agency Applied Physics Laboratory 8621 Georgia Avenue Silver Spring, Maryland 20910 Attn: Technical Librarian	1
Chemical Propulsion CPIA Information Agency Applied Physics Laboratory 8621 Georgia Avenue Silver Spring, Maryland 20910 Attn: Mr. P. Martin	Ltr. Only
Aerojet-General Corporation P. O. Box 296 Azusa, California 91703 Attn: Technical Librarian	1
Aerojet-General Corporation P. O. Box 296 Azusa, California 91703 Attn: Mr. L. F. Kohrs	Ltr. Only
Aerojet-General Corporation P. O. Box 1947 Technical Library, Bldg. 2015, Dept. 2410 Sacramento, California 95809 Attn: Technical Librarian	1
Aerojet-General Corporation P. O. Box 1947 Sacramento, California 95809 Attn: Dr. C. B. McGough	Ltr. Only
Aeronutronic Division Philco Corporation Ford Road Newport Beach, California 92663 Attn: Technical Librarian	1
Aeronutronic Division Philco Corporation Ford Road Newport Beach, California 92663 Attn: Mr. N. Stern	Ltr. Only
Aerospace Corporation 2400 East El Segundo Boulevard P. O. Box 95085 Los Angeles, California 90045 Attn: Technical Librarian	1
Aerospace Corporation 2400 East El Segundo Boulevard P. O. Box 95085 Los Angeles, California 90045 Attn: Mr. M. J. Russi	Ltr. Only
Aerospace Corporation 2400 East El Segundo Boulevard P. O. Box 95085 Los Angeles, California 90045 Attn: Mr. H. Greer, Propulsion Dept.	Ltr. Only
Arthur D. Little, Incorporated 20 Acorn Park Cambridge, Massachusetts 02140 Attn: Technical Librarian	1
Arthur D. Little, Incorporated 20 Acorn Park Cambridge, Massachusetts 02140 Attn: Mr. E. Karl Bastress	Ltr. Only
Astropower Laboratory Douglas Aircraft Company 2121 Paularino Newport Beach, California 92663 Attn: Technical Librarian	1
Astropower Laboratory Douglas Aircraft Company 212 Paularino Newport Beach, California 92663 Attn: Dr. George Moc, Dir. Research	Ltr. Only
Astrosystems International, Incorporated 1275 Bloomfield Avenue Fairfield, New Jersey 07007 Attn: Technical Librarian	1
Astrosystems International, Incorporated 1275 Bloomfield Avenue Fairfield, New Jersey 07007 Attn: Mr. A. Mendenhall	Ltr. Only
Atlantic Research Corporation Edsall Road and Shirley Highway Alexandria, Virginia 22314 Attn: Technical Librarian	1
Atlantic Research Corporation Edsall Road and Shirley Highway Alexandria, Virginia 22314 Attn: Mr. A. Scurlock	Ltr. Only
Beech Aircraft Corporation Boulder Division Box 631 Boulder, Colorado 80302 Attn: Technical Librarian	1

Addressee	Copies
Beech Aircraft Corporation Boulder Division Box 631 Boulder, Colorado 80302 Attn: Mr. J. H. Rodgers	Ltr. Only
Bell Aerosystems Company P. O. Box 1 Buffalo, New York 14240 Attn: Technical Librarian	1
Bell Aerosystems Company P. O. Box 1 Buffalo, New York 14240 Attn: Mr. N. Safeer	Ltr. Only
Bell Aerosystems Company P. O. Box 1 Buffalo, New York 14240 Attn: Mr. N. R. Roth	Ltr. Only
Bell Aerosystems Company P. O. Box 1 Buffalo, New York 14240 Attn: Mr. J. Flanagan	Ltr. Only
Bendix Systems Division Bendix Corporation 3300 Plymouth Road Ann Arbor, Michigan 48105 Attn: Technical Librarian	1
Bendix Systems Division Bendix Corporation 3300 Plymouth Road Ann Arbor, Michigan 48105 Attn: Mr. John M. Brueger	Ltr. Only
Boeing Company P. O. Box 3707 Seattle, Washington 98124 Attn: Technical Librarian	1
Boeing Company P. O. Box 3707 Seattle, Washington 98124 Attn: Mr. J. D. Alexander	Ltr. Only
Missile Division Chrysler Corporation P. O. Box 2628 Detroit, Michigan 48231 Attn: Technical Librarian	1
Missile Division Chrysler Corporation P. O. Box 2628 Detroit, Michigan 48231 Attn: Mr. John Gates	Ltr. Only
Wright Aeronautical Division Curtiss-Wright Corporation Wood-Ridge, New Jersey 07075 Attn: Technical Librarian	1
Wright Aeronautical Division Curtiss-Wright Corporation Wood-Ridge, New Jersey 07075 Attn: Mr. G. Kelley	Ltr. Only
Missile and Space Systems Division Douglas Aircraft Company, Incorporated 3000 Ocean Park Boulevard Santa Monica, California 90406 Attn: Technical Librarian	1
Missile and Space Systems Division Douglas Aircraft Company, Incorporated 3000 Ocean Park Boulevard Santa Monica, California 90406 Attn: Mr. R. W. Hallet, Chief Engineer Advanced Space Tech.	Ltr. Only
Missile and Space Systems Division Douglas Aircraft Company, Incorporated 3000 Ocean Park Boulevard Santa Monica, California 90406 Attn: Mr. A. Pisciotta, Jr.	Ltr. Only
Aircraft Missiles Division Fairchild Hiller Corporation Hagerstown, Maryland 21740 Attn: Technical Librarian	1
Aircraft Missiles Division Fairchild Hiller Corporation Hagerstown, Maryland 21740 Attn: Mr. J. S. Kerr	Ltr. Only
General Dynamics Convair Division 5001 Kearny Villa Road P. O. Box 1628 San Diego, California 92112 Attn: Technical Librarian	1
General Dynamics Convair Division 5001 Kearny Villa Road P. O. Box 1628 San Diego, California 92112 Attn: Mr. E. R. Peterson V.P., Research and Eng.	Ltr. Only
General Dynamics Convair Division 5001 Kearny Villa Road P. O. Box 1628 San Diego, California 92112 Attn: Mr. Frank Dore	Ltr. Only
Missile and Space Systems Center General Electric Company Valley Forge Space Technology Center P. O. Box 8555 Philadelphia, Pennsylvania Attn: Technical Librarian	1
Missile and Space Systems Center General Electric Company Valley Forge Space Technology Center P. O. Box 8555 Philadelphia, Pennsylvania Attn: Mr. F. Mezger	Ltr. Only
Missile and Space Systems Center General Electric Company Valley Forge Space Technology Center P. O. Box 8555 Philadelphia, Pennsylvania Attn: Mr. R. E. Emmer	Ltr. Only
Missile and Space Systems Center General Electric Company Valley Forge Space Technology Center P. O. Box 8555 Philadelphia, Pennsylvania Attn: Mr. B. H. Caldwell	Ltr. Only
Advanced Engine & Technology Department General Electric Company Cincinnati, Ohio 45215 Attn: Technical Librarian	1

Addressee	Copies
Advanced Engine & Technology Department General Electric Company Cincinnati, Ohio 45215 Attn: Mr. D. Suichu	Ltr. Only
Grumman Aircraft Engineering Corporation Bethpage, Long Island, New York 11714 Attn: Technical Librarian	1
Grumman Aircraft Engineering Corporation Bethpage, Long Island, New York 11714 Attn: Mr. Joseph Gavin	Ltr. Only
Hughes Aircraft Company Aerospace Group Centinela and Teale Streets Culver City, California Attn: Technical Librarian	1
Hughes Aircraft Company Aerospace Group Centinela and Teale Streets Culver City, California Attn: Mr. E. H. Meier, V.P. & Div. Mgr. Research and Dev. Div.	Ltr. Only
Walter Kidde & Company, Incorporated 675 Main Street Belleville, New Jersey 07109 Attn: Technical Librarian	1
Walter Kidde & Company, Incorporated 675 Main Street Belleville, New Jersey 07109 Attn: Mr. K. A. Traynelis	Ltr. Only
Ling-Temco-Vought Corporation Astronautics P. O. Box 5907 Dallas, Texas 75222 Attn: Technical Librarian	1
Ling-Temco-Vought Corporation Astronautics P. O. Box 5907 Dallas, Texas 75222 Attn: Mr. Garland Whisenhunt	Ltr. Only
Lockheed Missiles and Space Company Attn: Technical Information Center P. O. Box 504 Sunnyvale, California 94088 Attn: Technical Librarian	1
Lockheed Missiles and Space Company Attn: Technical Information Center P. O. Box 504 Sunnyvale, California 94088 Attn: Mr. Y. C. Lee	Ltr. Only
Lockheed Propulsion Company P. O. Box 111 Redlands, California 92374 Attn: Technical Librarian	1
Lockheed Propulsion Company P. O. Box 111 Redlands, California 92374 Attn: Mr. H. L. Thackwell	Ltr. Only
Lockheed Propulsion Company P. O. Box 111 Redlands, California 92374 Attn: Mr. J. E. Fitzgerald	Ltr. Only
The Marquardt Corporation 16555 Saricoy Street Van Nuys, California 91409 Attn: Technical Librarian	1
The Marquardt Corporation 16555 Saricoy Street Van Nuys, California 91409 Attn: Mr. Warren P. Boardman, Jr.	Ltr. Only
The Marquardt Corporation 16555 Saricoy Street Van Nuys, California 91409 Attn: Mr. R. Knox	Ltr. Only
Baltimore Division Martin Marietta Corporation Baltimore, Maryland 21203 Attn: Technical Librarian	1
Baltimore Division Martin Marietta Corporation Baltimore, Maryland 21203 Attn: Mr. John Calathes (3214)	Ltr. Only
Denver Division Martin Marietta Corporation P. O. Box 179 Denver, Colorado 80201 Attn: Technical Librarian	1
Denver Division Martin Marietta Corporation P. O. Box 179 Denver, Colorado 80201 Attn: Mr. J. D. Goodlette (A-241)	Ltr. Only
Denver Division Martin Marietta Corporation P. O. Box 179 Denver, Colorado 80201 Attn: Mr. A. J. Kullas	Ltr. Only
Orland Division Martin Marietta Corporation Box 5837 Orlando, Florida Attn: Technical Librarian	1
Orland Division Martin Marietta Corporation Box 5837 Orlando, Florida Attn: Mr. J. Ferm	Ltr. Only
McDonnell Aircraft Corporation P. O. Box 516 Municipal Airport St. Louis, Missouri 63166 Attn: Technical Librarian	1
McDonnell Aircraft Corporation P. O. Box 516 Municipal Airport St. Louis, Missouri 63166 Attn: Mr. R. A. Herzmark	Ltr. Only
McDonnell Aircraft Corporation P. O. Box 516 Municipal Airport St. Louis, Missouri 63166 Attn: Mr. P. Kelley	Ltr. Only
Rocket Research Corporation 520 South Portland Street Seattle, Washington 98108 Attn: Technical Librarian	1
Rocket Research Corporation 520 South Portland Street Seattle, Washington 98108 Attn: Mr. Foy McCullough, Jr.	Ltr. Only

Addressee	Copies
Rocket Research Corporation 520 South Portland Street Seattle, Washington 98108 Attn: Mr. Bruce Schmitz	Ltr. Only
Rocket Research Corporation 520 South Portland Street Seattle, Washington 98108 Attn: Dr. Duane Williams	Ltr. Only
Space & Information Systems Division North American Aviation, Incorporated 12214 Lakewood Boulevard Downey, California 90241 Attn: Technical Librarian	1
Space & Information Systems Division North American Aviation, Incorporated 12214 Lakewood Boulevard Downey, California 90241 Attn: Mr. H. Storms	Ltr. Only
Rocketdyne (Library 586-306) North American Aviation, Incorporated 6633 Canoga Avenue Canoga Park, California 91304 Attn: Technical Librarian	1
Rocketdyne (Library 586-306) North American Aviation, Incorporated 6633 Canoga Avenue Canoga Park, California 91304 Attn: Mr. E. B. Monteath	Ltr. Only
Rocketdyne (Library 586-306) North American Aviation, Incorporated 6633 Canoga Avenue Canoga Park, California 91304 Attn: Mr. E. V. Zettle	Ltr. Only
Rocketdyne (Library 586-306) North American Aviation, Incorporated 6633 Canoga Avenue Canoga Park, California 91304 Attn: Mr. N. Rodewald	Ltr. Only
Northrop Space Laboratories 3401 West Broadway Hawthorne, California 90250 Attn: Technical Librarian	1
Northrop Space Laboratories 3401 West Broadway Hawthorne, California 90250 Attn: Dr. William Howard	Ltr. Only
Astro-Electronics Division Radio Corporation of America Princeton, New Jersey 08540 Attn: Technical Librarian	1
Astro-Electronics Division Radio Corporation of America Princeton, New Jersey 08540 Attn: Mr. S. Fairweather	Ltr. Only
Reaction Motors Division Thiokol Chemical Corporation Denville, New Jersey 07832 Attn: Technical Librarian	1
Reaction Motors Division Thiokol Chemical Corporation Denville, New Jersey 07832 Attn: Mr. Arthur Sherman	Ltr. Only
Reaction Motors Division Thiokol Chemical Corporation Denville, New Jersey 07832 Attn: Mr. Robert Gere	Ltr. Only
Republic Aviation Corporation Farmingdale, Long Island, New York Attn: Technical Librarian	1
Republic Aviation Corporation Farmingdale, Long Island, New York Attn: Dr. William O'Donnell	Ltr. Only
Space General Corporation 9200 East Flair Avenue El Monte, California 91734 Attn: Technical Librarian	1
Space General Corporation 9200 East Flair Avenue El Monte, California 91734 Attn: Mr. C. E. Roth	Ltr. Only
Stanford Research Institute 333 Ravenswood Avenue Menlo Park, California 94025 Attn: Technical Librarian	1
Stanford Research Institute 333 Ravenswood Avenue Menlo Park, California 94025 Attn: Mr. Lionel Dickinson	Ltr. Only
TRW Systems One Space Park Redondo Beach, California 90278 Attn: Technical Librarian	1
TRW Systems One Space Park Redondo Beach, California 90278 Attn: Mr. D. Lee	Ltr. Only
TRW Systems One Space Park Redondo Beach, California 90278 Attn: Mr. V. Moseley	Ltr. Only
Tapco Division TRW, Incorporated 23555 Euclid Avenue Cleveland, Ohio 44117 Attn: Technical Librarian	1
Tapco Division TRW, Incorporated 23555 Euclid Avenue Cleveland, Ohio 44117 Attn: Mr. P. T. Angell	Ltr. Only
Thiokol Chemical Corporation Huntsville Division Huntsville, Alabama 35807 Attn: Technical Librarian	1
Thiokol Chemical Corporation Huntsville Division Huntsville, Alabama 34807 Attn: Mr. John Goodloe	Ltr. Only
United Technology Center 587 Methilda Avenue P. O. Box 358 Sunnyvale, California 94088 Attn: Technical Librarian	1
United Technology Center 587 Methilda Avenue P. O. Box 358 Sunnyvale, California 94088 Attn: Mr. B. Adelman	Ltr. Only

Addressee	Copies
Florida Research & Development Center Pratt & Whitney Aircraft United Aircraft Corporation P. O. Box 2691 West Palm Beach, Florida 33402 Attn: Technical Librarian	1
Florida Research & Development Center Pratt & Whitney Aircraft United Aircraft Corporation P. O. Box 2691 West Palm Beach, Florida 33402 Attn: Mr. R. J. Coar	Ltr. Only
Vickers Incorporated Box 302 Troy, Michigan Attn: Technical Librarian	1
Sunstrand Aviation 2421 11th Street Rockford, Illinois 61101 Attn: Technical Librarian	1
Sunstrand Aviation 2421 11th Street Rockford, Illinois 61101 Attn: Mr. R. W. Reynolds	Ltr. Only
Hamilton Standard Division United Aircraft Corporation Windsor Locks, Connecticut 06096 Attn: Technical Librarian	1
Hamilton Standard Division United Aircraft Corporation Windsor Locks, Connecticut 06096 Attn: Mr. R. Hatch	Ltr. Only
Technical Library Air Research Manufacturing Company 9851 Sepulveda Boulevard Los Angeles, California 90009 Attn: Technical Librarian	
Air Research Manufacturing Company 9851 Sepulveda Boulevard Los Angeles, California 90009 Attn: Mr. C. S. Coe	Ltr. Only
Air Research Manufacturing Company 9851 Sepulveda Boulevard Los Angeles, California 90009 Attn: Mr. A. C. Standiffe	Ltr. Only
Shell Development Company 1400 53rd Street Emeryville, California 94608 Attn: Technical Librarian	1
Shell Development Company 1400 53rd Street Emeryville, California 94608 Attn: Dr. H. Voge	Ltr. Only
Shell Development Company 1400 53rd Street Emeryville, California 94608 Attn: Dr. T. J. Jennings	Ltr. Only
Brooklyn Polytechnic Institute Department of Chemical Engineering 333 Jay Street Brooklyn, New York 11201 Attn: Technical Librarian	1
Brooklyn Polytechnic Institute Department of Chemical Engineering 333 Jay Street Brooklyn, New York 11201 Attn: Prof. I. Miller	Ltr. Only

FIG. 1

COMPARISON OF THEORETICAL AND EXPERIMENTAL TRANSIENT TEMPERATURE PROFILES

STEADY-STATE CHAMBER PRESSURE = 200 PSIA STEADY-STATE MASS FLOW RATE = 6.5 LB/FT^2 - SEC
CATALYST BED CONFIGURATION: MIXED BED #1 (SEE TEXT)
INITIAL BED TEMPERATURE = 530 DEG R
SEE TEXT FOR ADDITIONAL REACTOR PARAMETERS

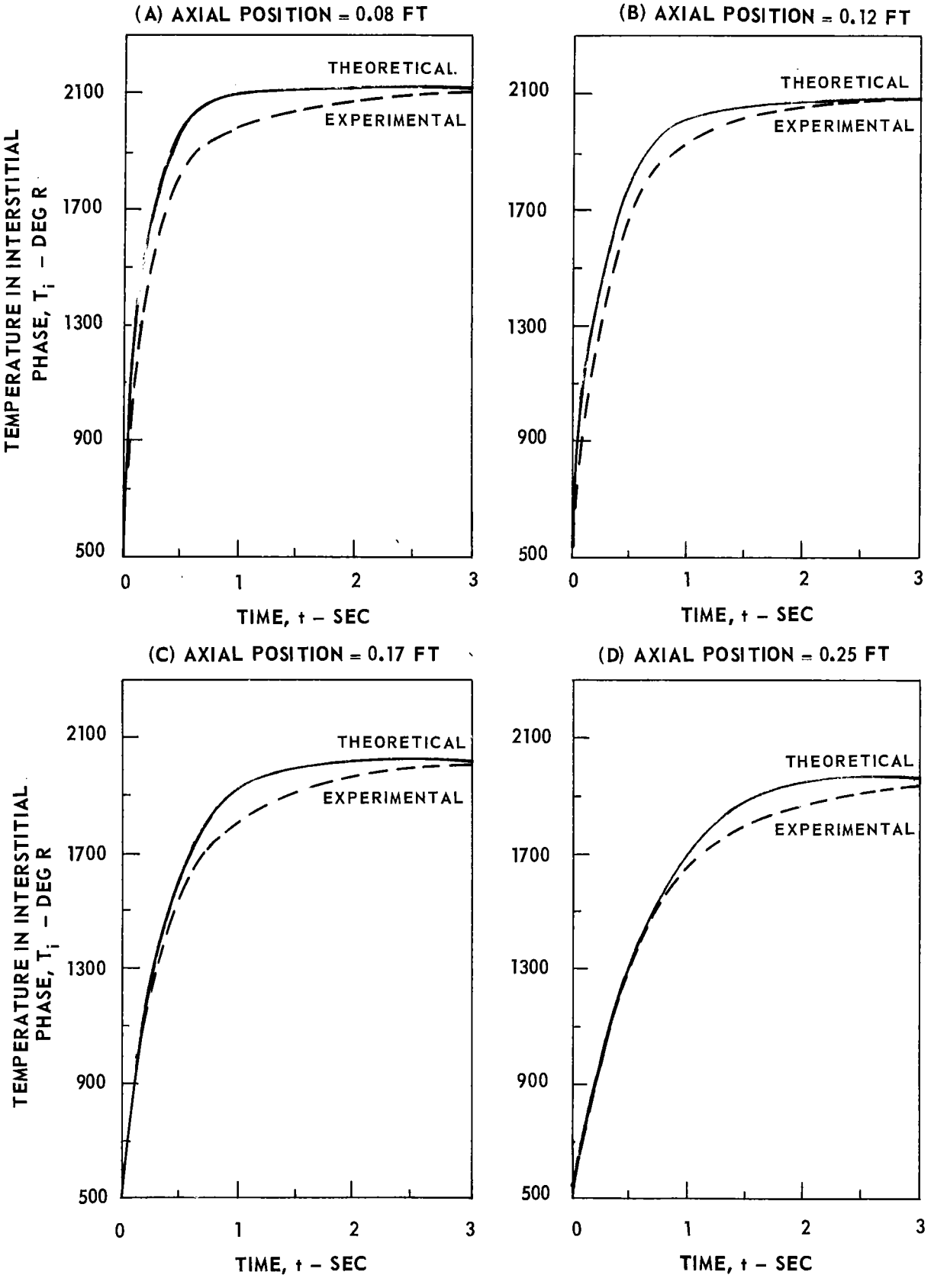

FIG. 2

TRANSIENT AXIAL PROFILES OF MOLE-FRACTIONS OF HYDRAZINE AND AMMONIA

INITIAL BED TEMPERATURE = 530 DEG R

STEADY-STATE CHAMBER PRESSURE = 200 PSIA
STEADY-STATE MASS FLOW RATE = 6.5 LB/FT^2 - SEC
CATALYST BED CONFIGURATION: MIXED BED # 1 (SEE TEXT)
SEE TEXT FOR ADDITIONAL REACTOR PARAMETERS

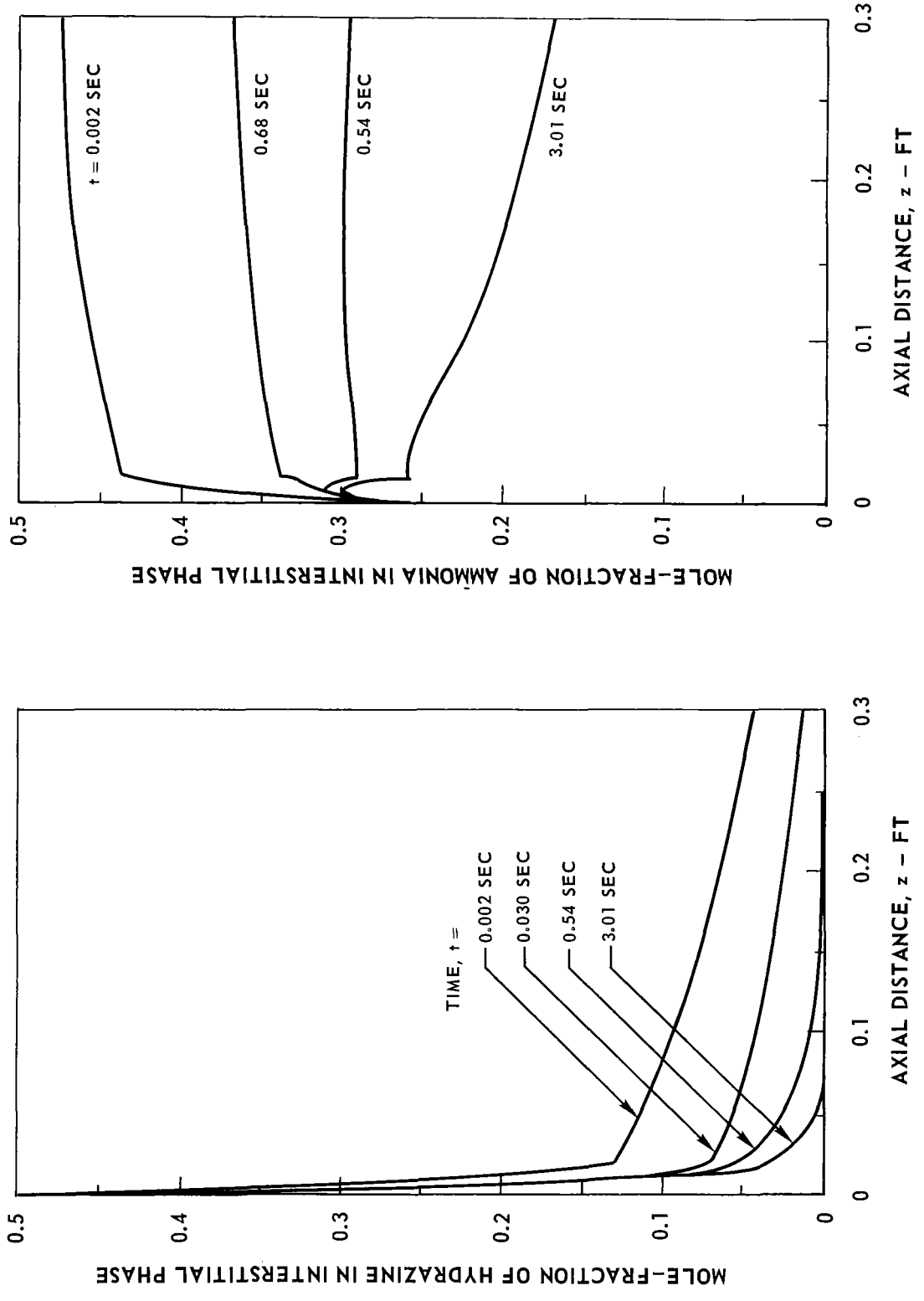

FIG. 3

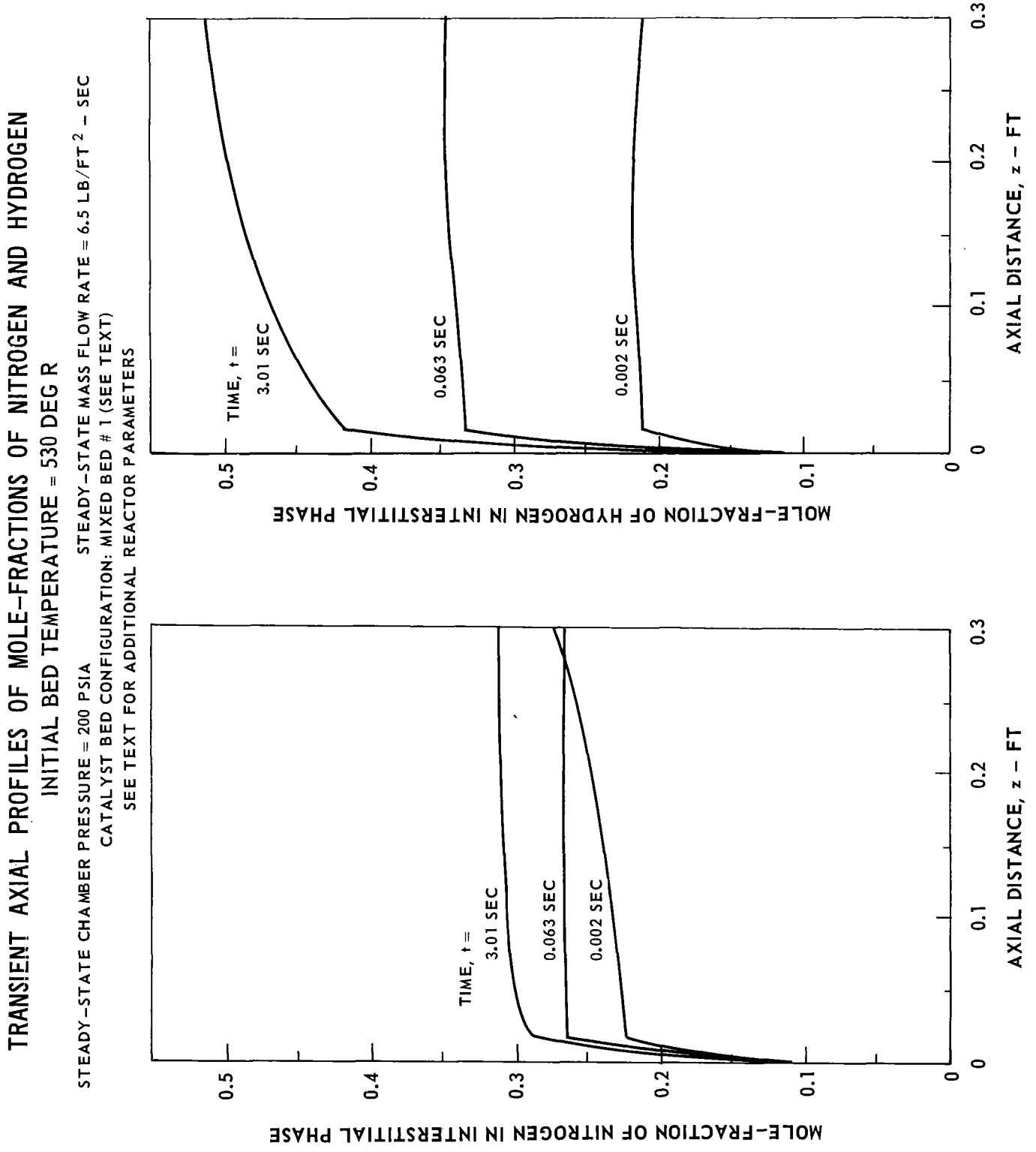
TRANSIENT AXIAL PROFILES OF MOLE-FRACTIONS OF NITROGEN AND HYDROGEN
INITIAL BED TEMPERATURE = 530 DEG R
STEADY-STATE CHAMBER PRESSURE = 200 PSIA
STEADY-STATE MASS FLOW RATE = 6.5 LB/FT^2 - SEC
CATALYST BED CONFIGURATION: MIXED BED # 1 (SEE TEXT)
SEE TEXT FOR ADDITIONAL REACTOR PARAMETERS
MOLE-FRACTION OF HYDROGEN IN INTERSTITIAL PHASE
TIME, t =
3.01 SEC
0.063 SEC
0.002 SEC
AXIAL DISTANCE, z - FT
MOLE-FRACTION OF NITROGEN IN INTERSTITIAL PHASE
TIME, t =
3.01 SEC
0.063 SEC
0.002 SEC
AXIAL DISTANCE, z - FT

COMPARISON OF THEORETICAL AND EXPERIMENTAL TRANSIENT TEMPERATURE PROFILES FOR VARIOUS INITIAL BED TEMPERATURES

AXIAL POSITION = 0.12 FT

STEADY-STATE CHAMBER PRESSURE = 200 PSIA

STEADY-STATE MASS FLOW RATE = 6.5 LB/FT^2 - SEC

CATALYST BED CONFIGURATION: MIXED BED # 1 (SEE TEXT)

SEE TEXT FOR ADDITIONAL REACTOR PARAMETERS

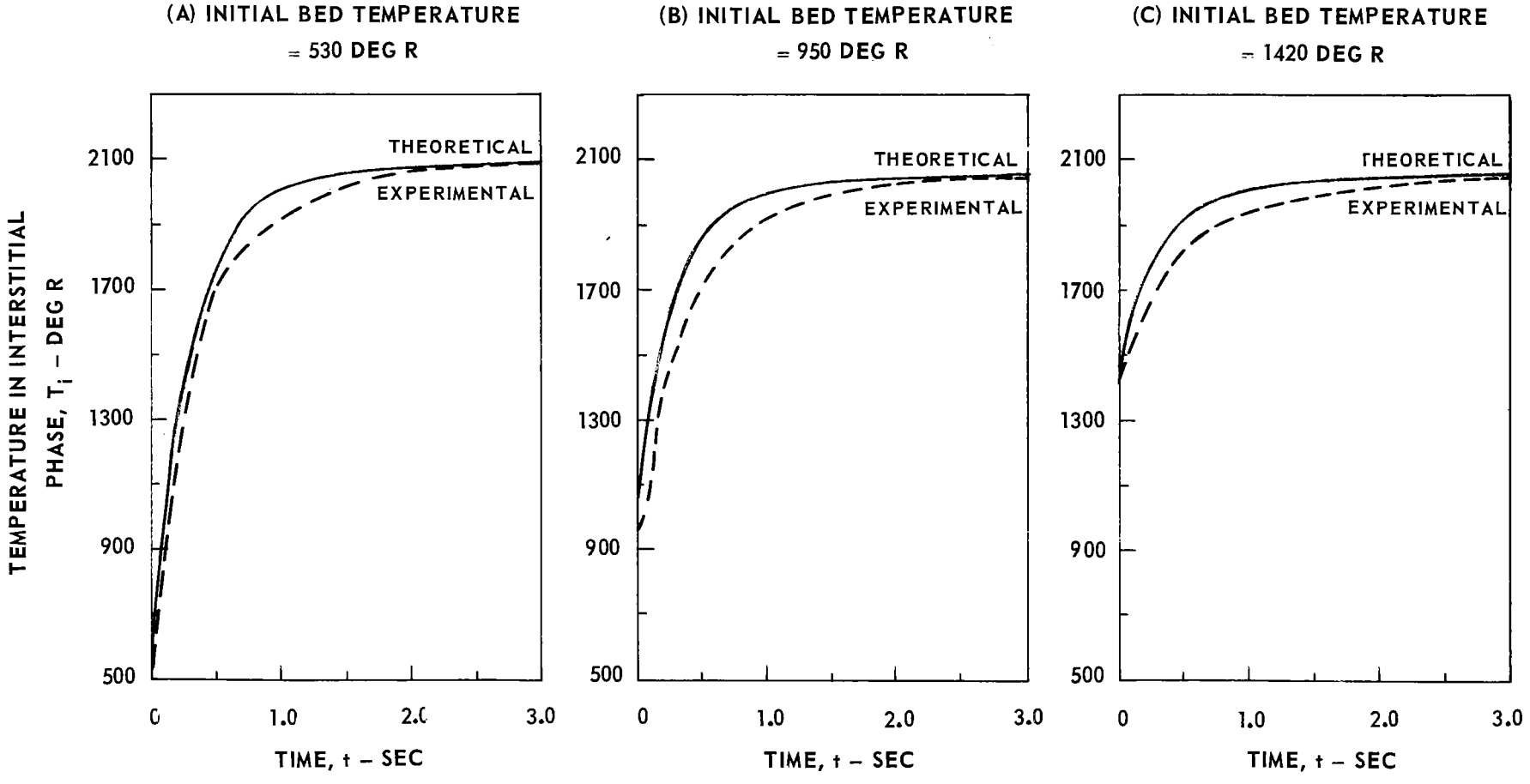

FIG. 4

VARIATION OF INTERSTITIAL TEMPERATURE WITH TIME AT VARIOUS AXIAL POSITIONS

STEADY-STATE CHAMBER PRESSURE = 260 PSIA STEADY-STATE MASS FLOW RATE = 5.8 LB/FT^2 - SEC
CATALYST BED CONFIGURATION: MIXED BED # 1 (SEE TEXT)
SEE TEXT FOR ADDITIONAL REACTOR PARAMETERS

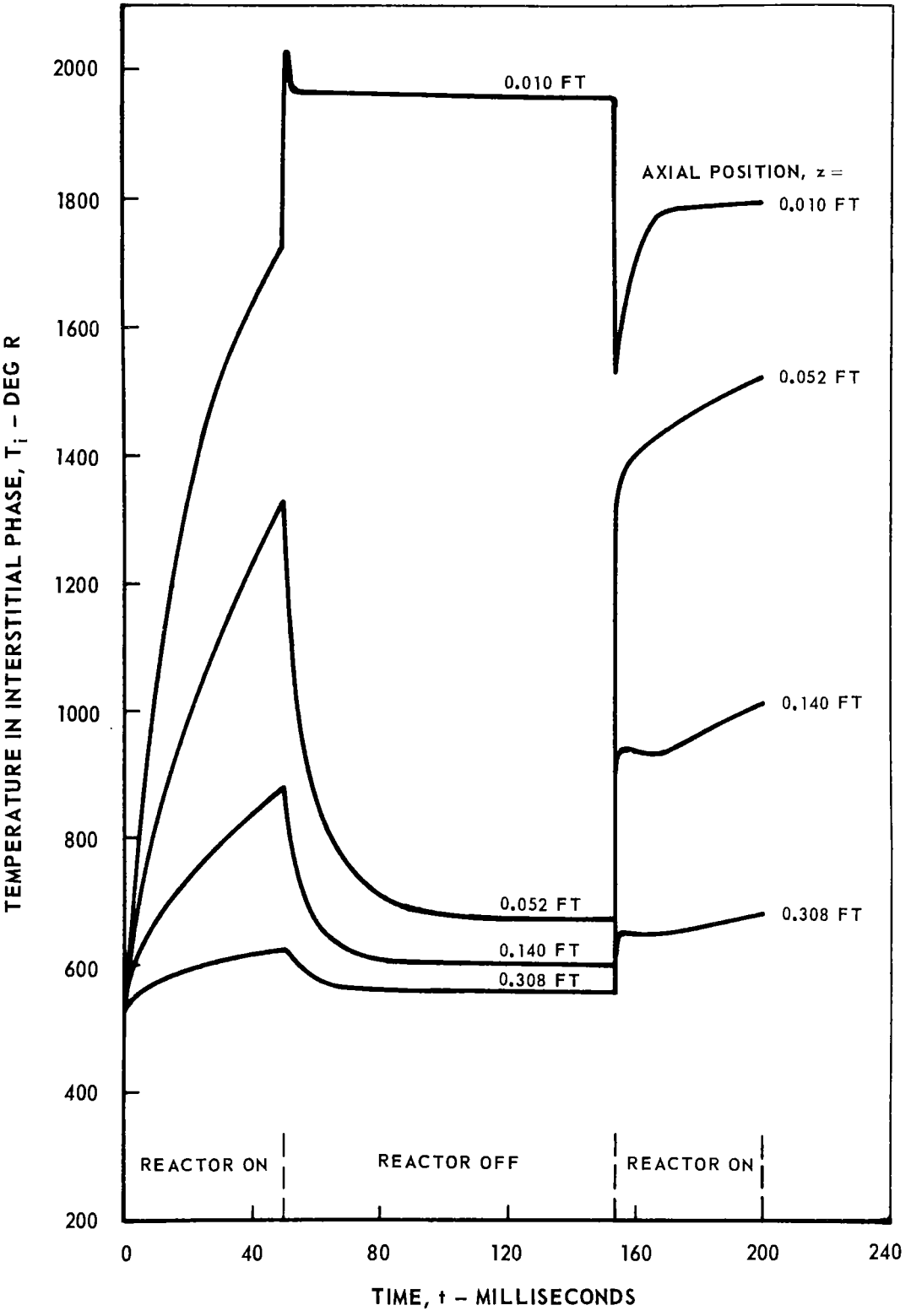

VARIATION OF CATALYST PARTICLE TEMPERATURE WITH TIME AT VARIOUS AXIAL POSITIONS

STEADY-STATE CHAMBER PRESSURE = 260 PSIA

STEADY-STATE MASS FLOW RATE = 5.8 LB/FT^2 - SEC

CATALYST BED CONFIGURATION: MIXED BED # 1 (SEE TEXT)

SEE TEXT FOR ADDITIONAL REACTOR PARAMETERS

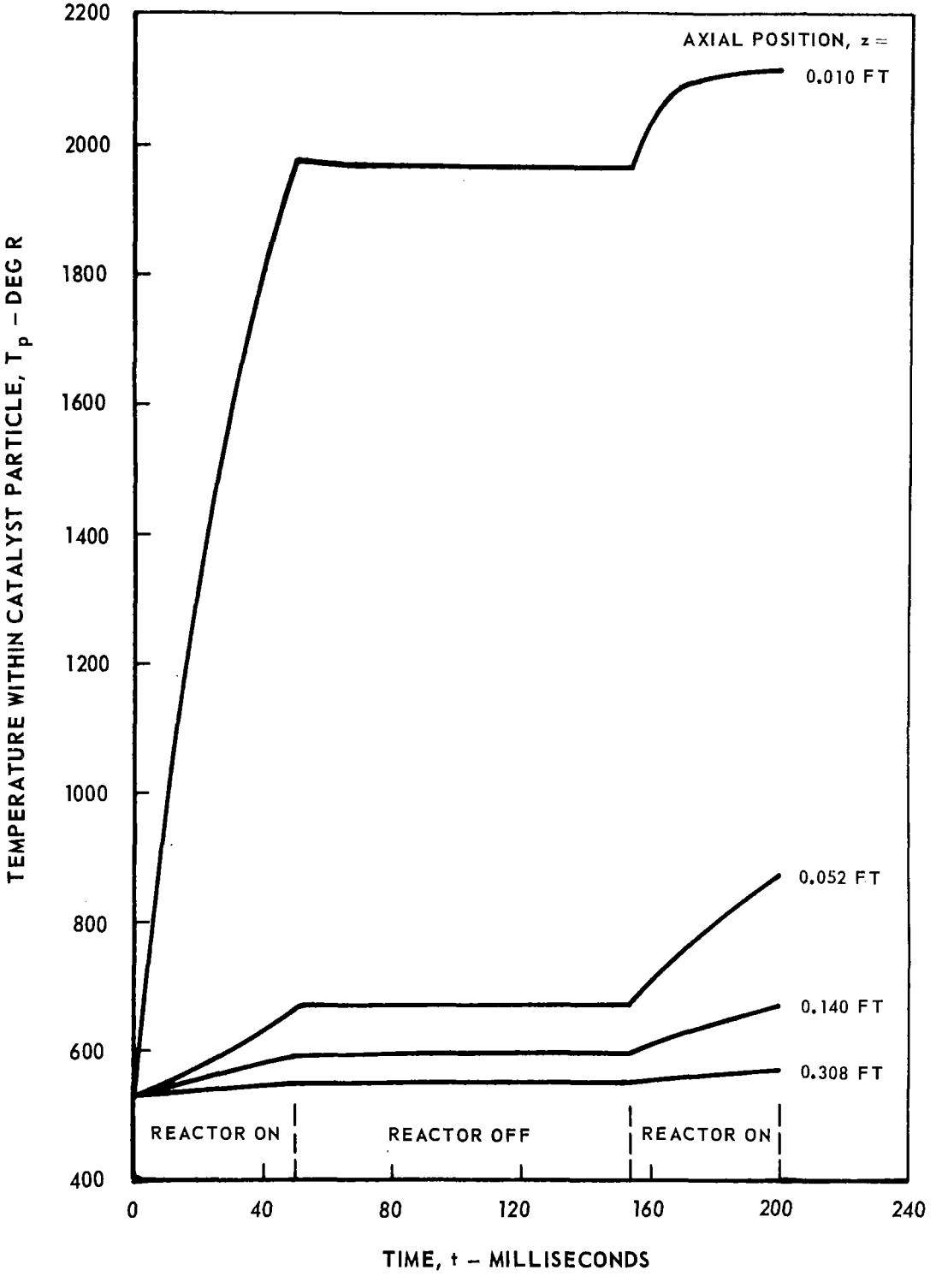

FIG. 7

VARIATION OF CHAMBER PRESSURE WITH TIME

STEADY-STATE CHAMBER PRESSURE = 260 PSIA STEADY-STATE MASS FLOW RATE = 5.8 LB/FT^2 - SEC

CATALYST BED CONFIGURATION: MIXED BED # 1 (SEE TEXT)

SEE TEXT FOR ADDITIONAL REACTOR PARAMETERS

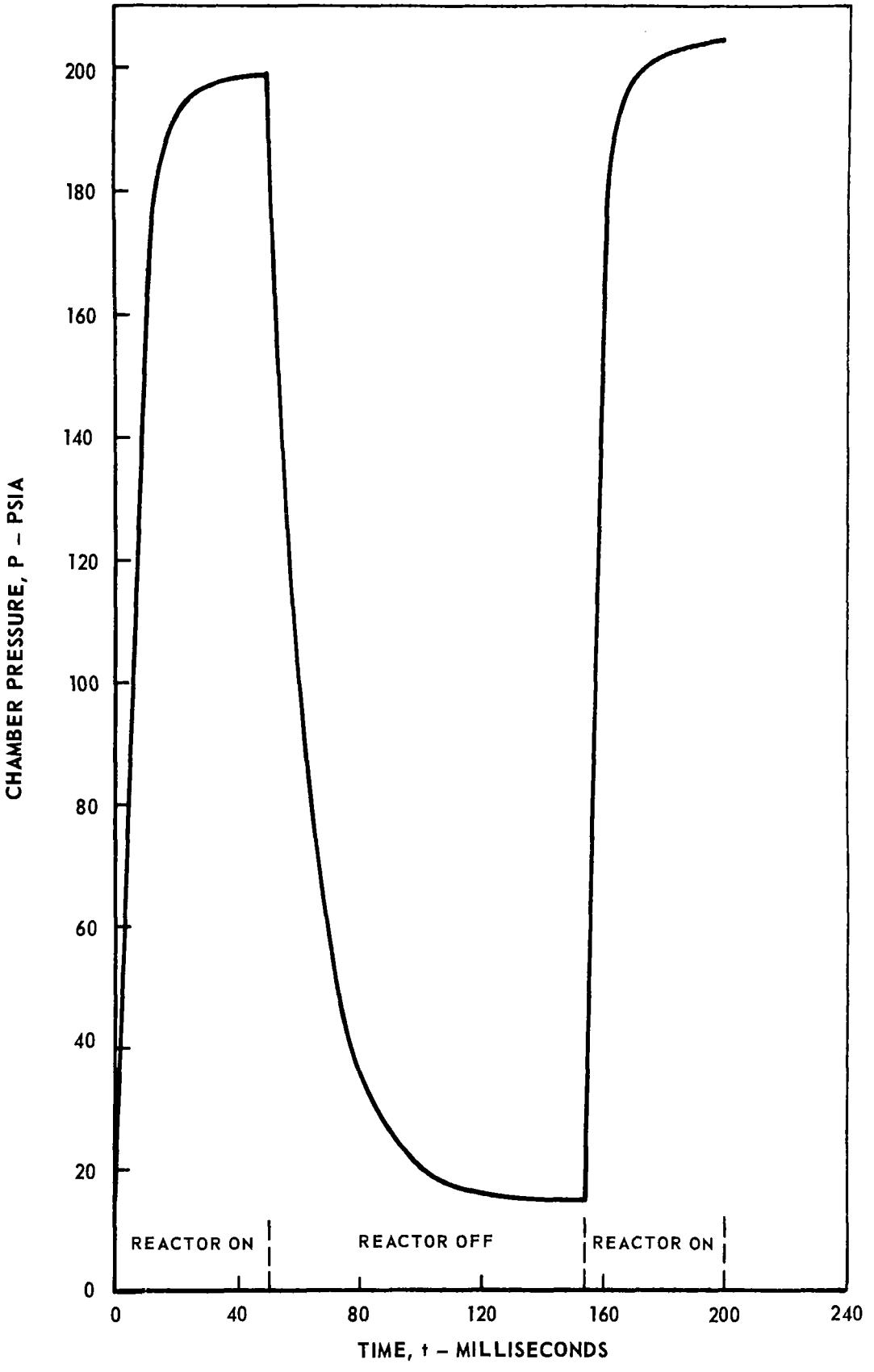

VARIATION OF MOLE-FRACTION OF HYDRAZINE WITH TIME AT VARIOUS AXIAL POSITIONS

STEADY-STATE CHAMBER PRESSURE = 260 PSIA
STEADY-STATE MASS FLOW RATE = 5.8 LB/FT^2 - SEC
CATALYST BED CONFIGURATION: MIXED BED # 1 (SEE TEXT)
SEE TEXT FOR ADDITIONAL REACTOR PARAMETERS

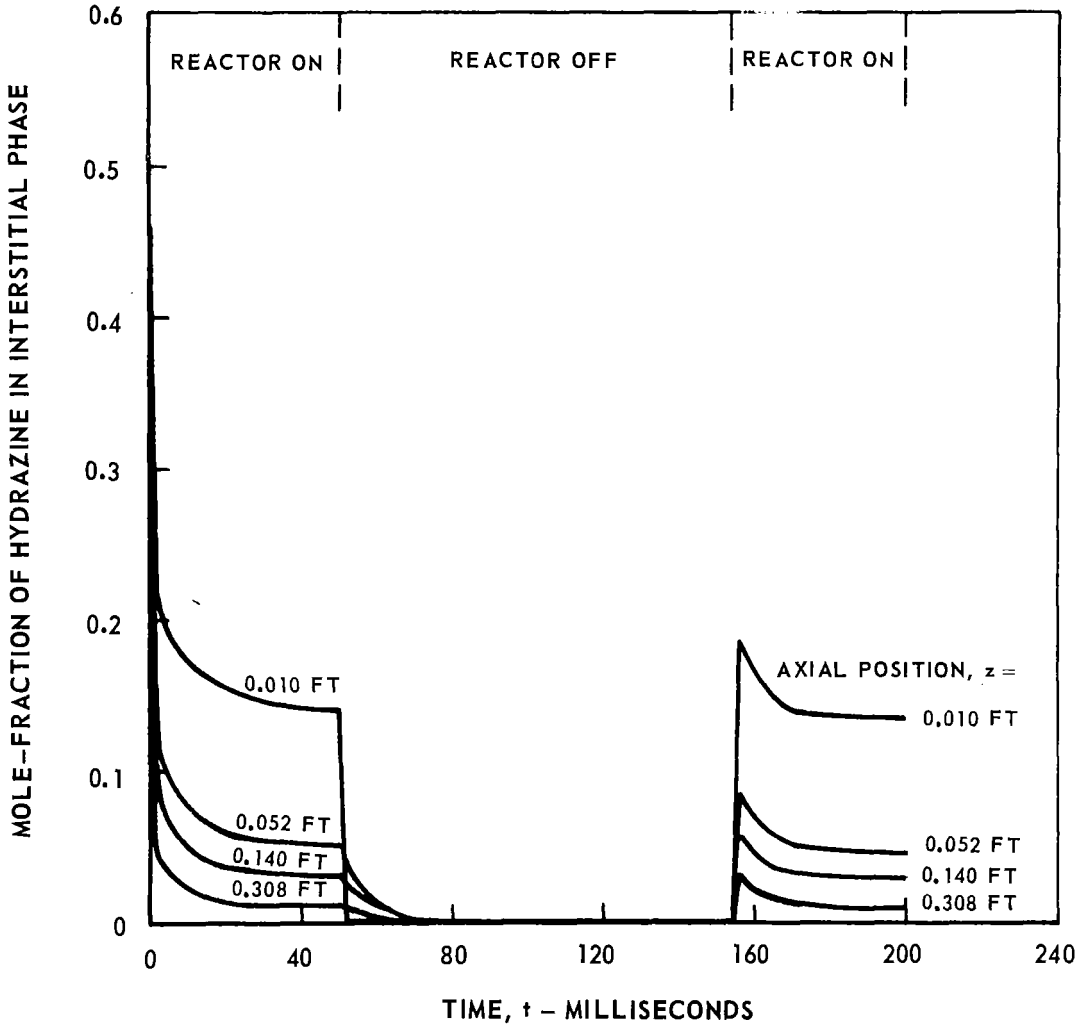

VARIATION OF MOLE-FRACTION OF AMMONIA WITH TIME AT VARIOUS AXIAL POSITIONS

STEADY-STATE CHAMBER PRESSURE = 260 PSIA

STEADY-STATE MASS FLOW RATE = 5.8 LB/FT^2 - SEC

CATALYST BED CONFIGURATION: MIXED BED # 1 (SEE TEXT)

SEE TEXT FOR ADDITIONAL REACTOR PARAMETERS

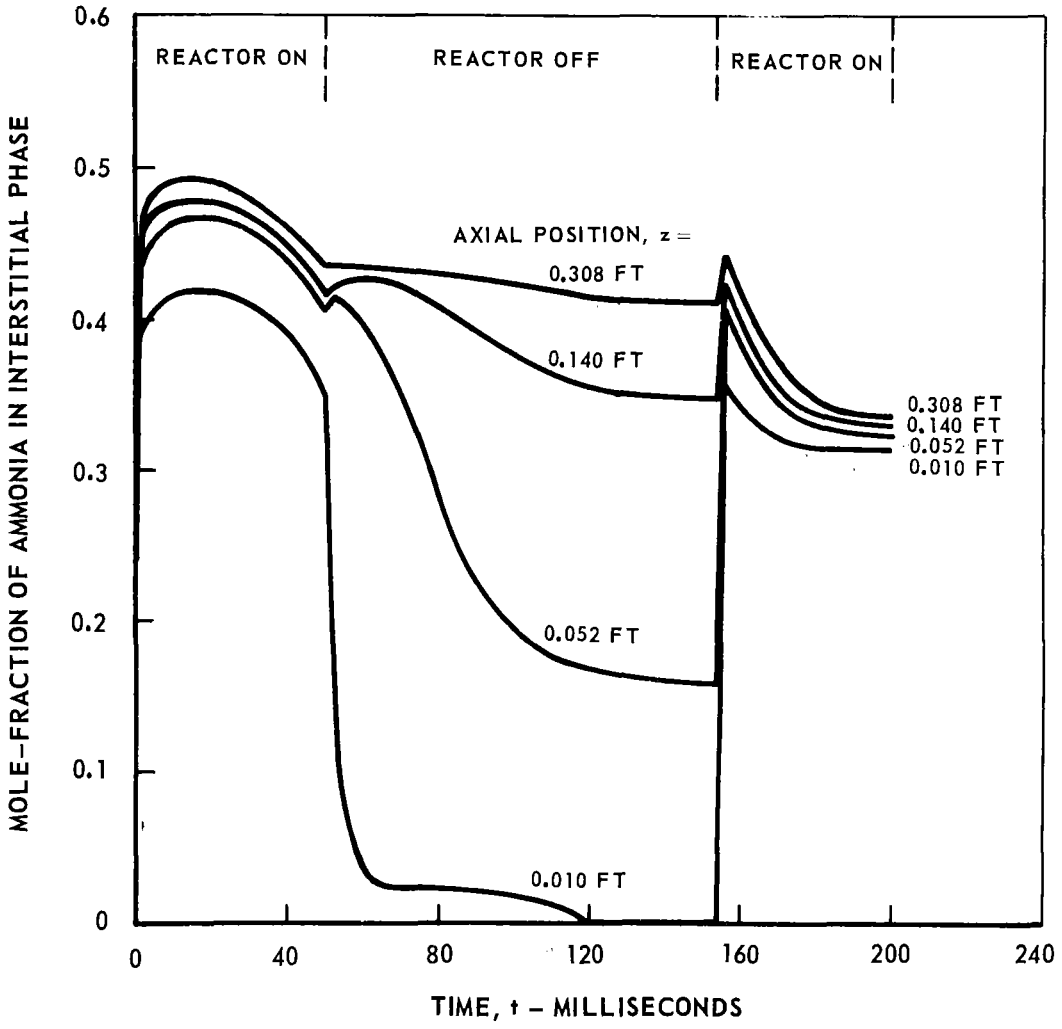

VARIATION OF MOLE-FRACTION OF NITROGEN WITH TIME AT VARIOUS AXIAL POSITIONS

STEADY-STATE CHAMBER PRESSURE = 260 PSIA
STEADY-STATE MASS FLOW RATE = 5.8 LB/FT^2 - SEC
CATALYST BED CONFIGURATION: MIXED BED # 1 (SEE TEXT)
SEE TEXT FOR ADDITIONAL REACTOR PARAMETERS

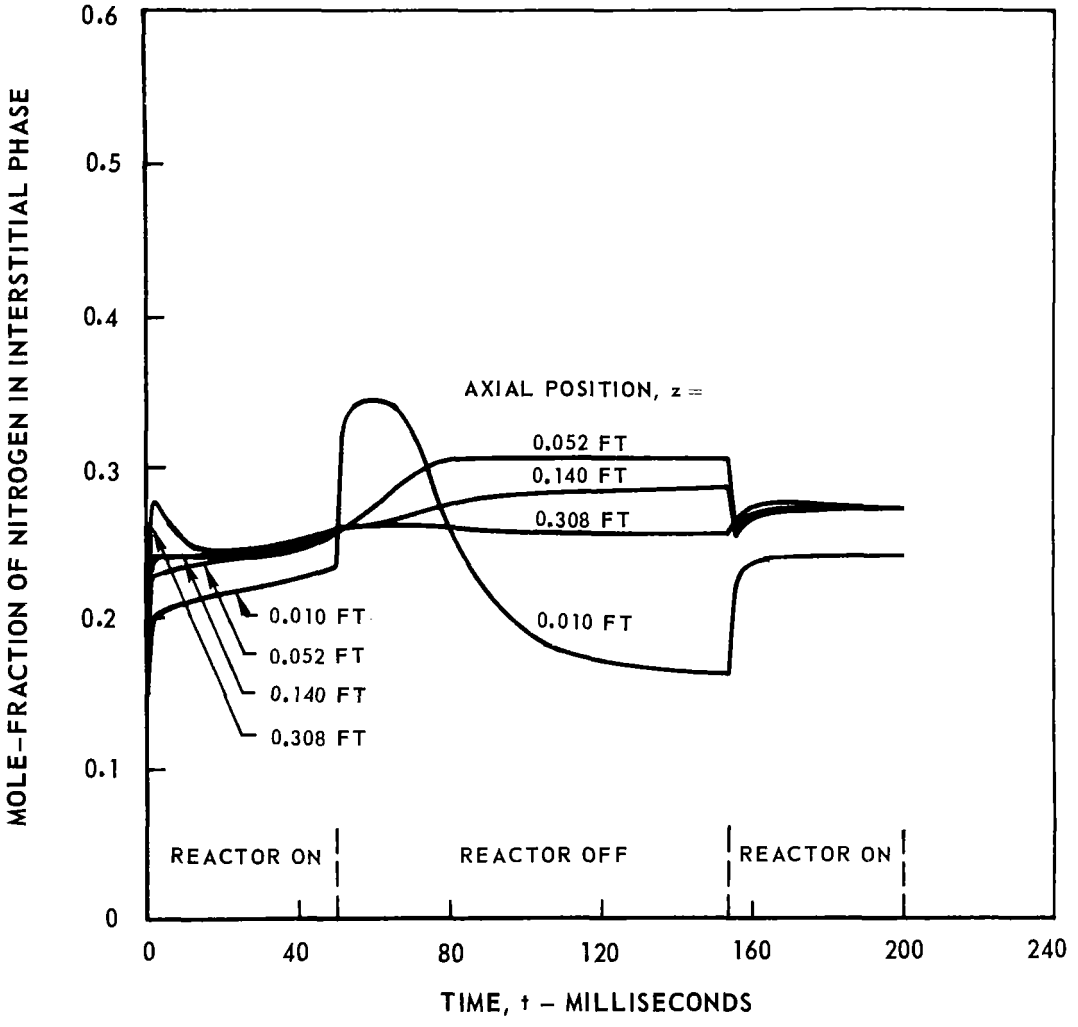

VARIATION OF MOLE-FRACTION OF HYDROGEN WITH TIME AT VARIOUS AXIAL POSITIONS

STEADY-STATE CHAMBER PRESSURE = 260 PSIA
STEADY-STATE MASS FLOW RATE = 5.8 LB/FT^2 - SEC
CATALYST BED CONFIGURATION: MIXED BED # 1 (SEE TEXT)
SEE TEXT FOR ADDITIONAL REACTOR PARAMETERS

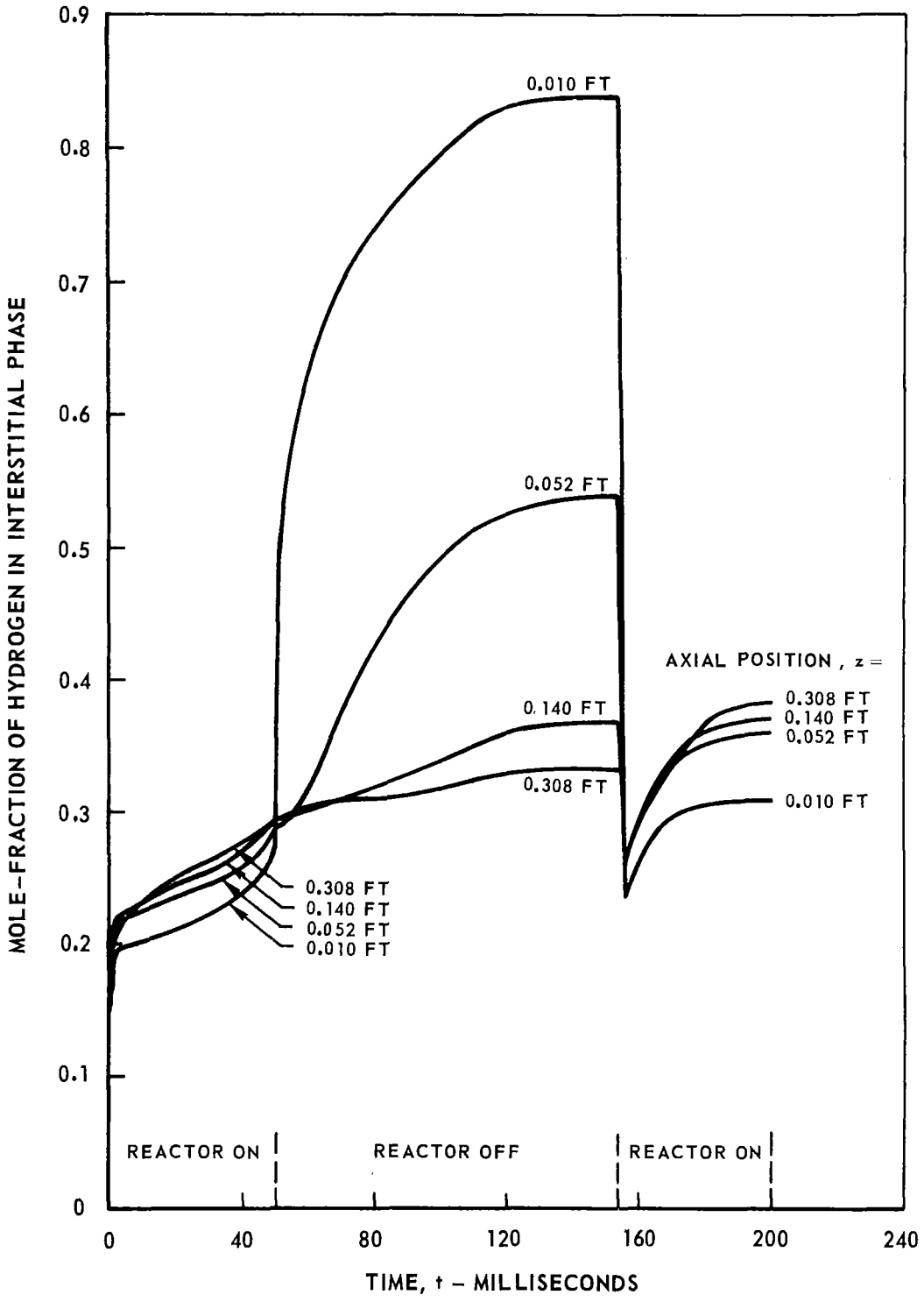

FIG. 12

TRANSIENT INTERSTITIAL TEMPERATURE PROFILES FOR THE REFERENCE OPERATING CONDITIONS

INJECTOR PRESSURE = 150 PSIA

STEADY-STATE MASS FLOW RATE = 5.76 LB/FT^2 – SEC

CATALYST BED CONFIGURATION: MIXED BED # 2 (SEE TEXT)

SEE TEXT FOR ADDITIONAL REACTOR PARAMETERS

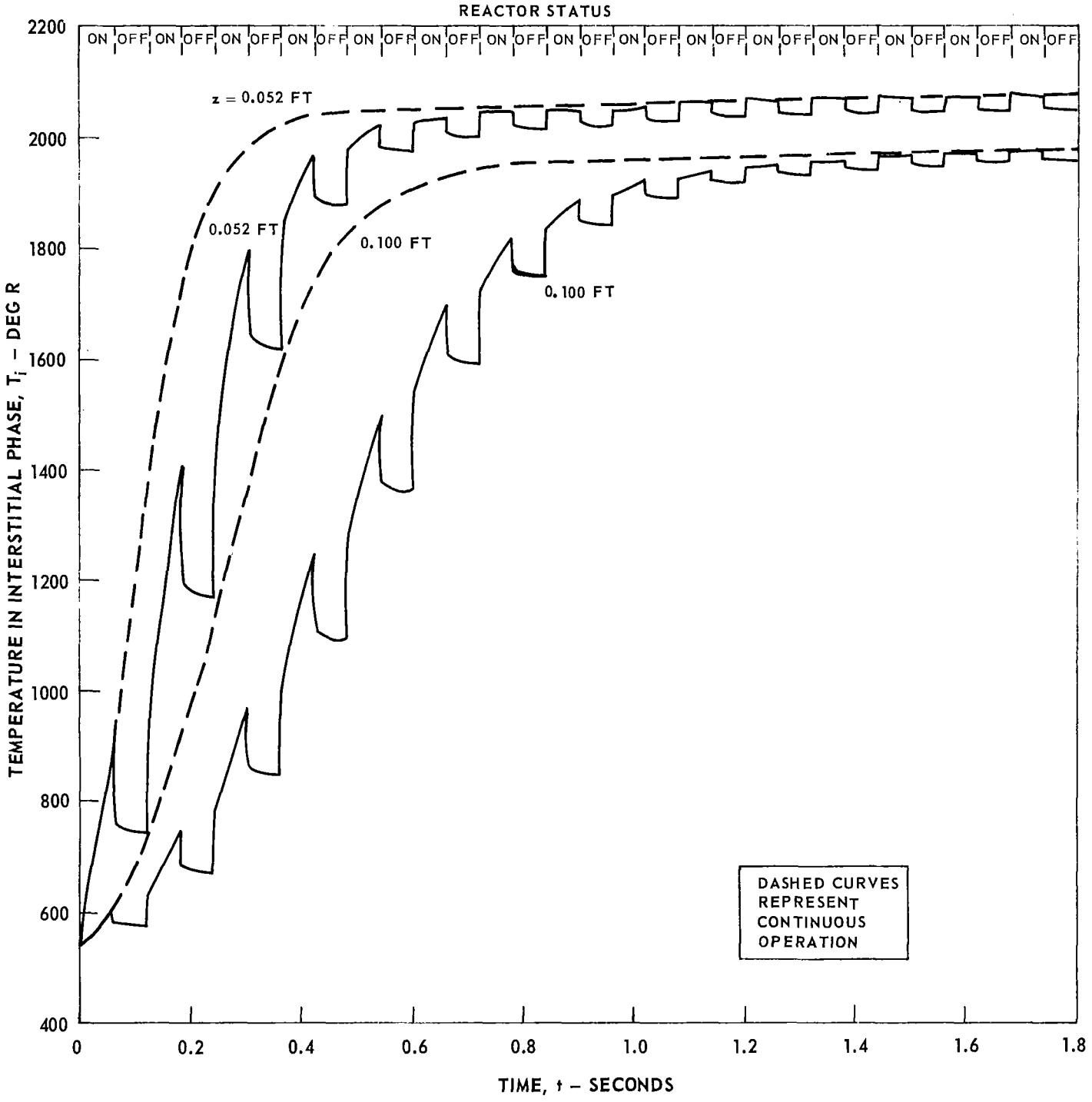

TRANSIENT PARTICLE TEMPERATURE PROFILES FOR THE REFERENCE OPERATING CONDITIONS

INJECTOR PRESSURE = 150 PSIA
STEADY-STATE MASS FLOW RATE = 5.76 LB/FT^2 - SEC
CATALYST BED CONFIGURATION: MIXED BED # 2 (SEE TEXT)
SEE TEXT FOR ADDITIONAL REACTOR PARAMETERS

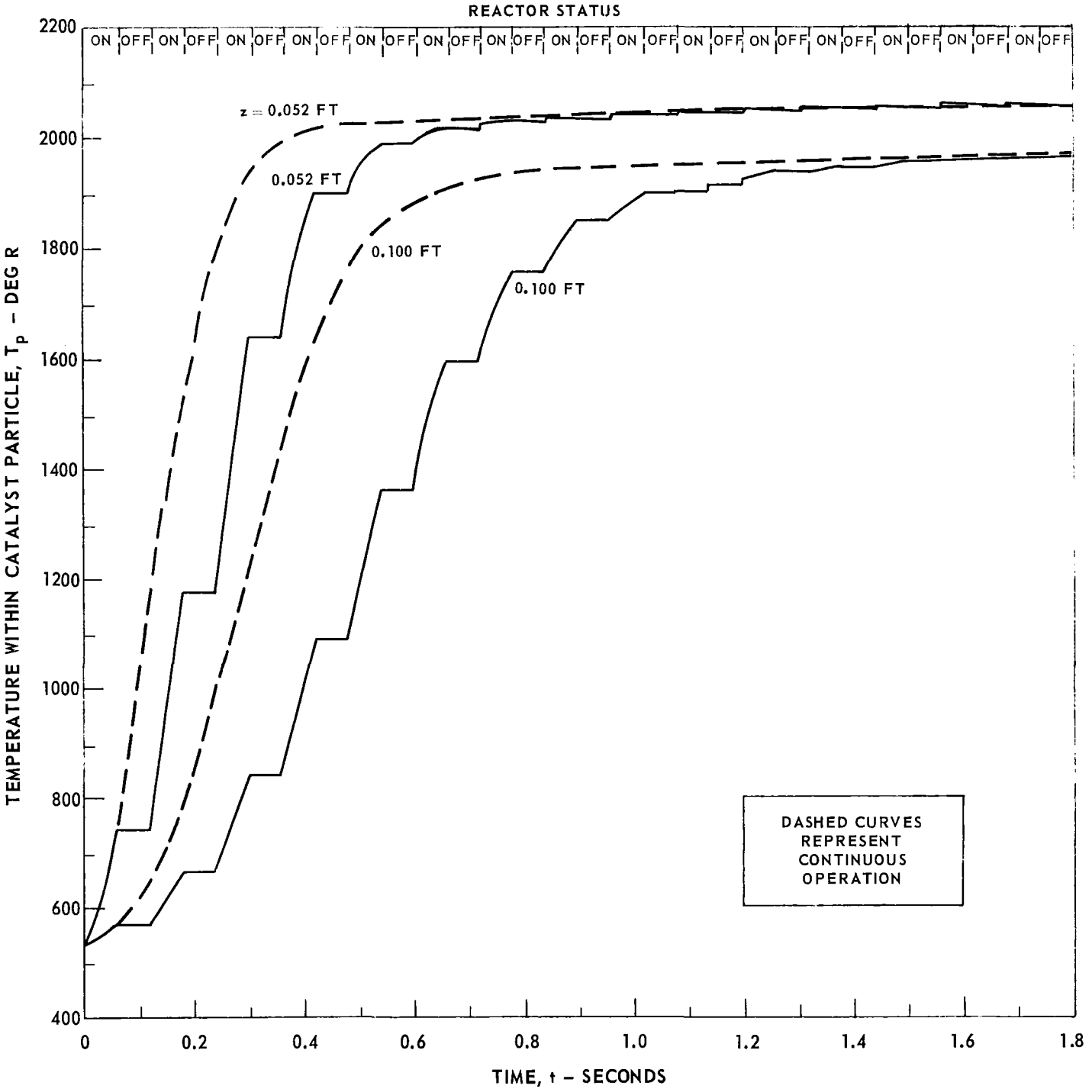

TRANSIENT CHAMBER PRESSURE PROFILE FOR THE REFERENCE OPERATING CONDITIONS

INJECTOR PRESSURE = 150 PSIA

STEADY-STATE MASS FLOW RATE = 5.76 LB/FT^2 - SEC

CATALYST BED CONFIGURATION: MIXED BED # 2 (SEE TEXT)

SEE TEXT FOR ADDITIONAL REACTOR PARAMETERS

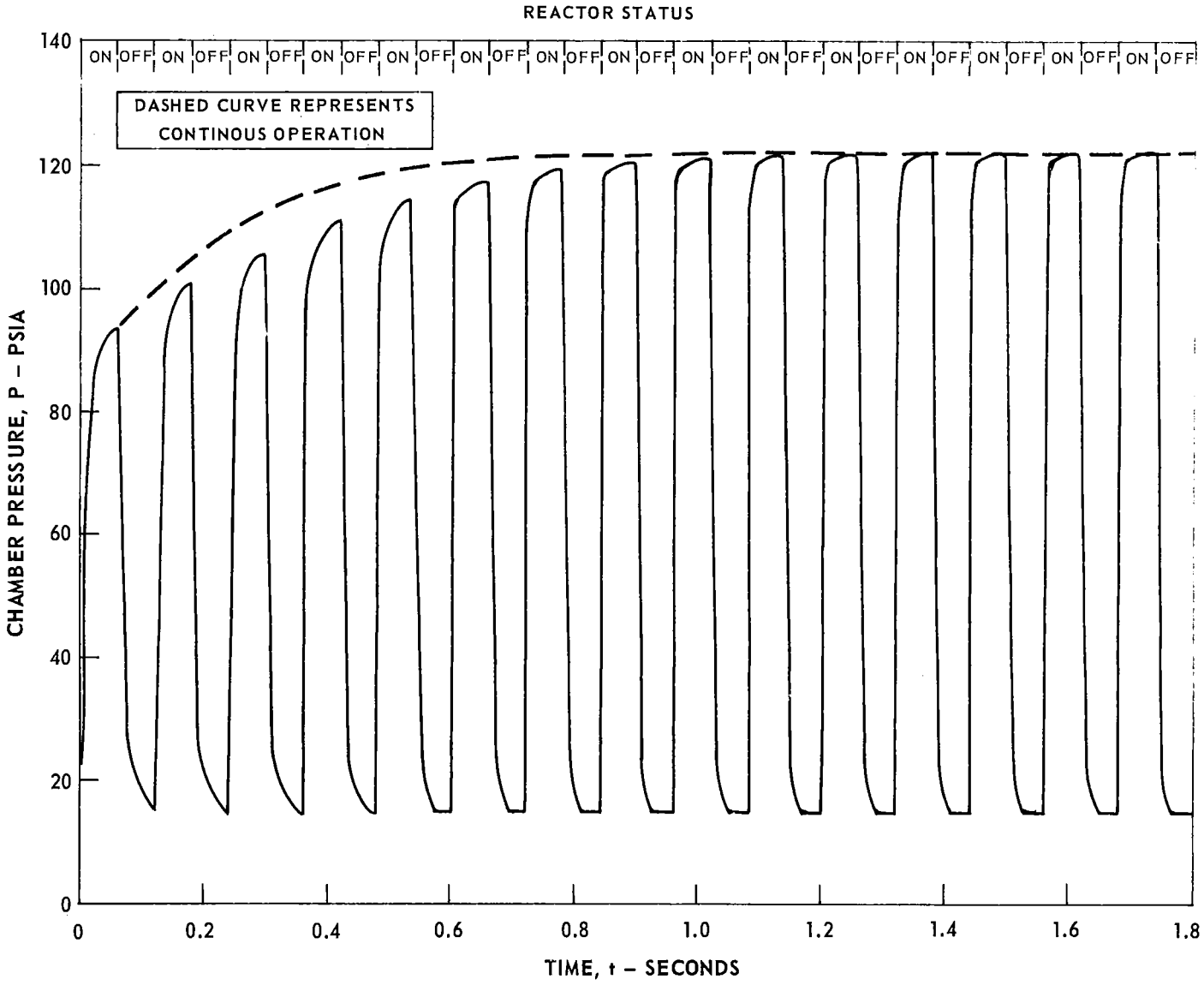

FIG. 15

TRANSIENT PROFILE OF MOLE-FRACTION OF HYDRAZINE FOR THE REFERENCE OPERATING CONDITIONS

INJECTOR PRESSURE = 150 PSIA

STEADY-STATE MASS FLOW RATE = 5.76 LB/FT^2 - SEC

CATALYST BED CONFIGURATION: MIXED BED # 2 (SEE TEXT)

SEE TEXT FOR ADDITIONAL REACTOR PARAMETERS

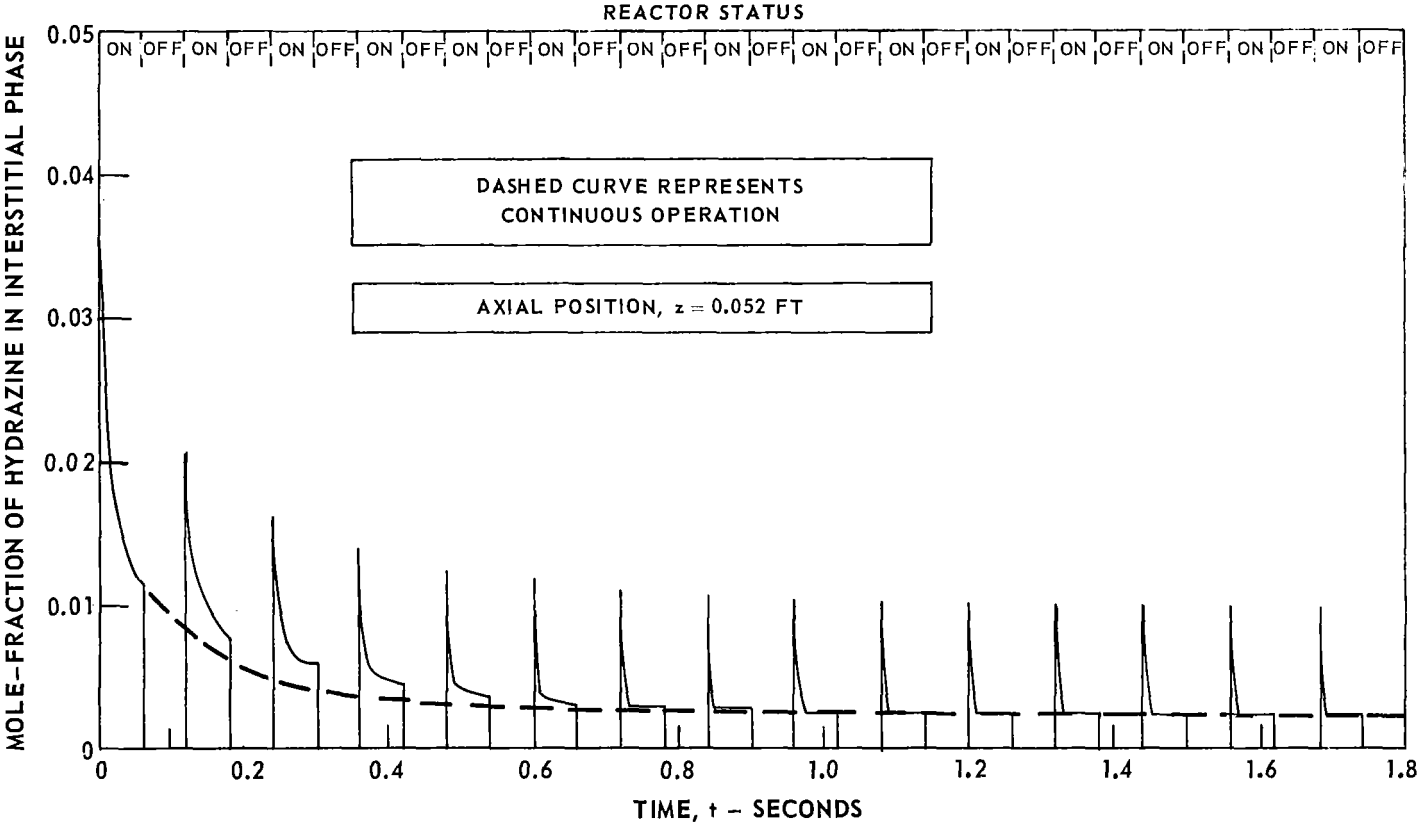

TRANSIENT PROFILE OF MOLE-FRACTION OF HYDRAZINE FOR THE REFERENCE OPERATING CONDITIONS

INJECTOR PRESSURE = 150 PSIA
STEADY-STATE MASS FLOW RATE = 5.76 LB/FT^2 - SEC
CATALYST BED CONFIGURATION: MIXED BED # 2 (SEE TEXT)
SEE TEXT FOR ADDITIONAL REACTOR PARAMETERS

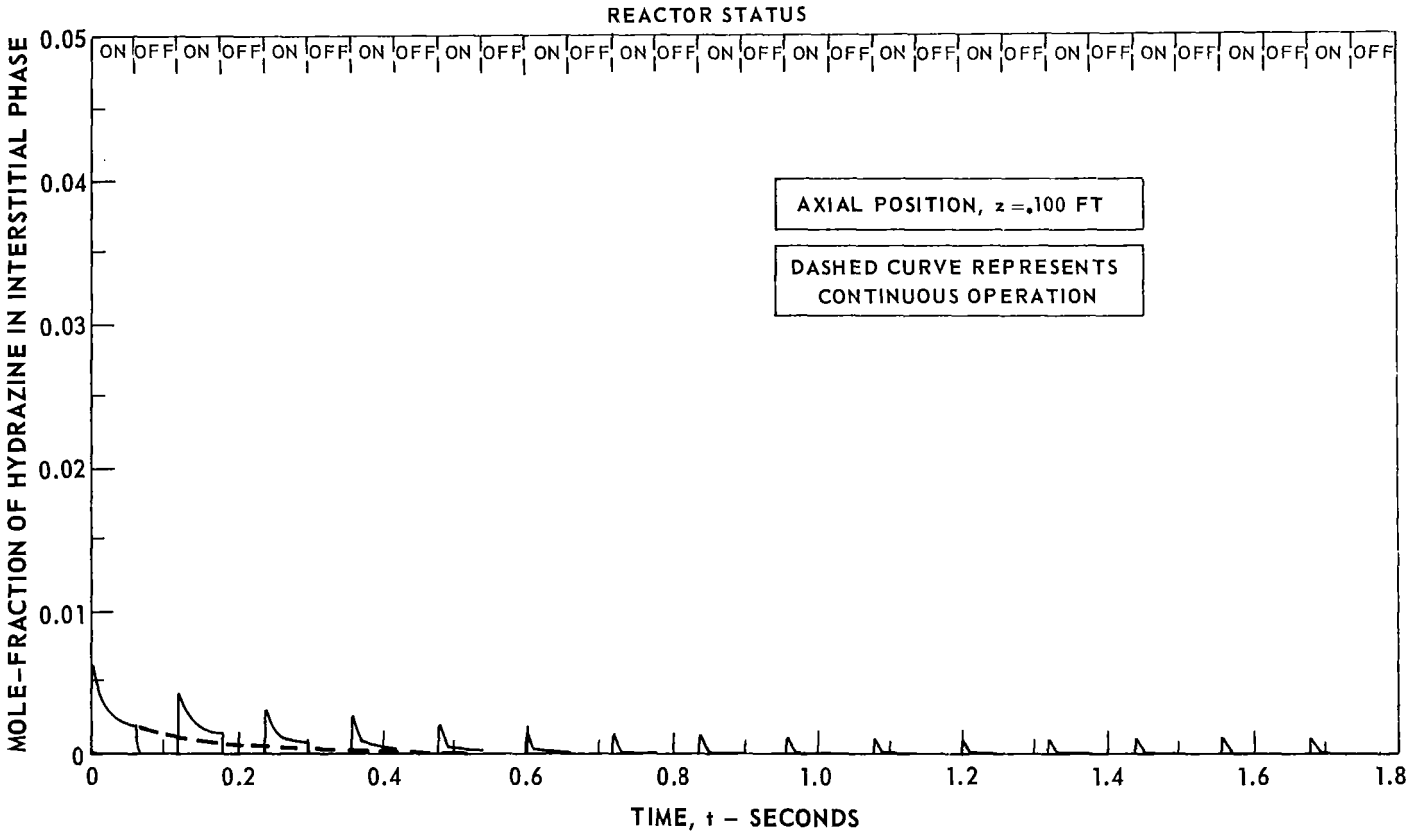

TRANSIENT PROFILE OF MOLE-FRACTION OF AMMONIA FOR THE REFERENCE OPERATING CONDITIONS

INJECTOR PRESSURE = 150 PSIA

STEADY-STATE MASS FLOW RATE = 5.76 LB/FT^2 - SEC

CATALYST BED CONFIGURATION : MIXED BED # 2 (SEE TEXT)

SEE TEXT FOR ADDITIONAL REACTOR PARAMETERS

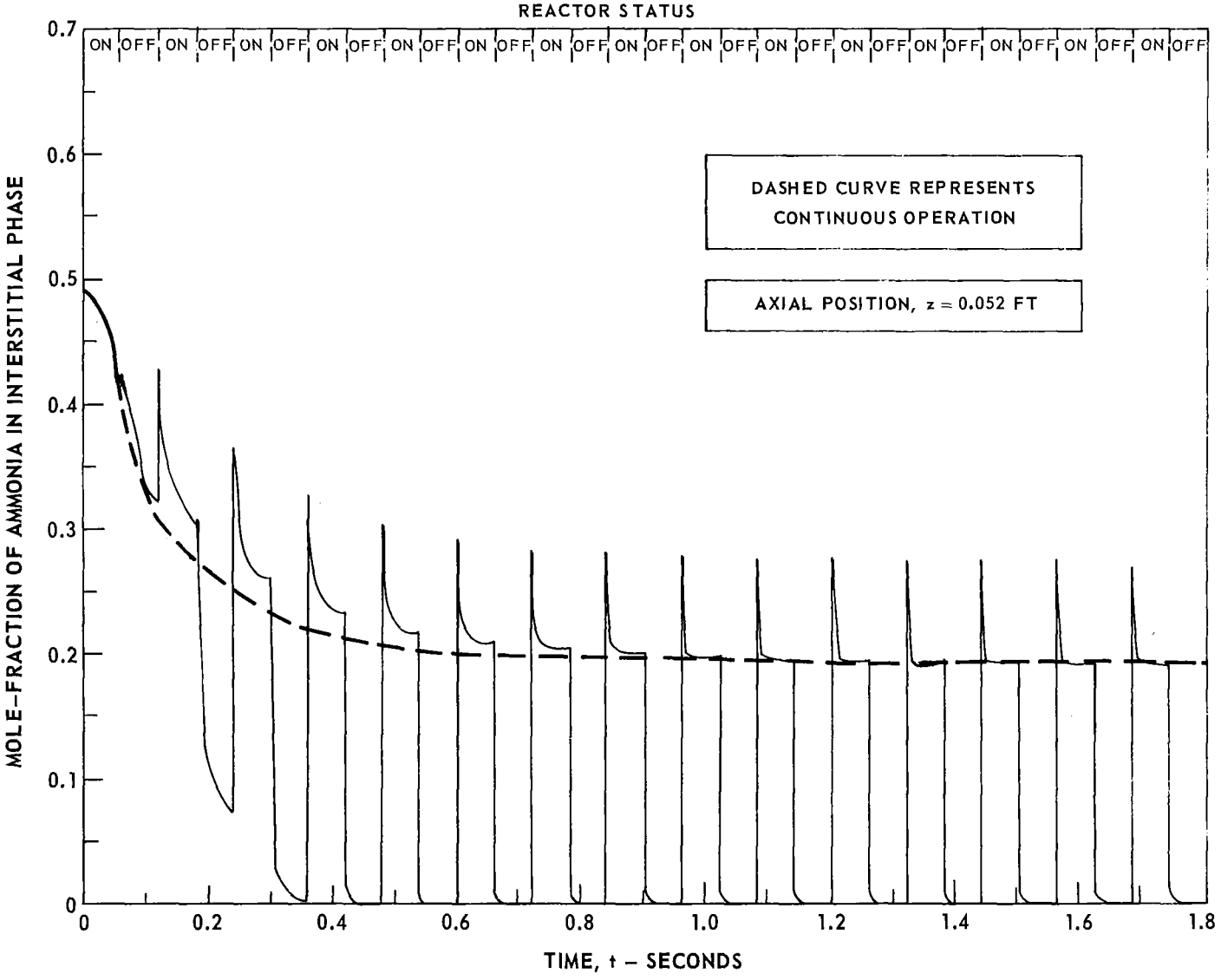

TRANSIENT PROFILE OF MOLE-FRACTION OF AMMONIA FOR THE REFERENCE OPERATING CONDITIONS

INJECTOR PRESSURE = 150 PSIA

STEADY-STATE MASS FLOW RATE = 5.76 LB/FT^2 - SEC

CATALYST BED CONFIGURATION: MIXED BED # 2 (SEE TEXT)

SEE TEXT FOR ADDITIONAL REACTOR PARAMETERS

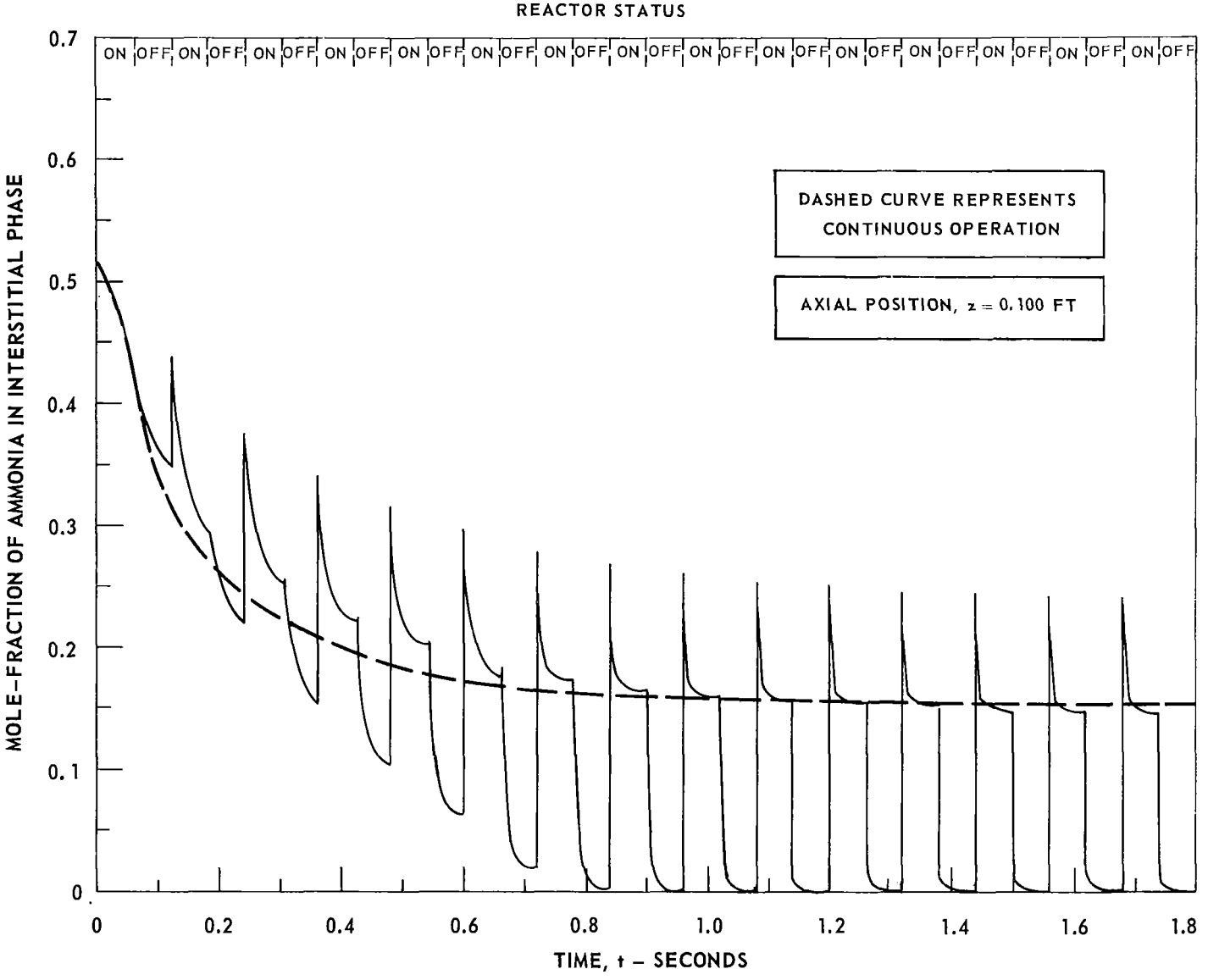

TRANSIENT PROFILE OF MOLE-FRACTION OF NITROGEN FOR THE REFERENCE OPERATING CONDITIONS

INJECTOR PRESSURE = 150 PSIA

STEADY-STATE MASS FLOW RATE = 5.76 LB/FT^2 - SEC

CATALYST BED CONFIGURATION: MIXED BED # 2 (SEE TEXT)

SEE TEXT FOR ADDITIONAL REACTOR PARAMETERS

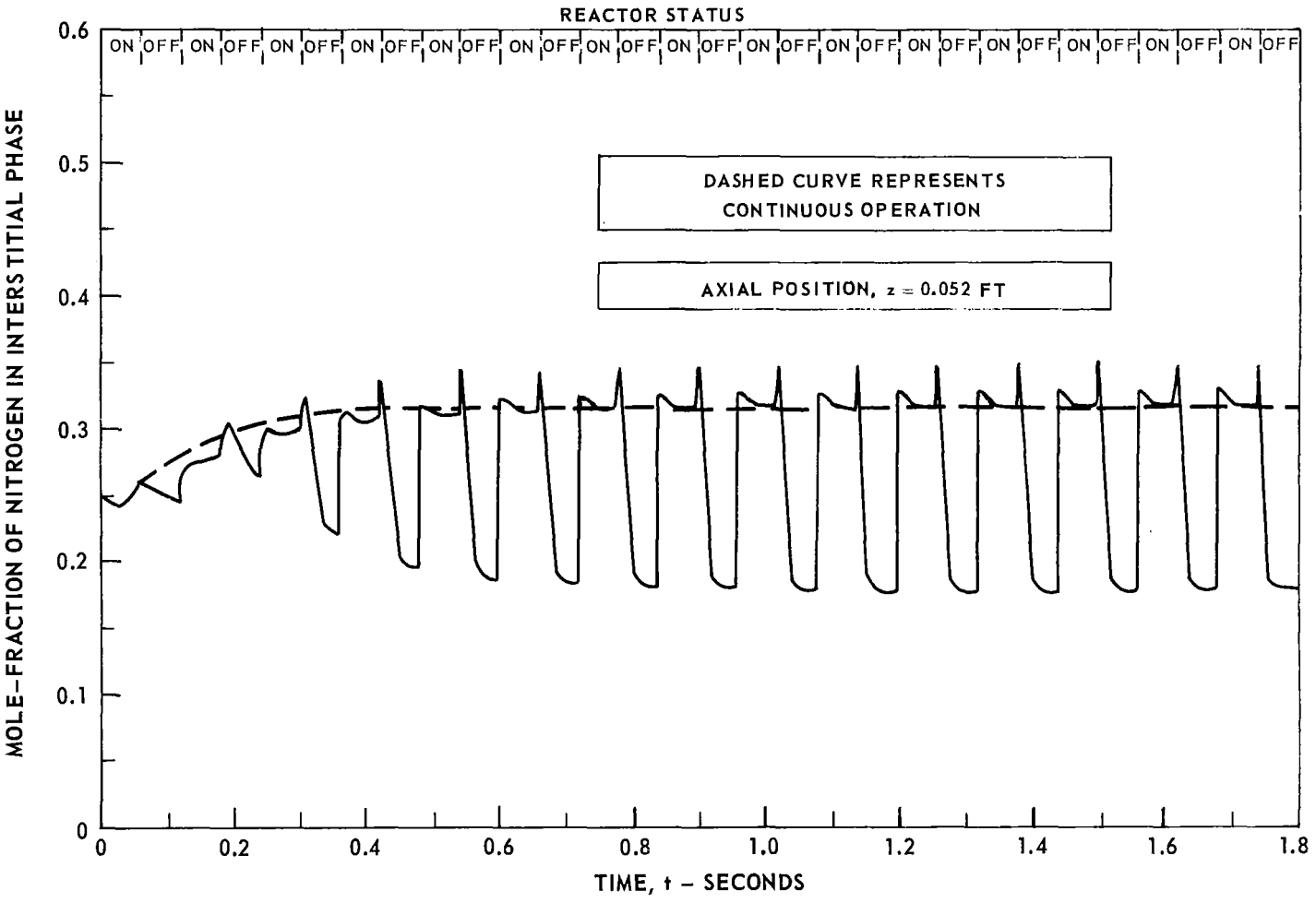

FIG. 20

TRANSIENT PROFILE OF MOLE-FRACTION OF NITROGEN FOR THE REFERENCE OPERATING CONDITIONS

INJECTOR PRESSURE = 150 PSIA

STEADY-STATE MASS FLOW RATE = 5.76 LB/FT^2 - SEC

CATALYST BED CONFIGURATION: MIXED BED # 2 (SEE TEXT)

SEE TEXT FOR ADDTIONAL REACTOR PARAMETERS

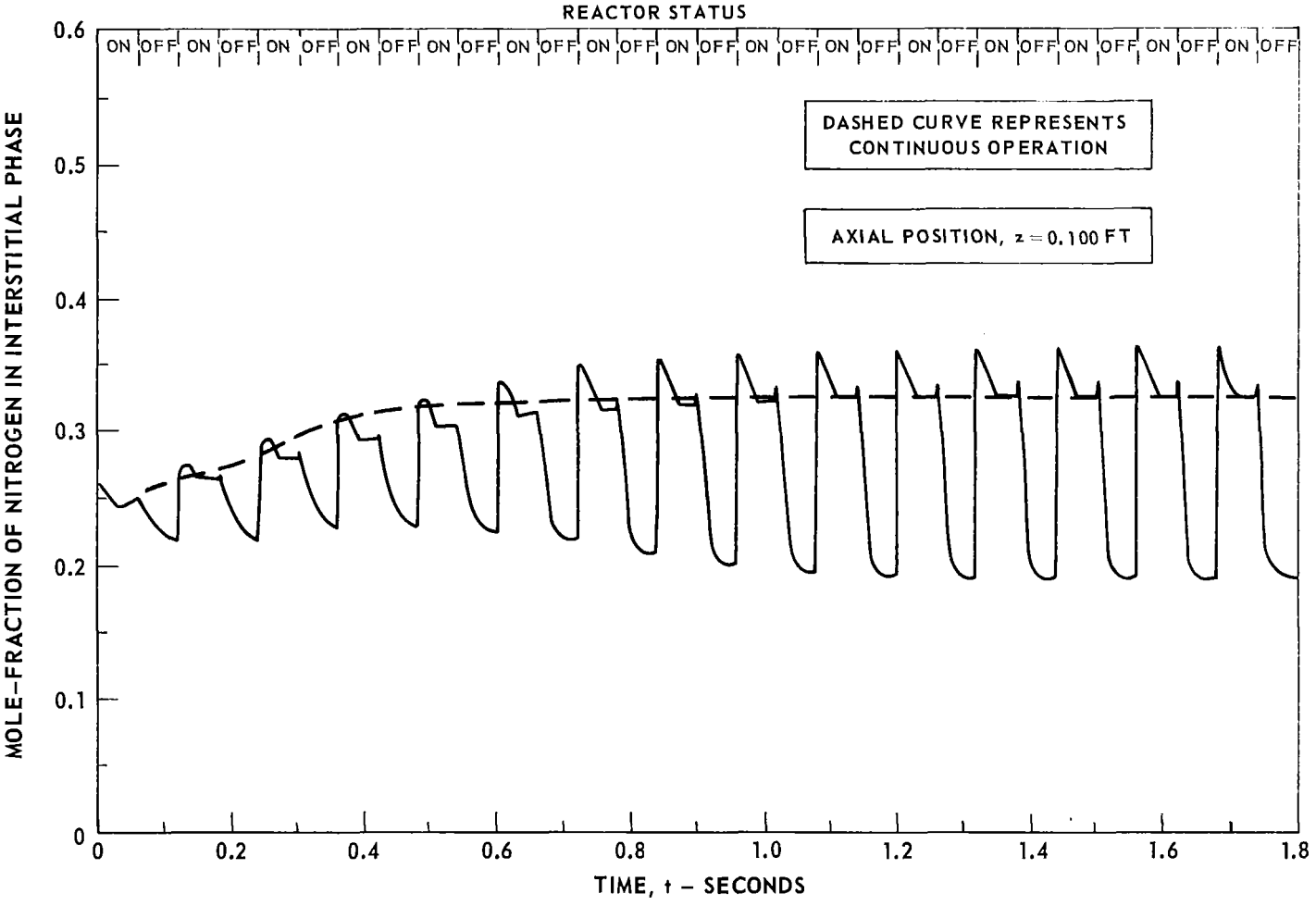

TRANSIENT PROFILE OF MOLE-FRACTION OF HYDROGEN FOR THE REFERENCE OPERATING CONDITIONS

INJECTOR PRESSURE = 150 PSIA

STEADY-STATE MASS FLOW RATE = 5.76 LB/FT^2 – SEC

CATALYST BED CONFIGURATION: MIXED BED # 2 (SEE TEXT)

SEE TEXT FOR ADDITIONAL REACTOR PARAMETERS

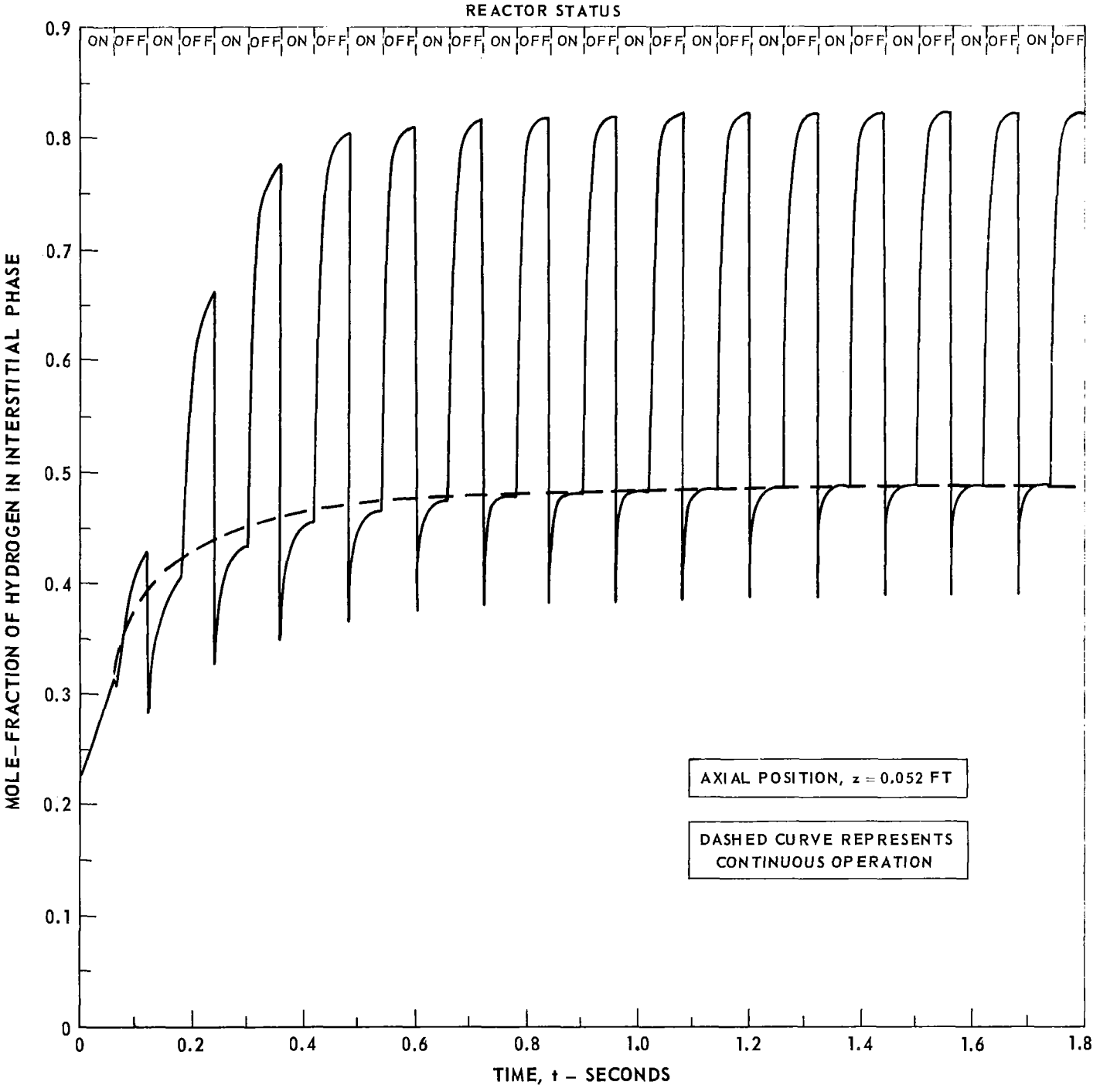

FIG. 22

TRANSIENT PROFILE OF MOLE-FRACTION OF HYDROGEN FOR THE REFERENCE OPERATING CONDITIONS

INJECTOR PRESSURE = 150 PSIA

STEADY-STATE MASS FLOW RATE = 5.76 LB/FT^2 -SEC

CATALYST BED CONFIGURATION: MIXED BED # 2 (SEE TEXT)

SEE TEXT FOR ADDITIONAL REACTOR PARAMETERS

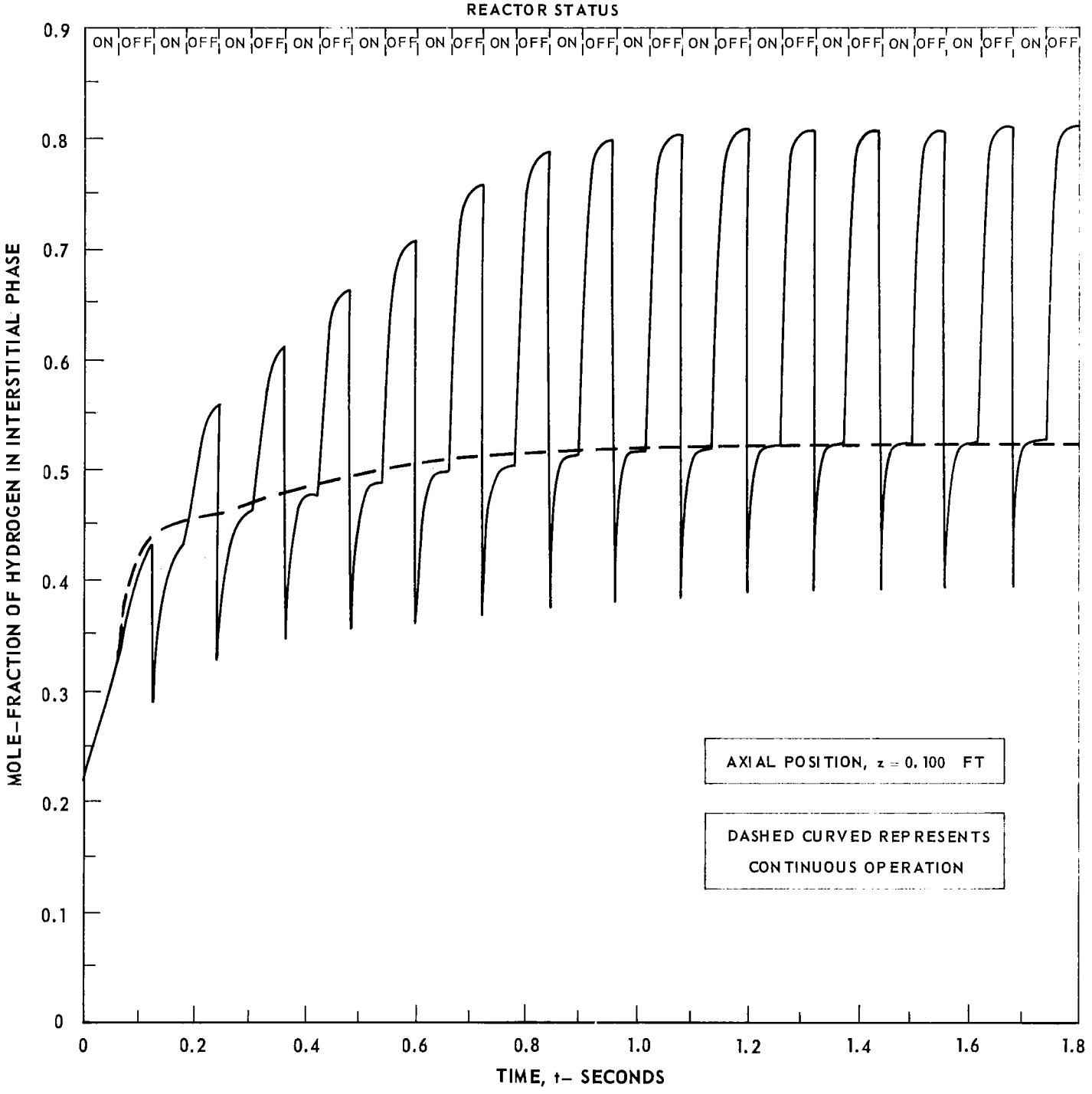

FIG. 23

TRANSIENT INTERSTITIAL TEMPERATURE PROFILES FOR AN INJECTOR PRESSURE OF 500 PSIA

STEADY-STATE MASS FLOW RATE = 5.76 LB/FT^2 -SEC

CATALYST BED CONFIGURATION: MIXED BED # 2 (SEE TEXT)

SEE TEXT FOR FOR ADDITIONAL REACTOR PARAMETERS

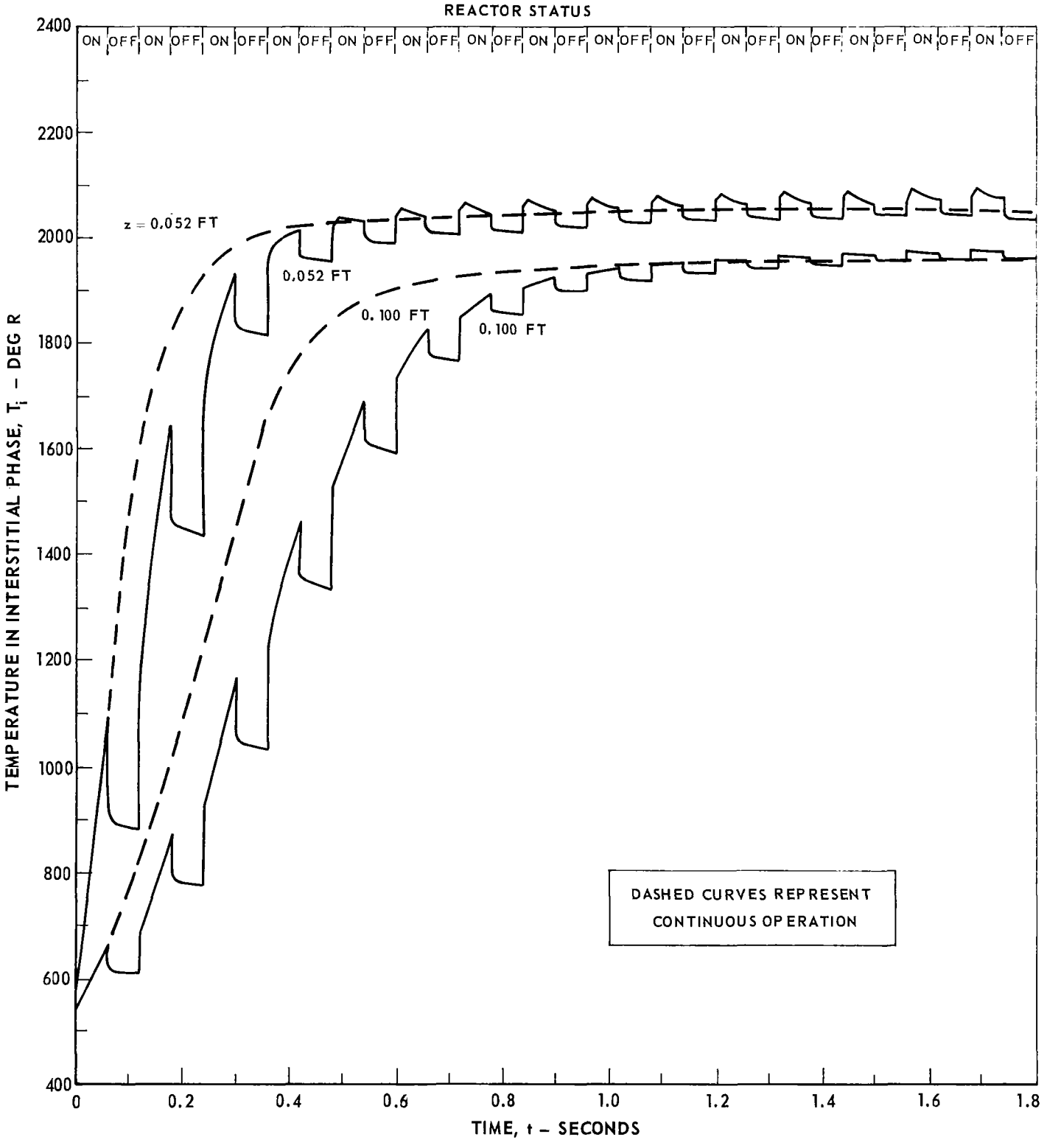

FIG. 24

COMPARISON OF TRANSIENT INTERSTITIAL TEMPERATURE PROFILES FOR TWO INJECTOR PRESSURES IN A CONTINUOUS FLOW SYSTEM

STEADY-STATE MASS FLOW RATE = 5.76 LB/FT^2 - SEC

CATALYST BED CONFIGURATION: MIXED BED # 2 (SEE TEXT)

SEE TEXT FOR ADDTITIONAL REACTOR PARAMETERS

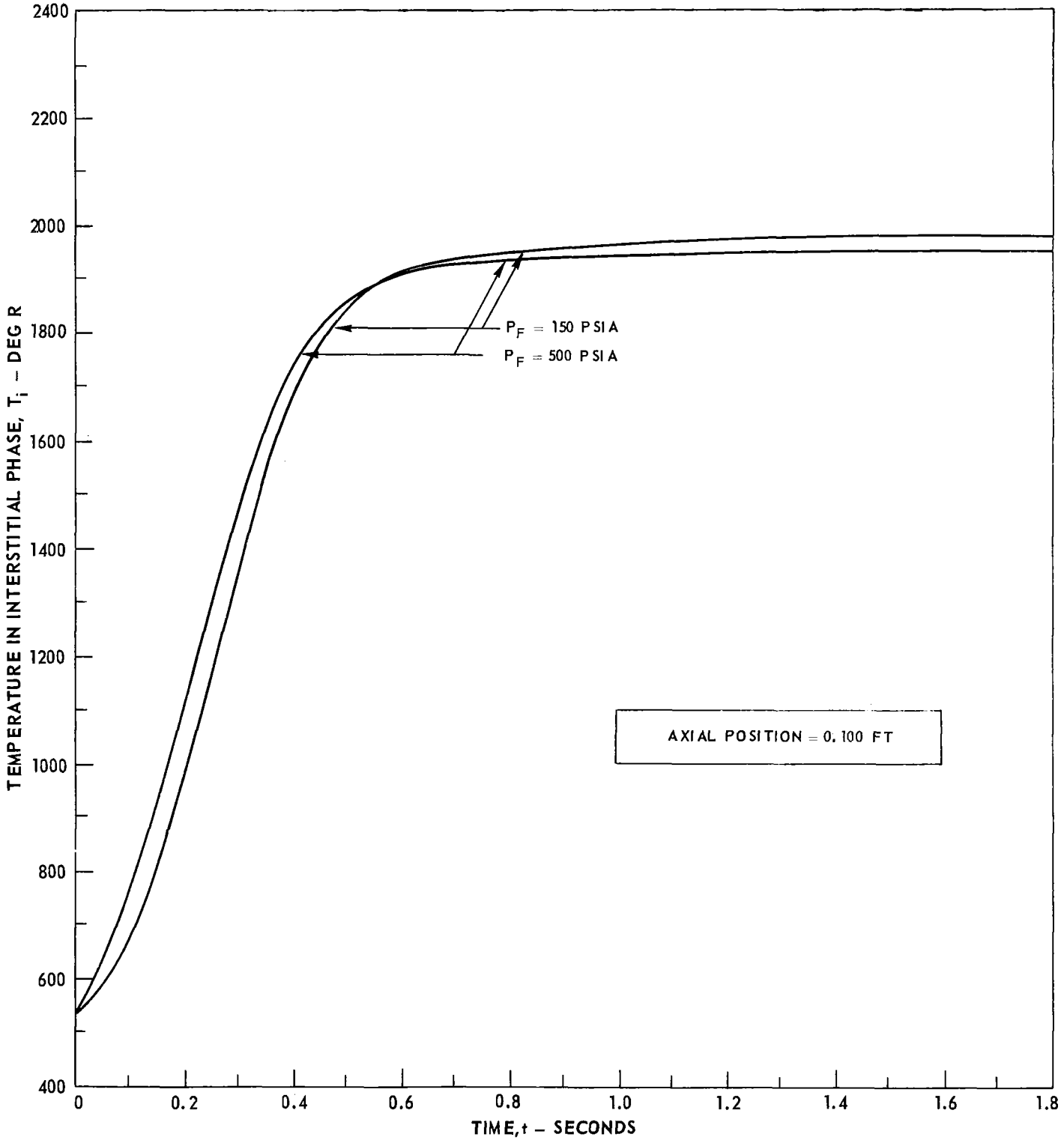

TRANSIENT INTERSTITIAL TEMPERATURE PROFILES FOR A STEADY-STATE MASS FLOW RATE OF 1.44 LB/FT^2 - SEC

INJECTOR PRESSURE = 150 PSIA
CATALYST BED CONFIGURATION: MIXED BED # 2 (SEE TEXT)
SEE TEXT FOR ADDITIONAL REACTOR PARAMETERS

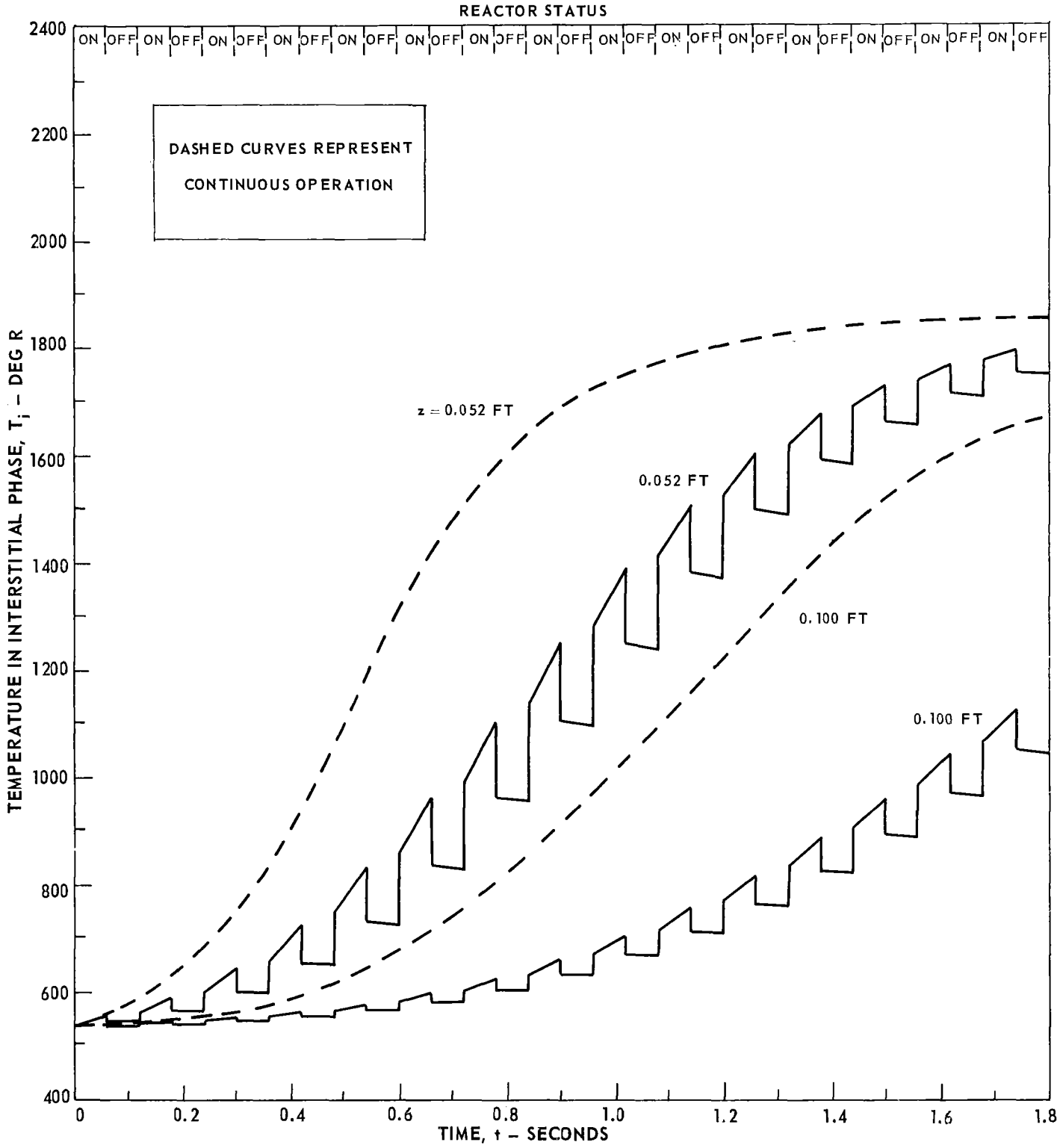

FIG. 26

TRANSIENT INTERSTITIAL TEMPERATURE PROFILES FOR A STEADY-STATE MASS FLOW RATE OF 14.4 LB/FT^2 - SEC

INJECTOR PRESSURE = 150 PSIA
CATALYST BED CONFIGURATION: MIXED BED # 2 (SEE TEXT)
SEE TEXT FOR ADDITIONAL REACTOR PARAMETERS

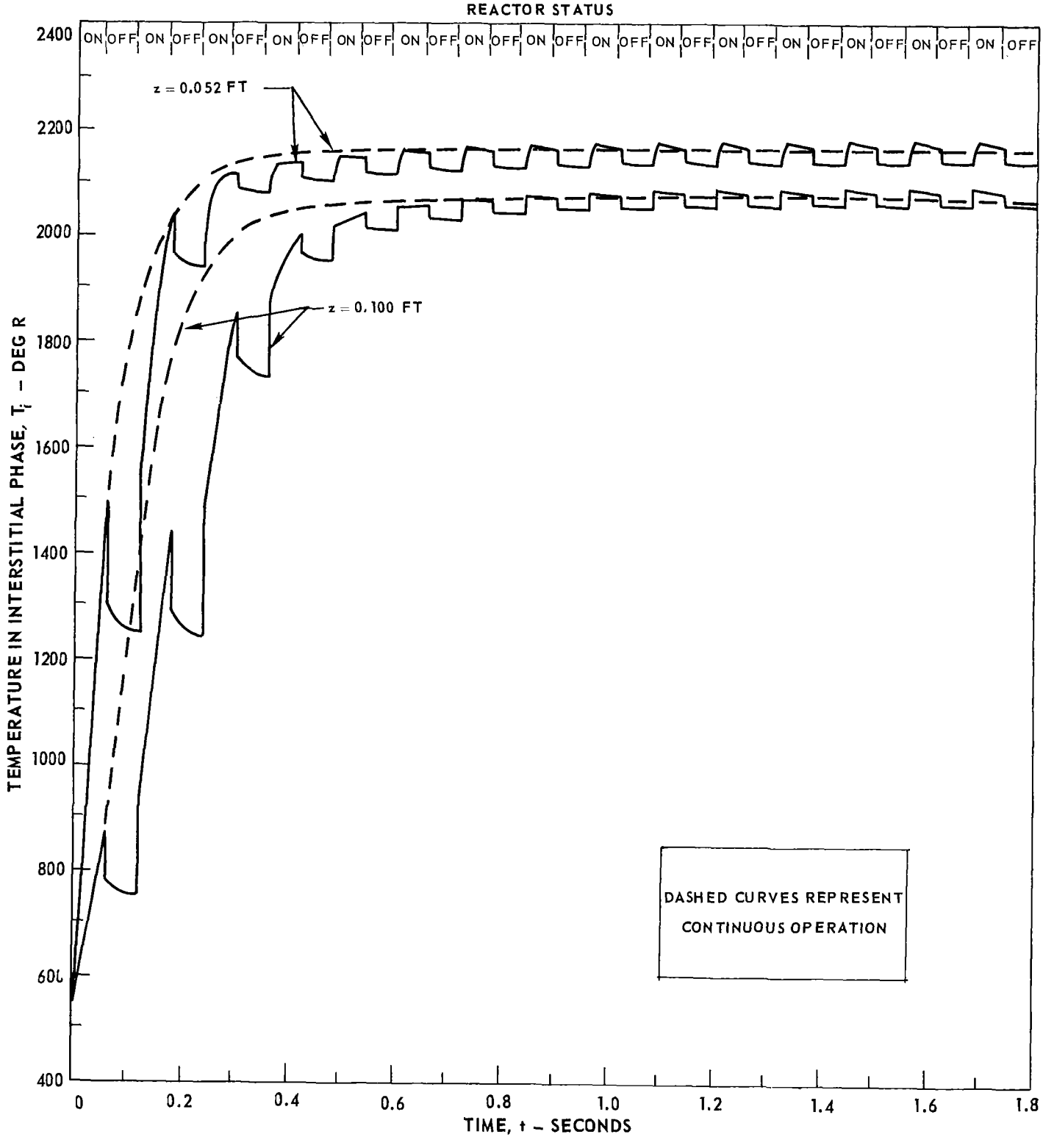

FIG. 27

COMPARISON OF TRANSIENT INTERSTITIAL TEMPERATURE PROFILES FOR VARIOUS STEADY-STATE MASS FLOW RATES IN A CONTINUOUS FLOW SYSTEM

INJECTOR PRESSURE = 150 PSIA

CATALYST BED CONFIGURATION: MIXED BED # 2 (SEE TEXT)

SEE TEXT FOR ADDITIONAL REACTOR PARAMETERS

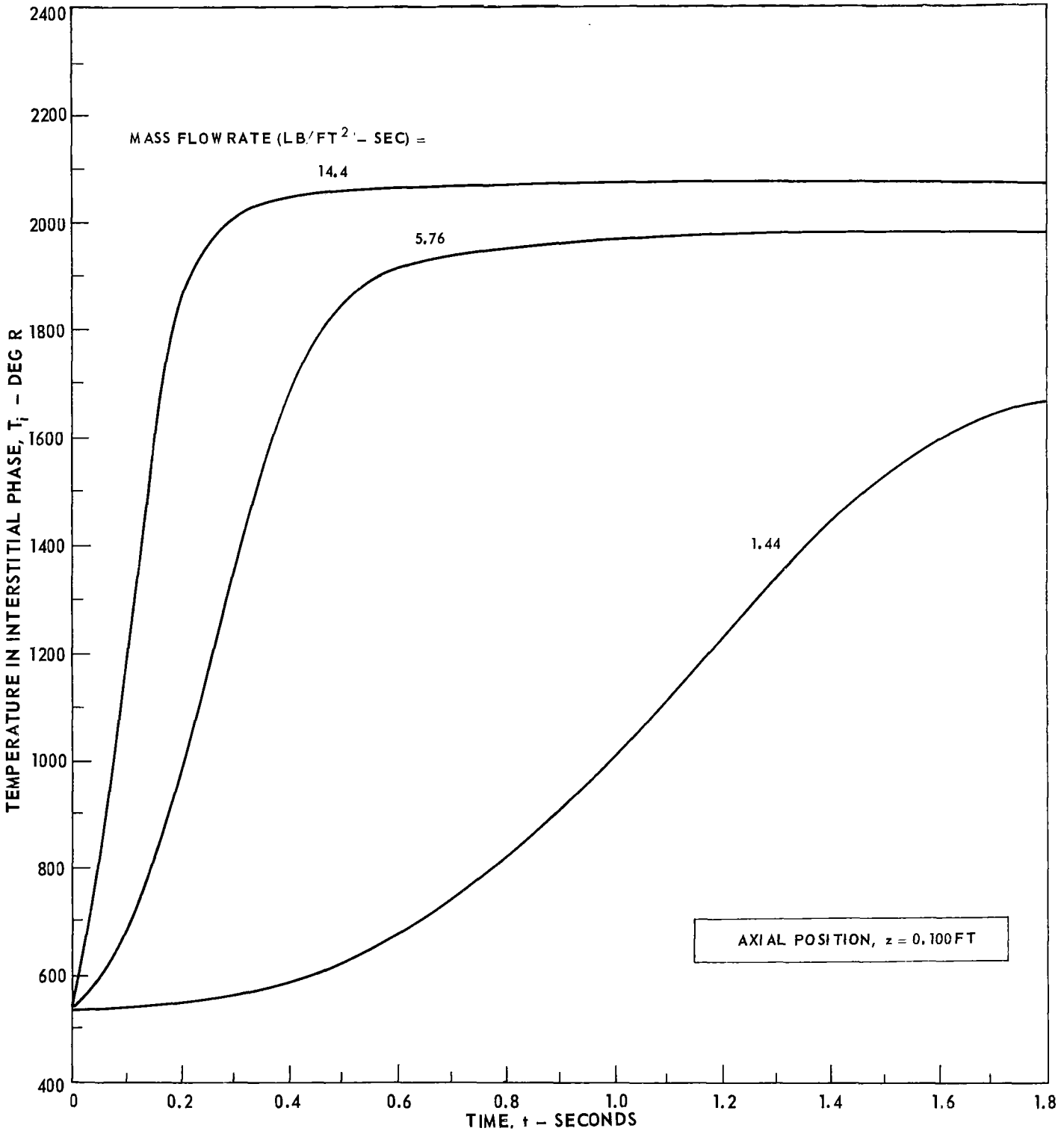

FIG. 28

TRANSIENT INTERSTITIAL TEMPERATURE PROFILE FOR A BURIED INJECTOR CONFIGURATION

INJECTOR PRESSURE = 150 PSIA

CATALYST BED CONFIGURATION: MIXED BED # 2 (SEE TEXT)

SEE TEXT FOR ADDITIONAL REACTOR PARAMETERS

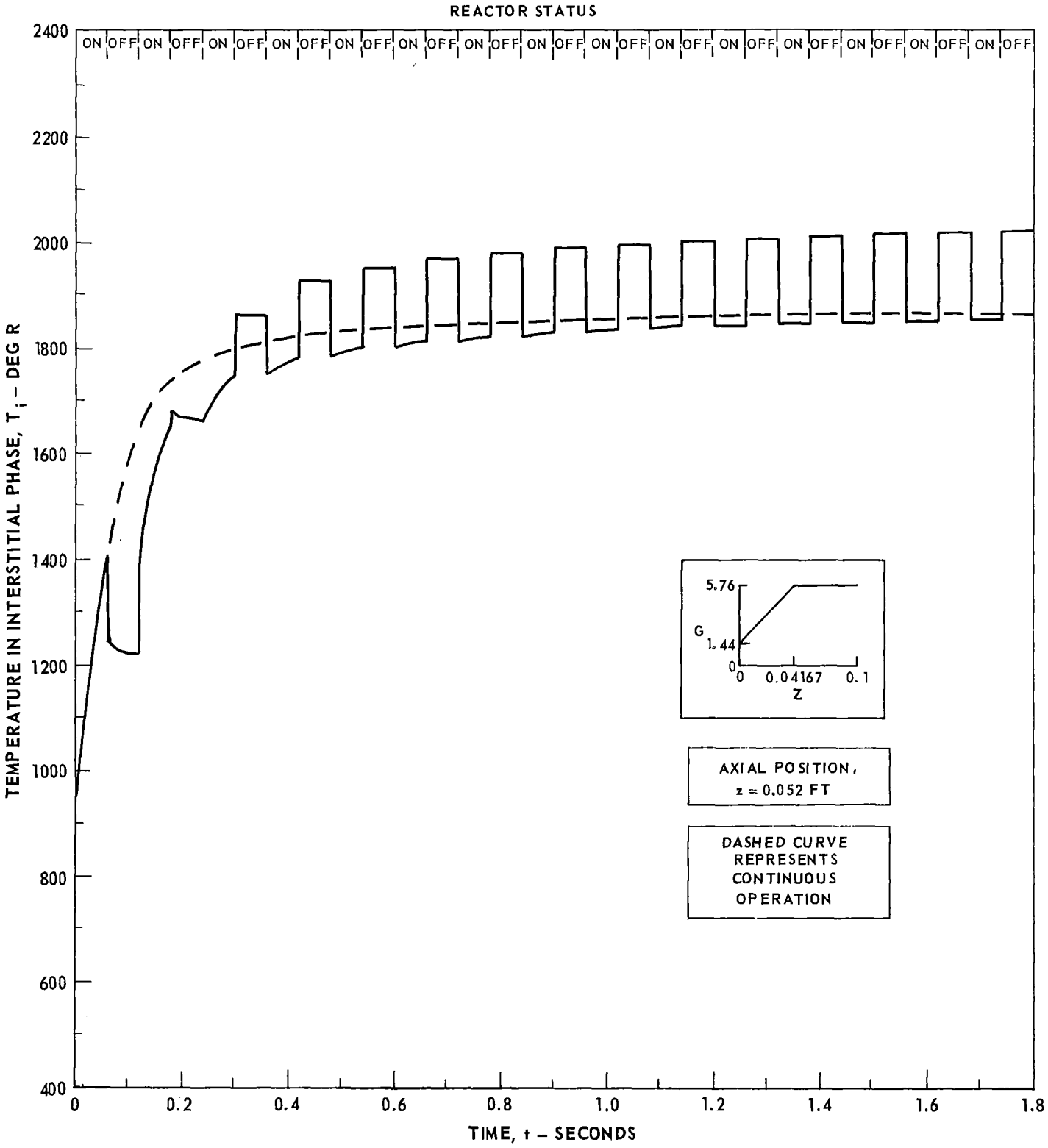

FIG. 29

TRANSIENT INTERSTITIAL TEMPERATURE PROFILE FOR A BURIED INJECTOR CONFIGURATION

INJECTOR PRESSURE = 150 PSIA
CATALYST BED CONFIGURATION: MIXED BED # 2 (SEE TEXT)
SEE TEXT FOR ADDITIONAL REACTOR PARAMETERS

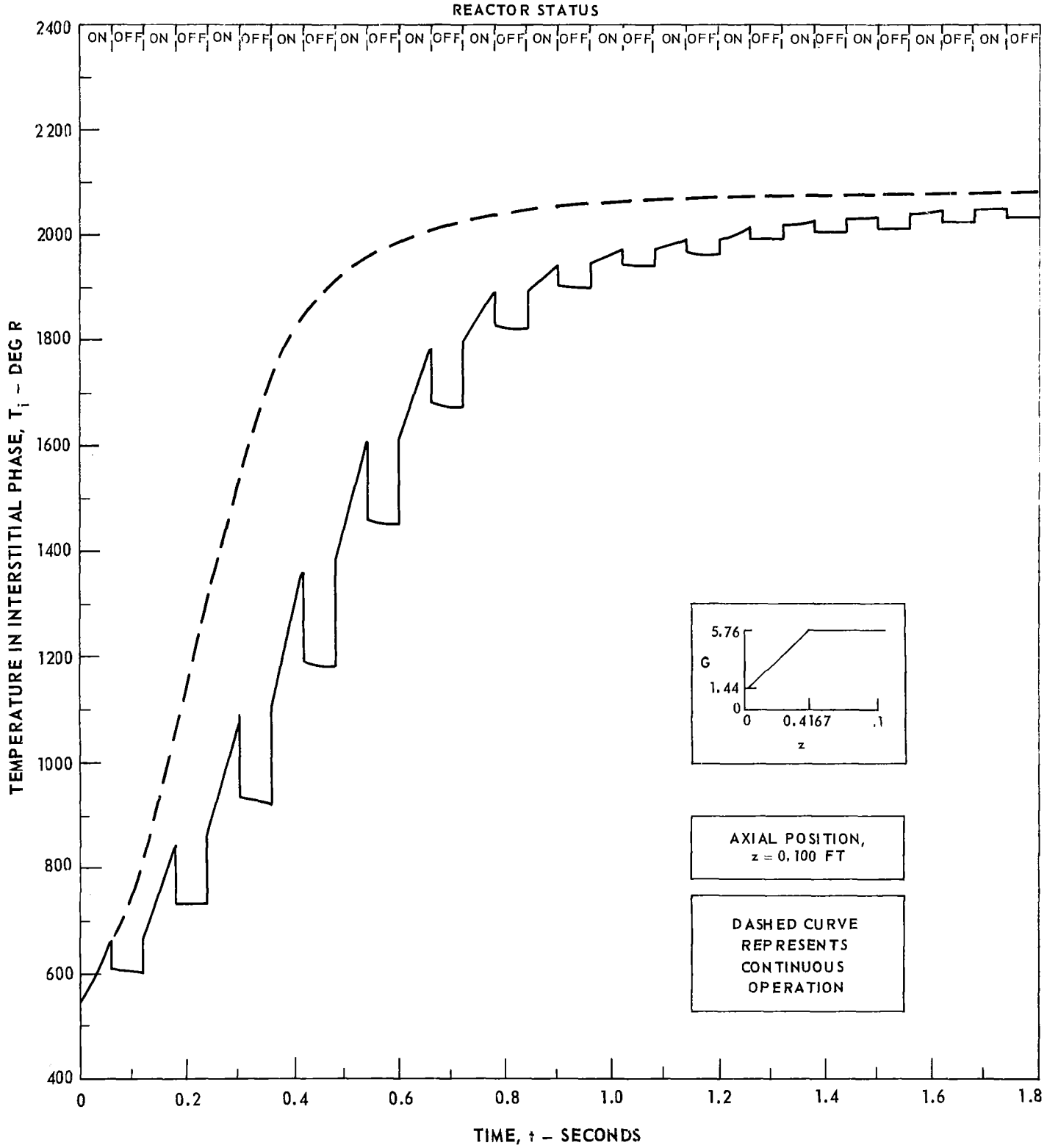

COMPARISON OF TRANSIENT INTERSTITIAL TEMPERATURE PROFILES FOR TWO INJECTION CONFIGURATIONS IN A CONTINUOUS FLOW SYSTEM

INJECTOR PRESSURE = 150 PSIA

CATALYST BED CONFIGURATION: MIXED BED # 2 (SEE TEXT)

SEE TEXT FOR ADDITIONAL REACTOR PARAMETERS

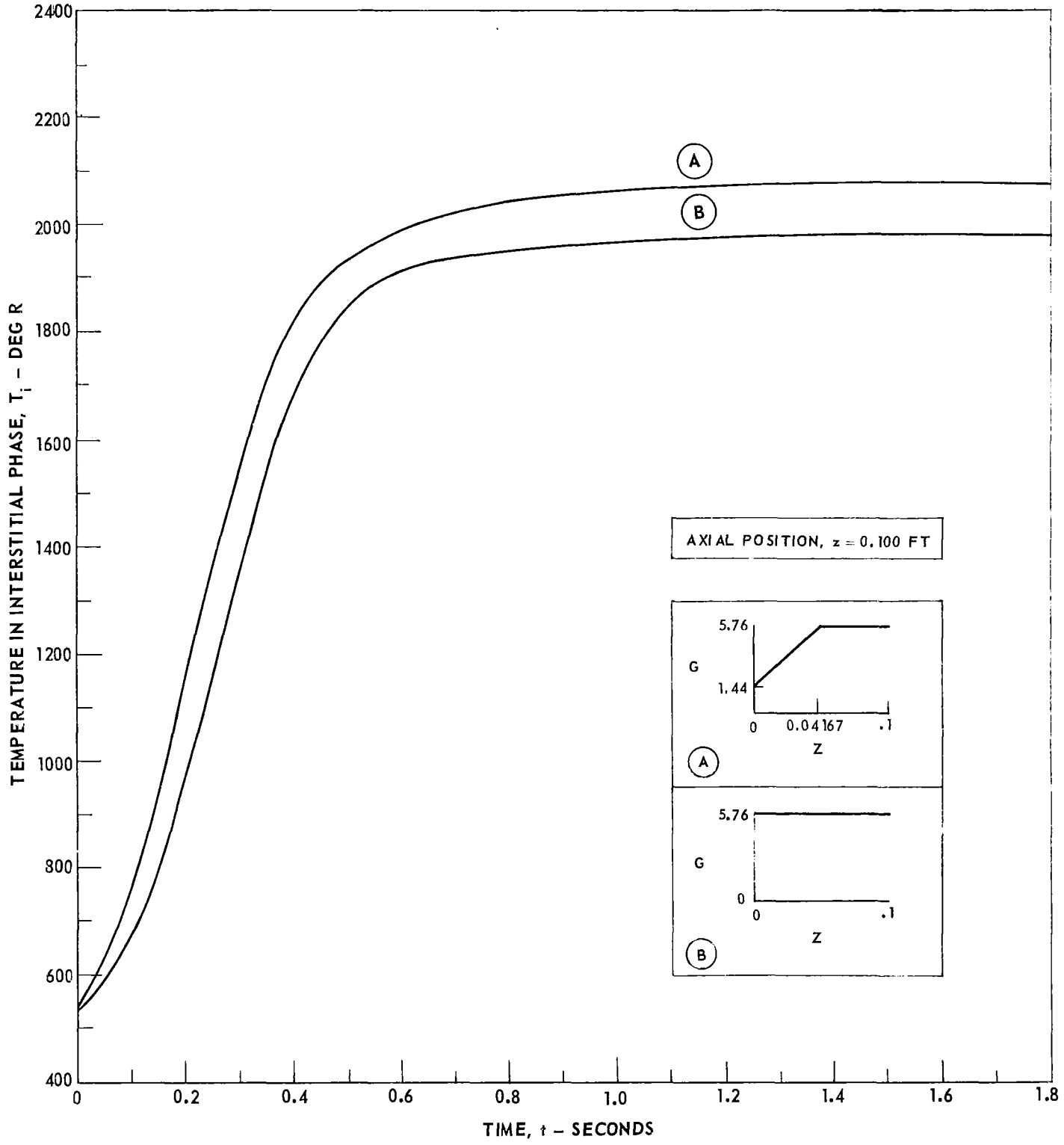

TRANSIENT INTERSTITIAL TEMPERATURE PROFILES FOR A CATALYST BED PACKED WITH ALL 25-30 MESH PARTICLES

INJECTOR PRESSURE = 150 PSIA
STEADY-STATE MASS FLOW RATE = 5.76 LB/FT^2 - SEC
SEE TEXT FOR ADDITIONAL REACTOR PARAMETERS

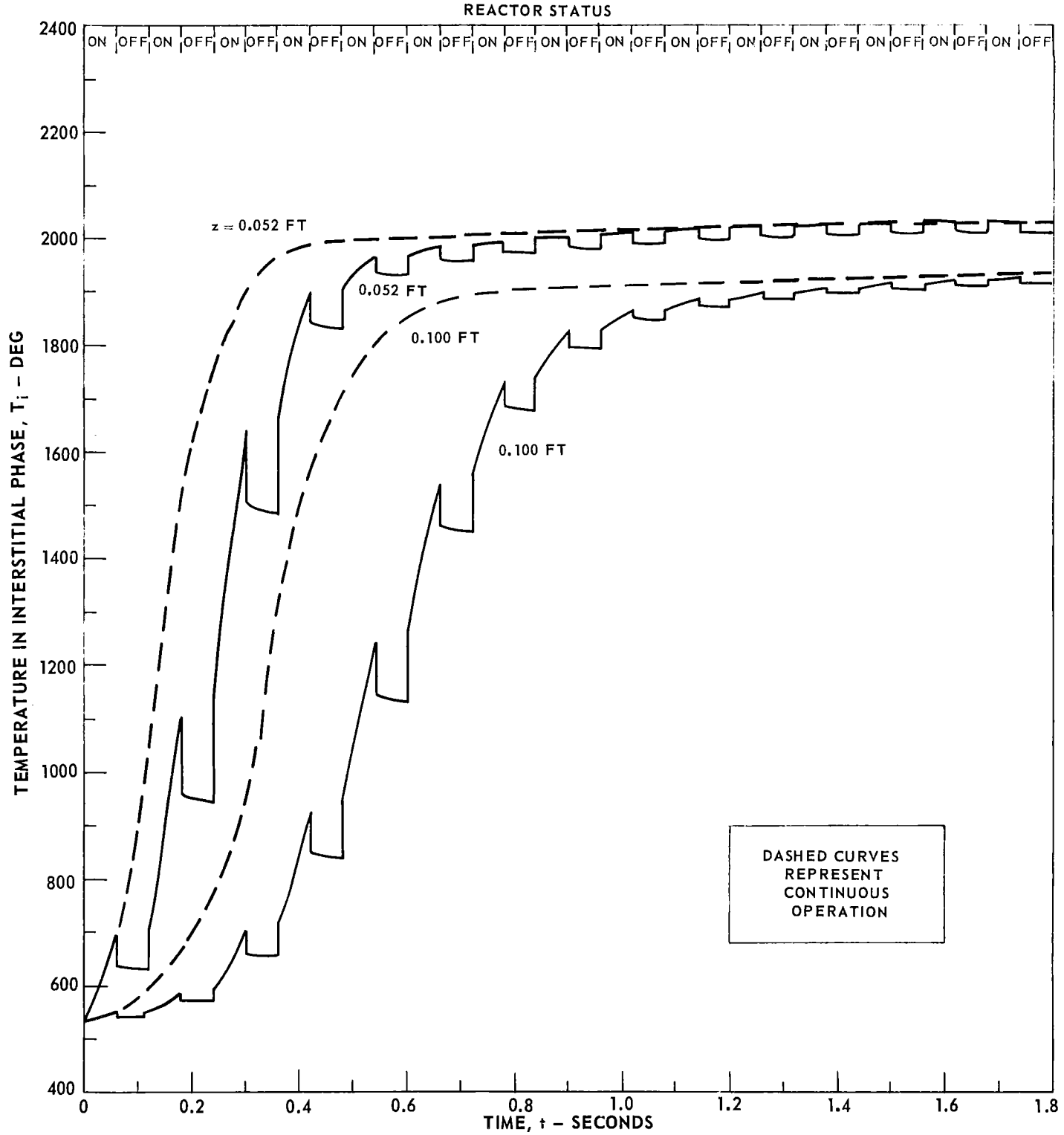

FIG. 32

TRANSIENT INTERSTITIAL TEMPERATURE PROFILES FOR A CATALYST BED PACKED WITH ALL 14-18 MESH PARTICLES

INJECTOR PRESSURE = 150 PSIA

STEADY-STATE MASS FLOW RATE = 5.76 LB/FT^2 - SEC

SEE TEXT FOR ADDITIONAL REACTOR PARAMETERS

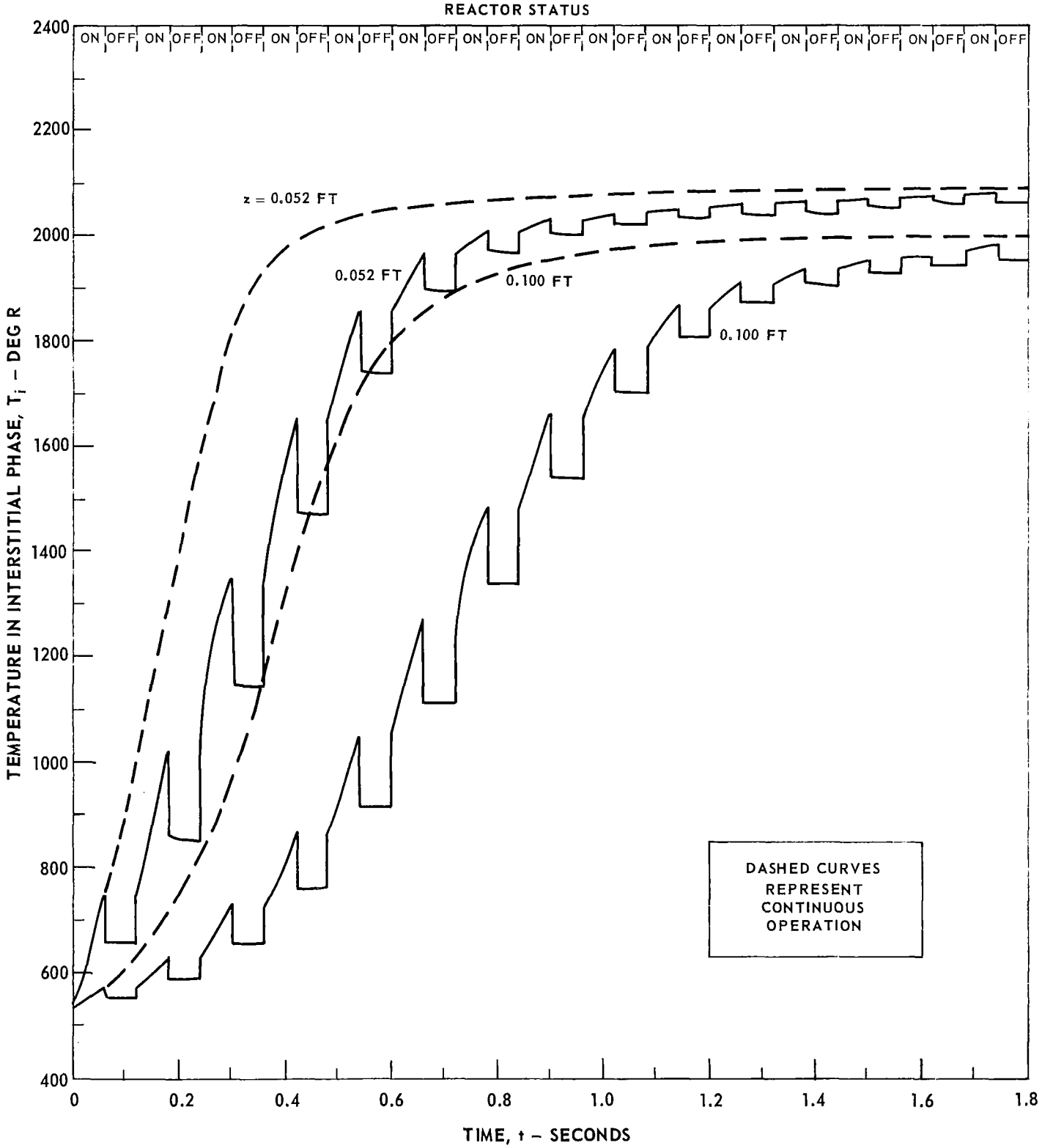

FIG. 33

TRANSIENT INTERSTITIAL TEMPERATURE PROFILE FOR THE "MIXED BED #1" CATALYST BED CONFIGURATION

INJECTOR PRESSURE = 150 PSIA

STEADY-STATE MASS FLOW RATE = 5.76 LB/FT^2 - SEC

SEE TEXT FOR ADDITIONAL REACTOR PARAMETERS

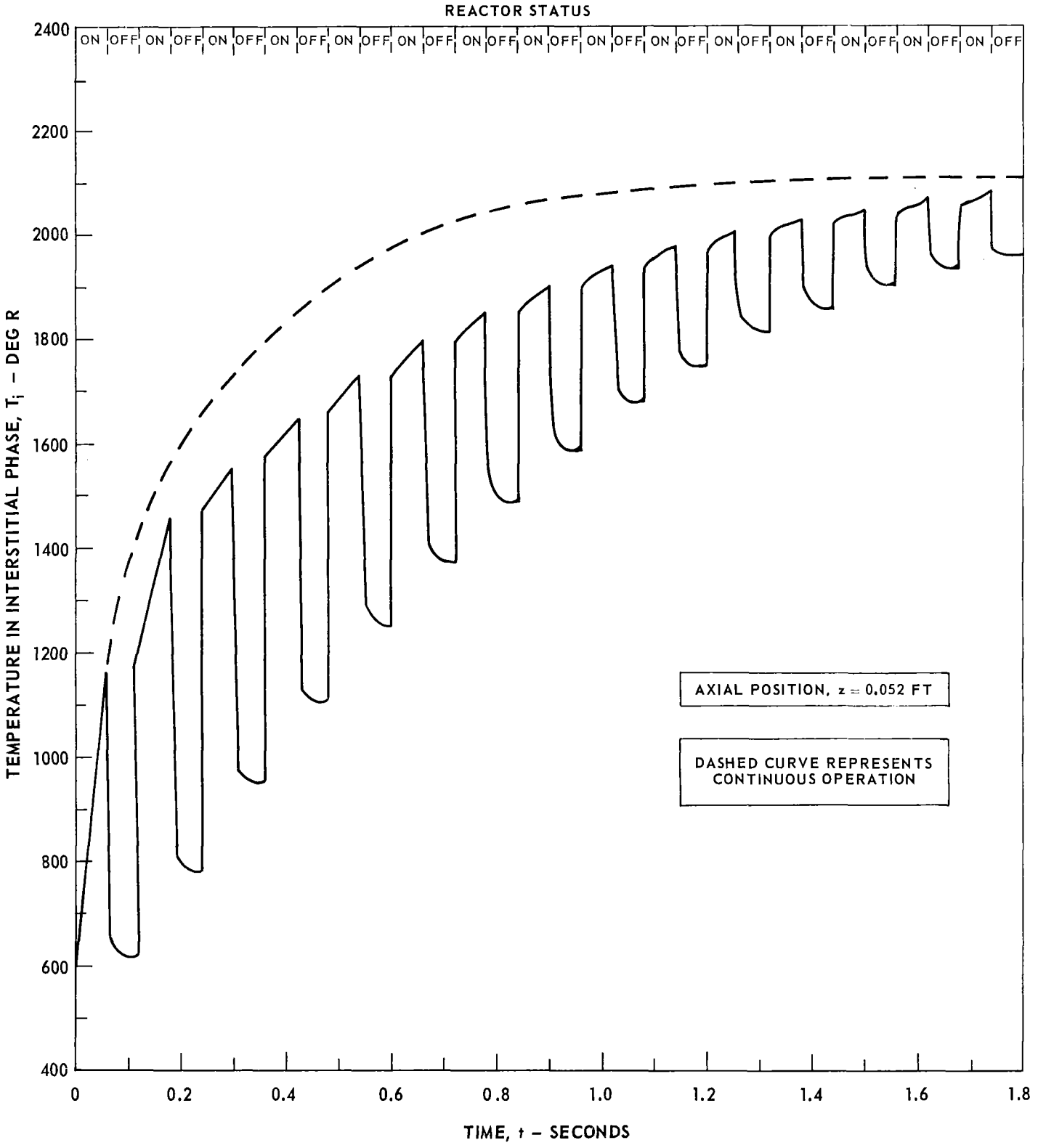

FIG. 34

TRANSIENT INTERSTITIAL TEMPERATURE PROFILE FOR THE "MIXED BED #1" CATALYST BED CONFIGURATION

INJECTOR PRESSURE = 150 PSIA

STEADY-STATE MASS FLOW RATE = 5.76 LB/FT^2 - SEC

SEE TEXT FOR ADDITIONAL REACTOR PARAMETERS

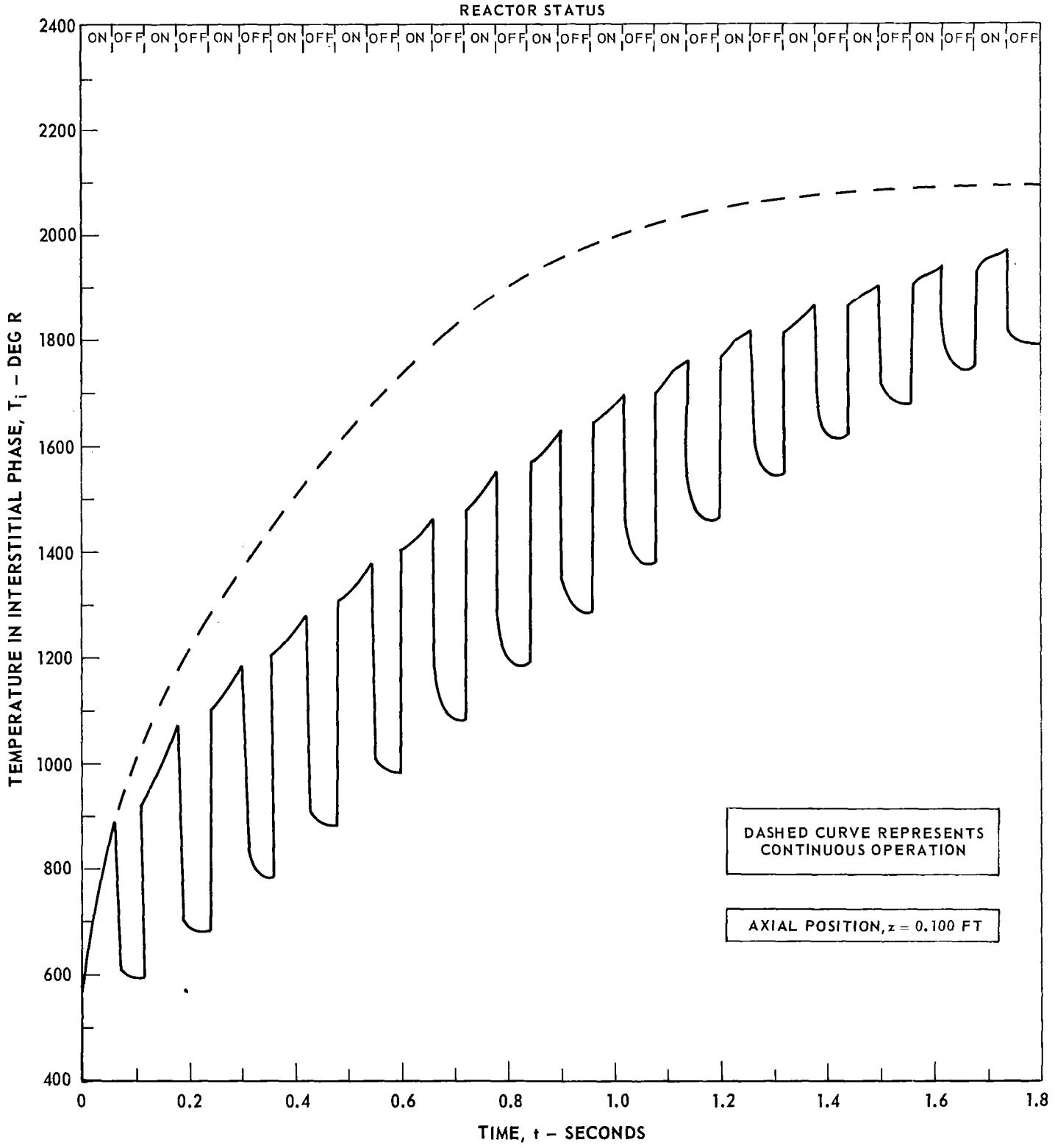

FIG. 35

COMPARISON OF TRANSIENT INTERSTITIAL TEMPERATURE PROFILES FOR VARIOUS BED CONFIGURATIONS IN A CONTINUOUS FLOW SYSTEM

INJECTOR PRESSURE = 150 PSIA

STEADY-STATE MASS FLOW RATE = 5.76 LB/FT^2 - SEC

SEE TEXT FOR ADDITIONAL REACTOR PARAMETERS

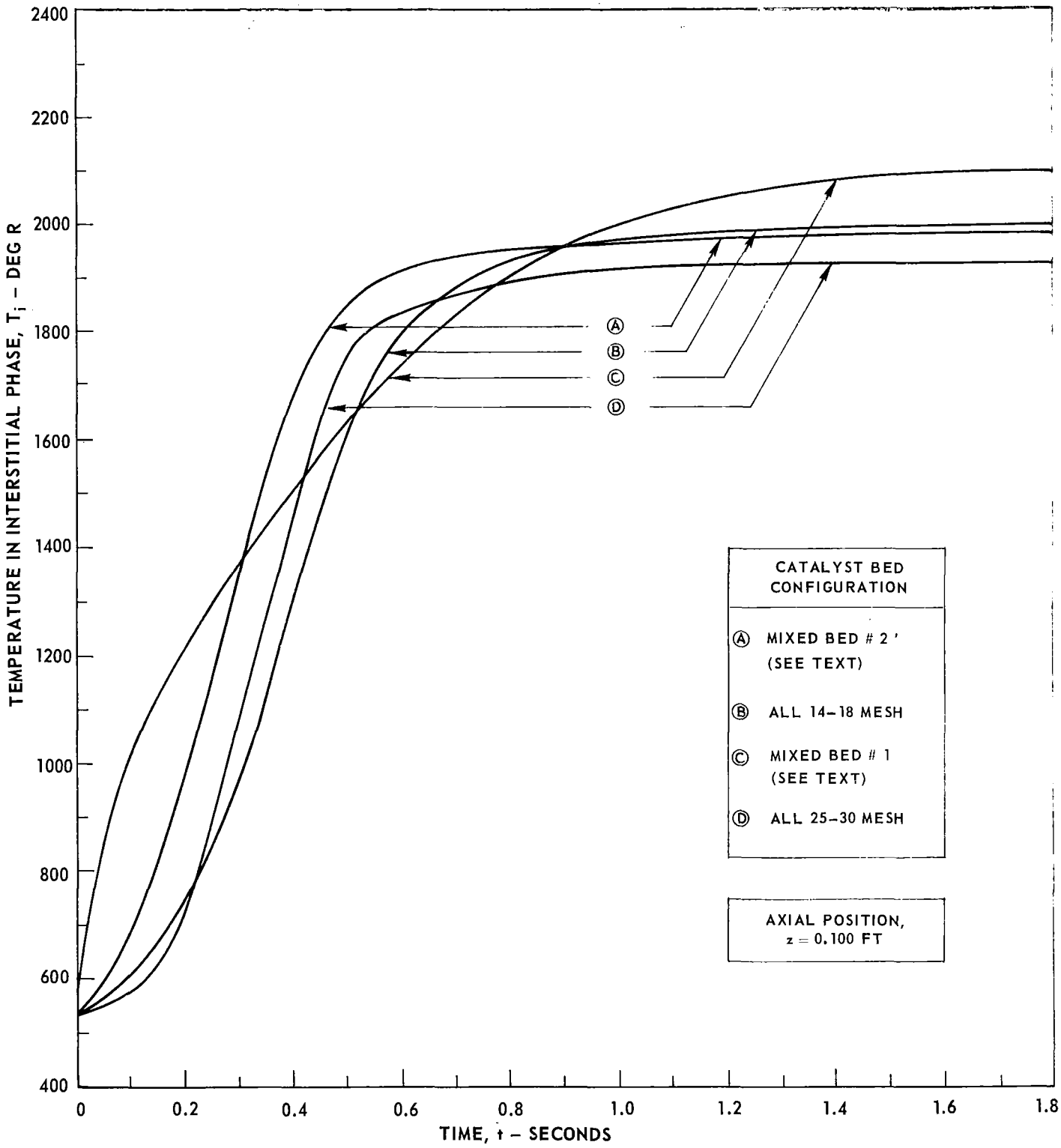

TRANSIENT INTERSTITIAL TEMPERATURE PROFILES FOR 60 msec/120 msec PULSE DUTY CYCLE

INJECTOR PRESSURE = 150 PSIA
STEADY-STATE MASS FLOW RATE = 5.76 LB/FT^2 - SEC
CATALYST BED CONFIGURATION: MIXED BED # 2 (SEE TEXT)
SEE TEXT FOR ADDITIONAL REACTOR PARAMETERS

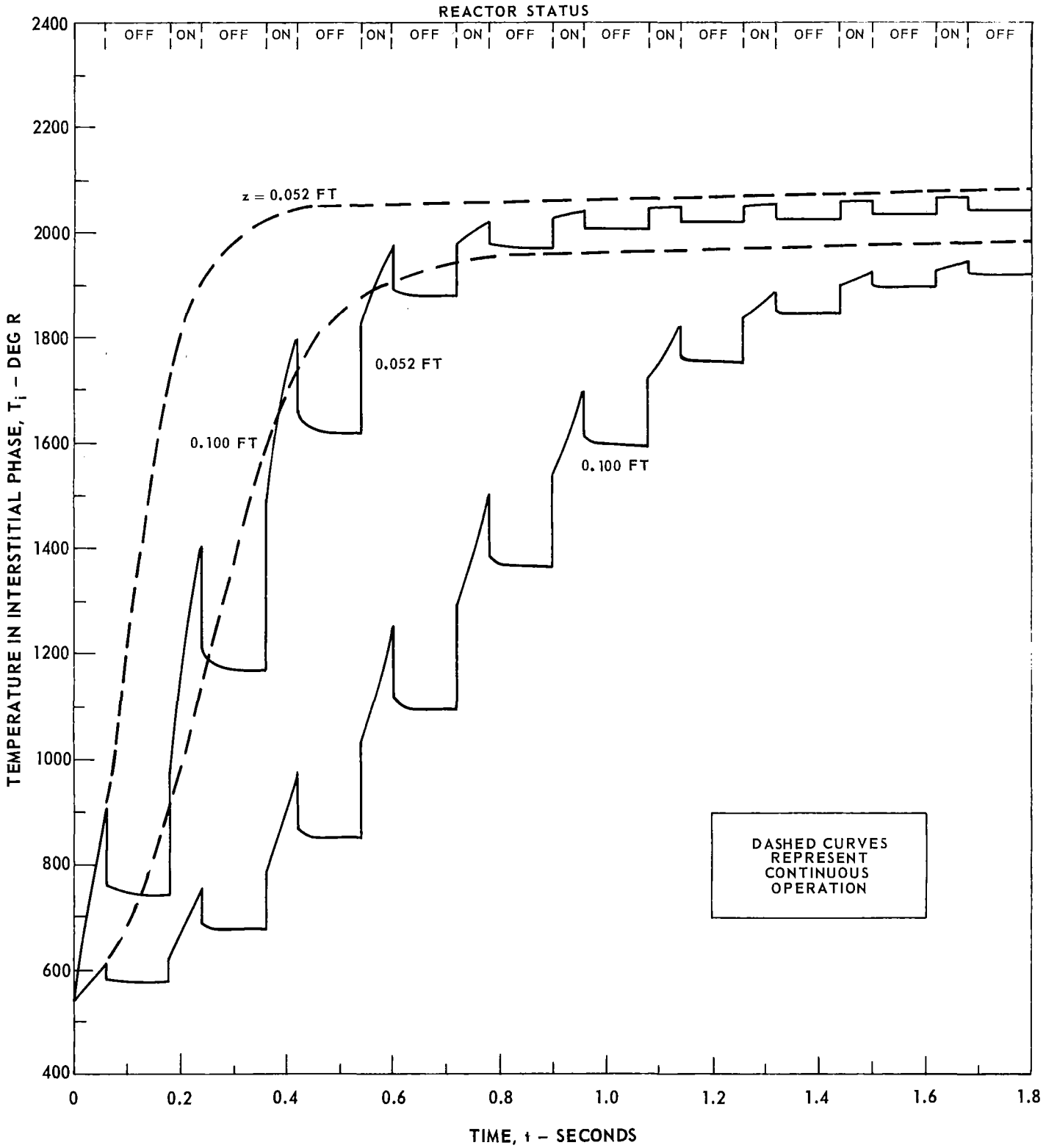

TRANSIENT INTERSTITIAL TEMPERATURE PROFILES FOR 60 msec/ 240 msec PULSE DUTY CYCLE

INJECTOR PRESSURE = 150 PSIA
STEADY-STATE MASS FLOW RATE = 5.76 LB/FT^2 - SEC
CATALYST BED CONFIGURATION: MIXED BED # 2 (SEE TEXT)
SEE TEXT FOR ADDITIONAL REACTOR PARAMETERS

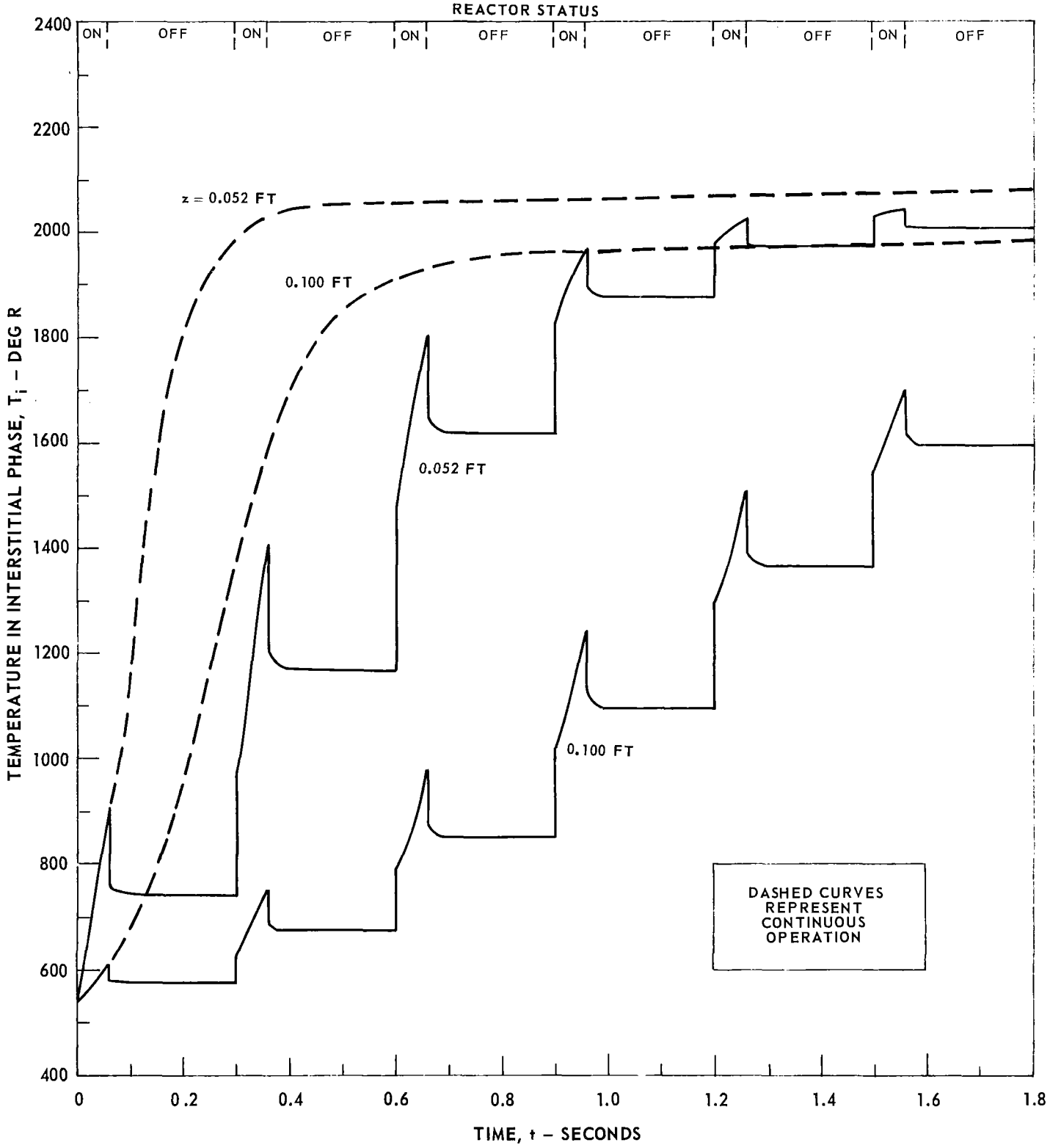

COMPARISON OF TRANSIENT INTERSTITIAL TEMPERATURE PROFILES FOR VARIOUS PULSE DUTY CYCLES

INJECTOR PRESSURE = 150 PSIA
STEADY-STATE MASS FLOW RATE = 5.76 LB/FT^2 - SEC
CATALYST BED CONFIGURATION: MIXED BED # 2 (SEE TEXT)
SEE TEXT FOR ADDITIONAL REACTOR PARAMETERS

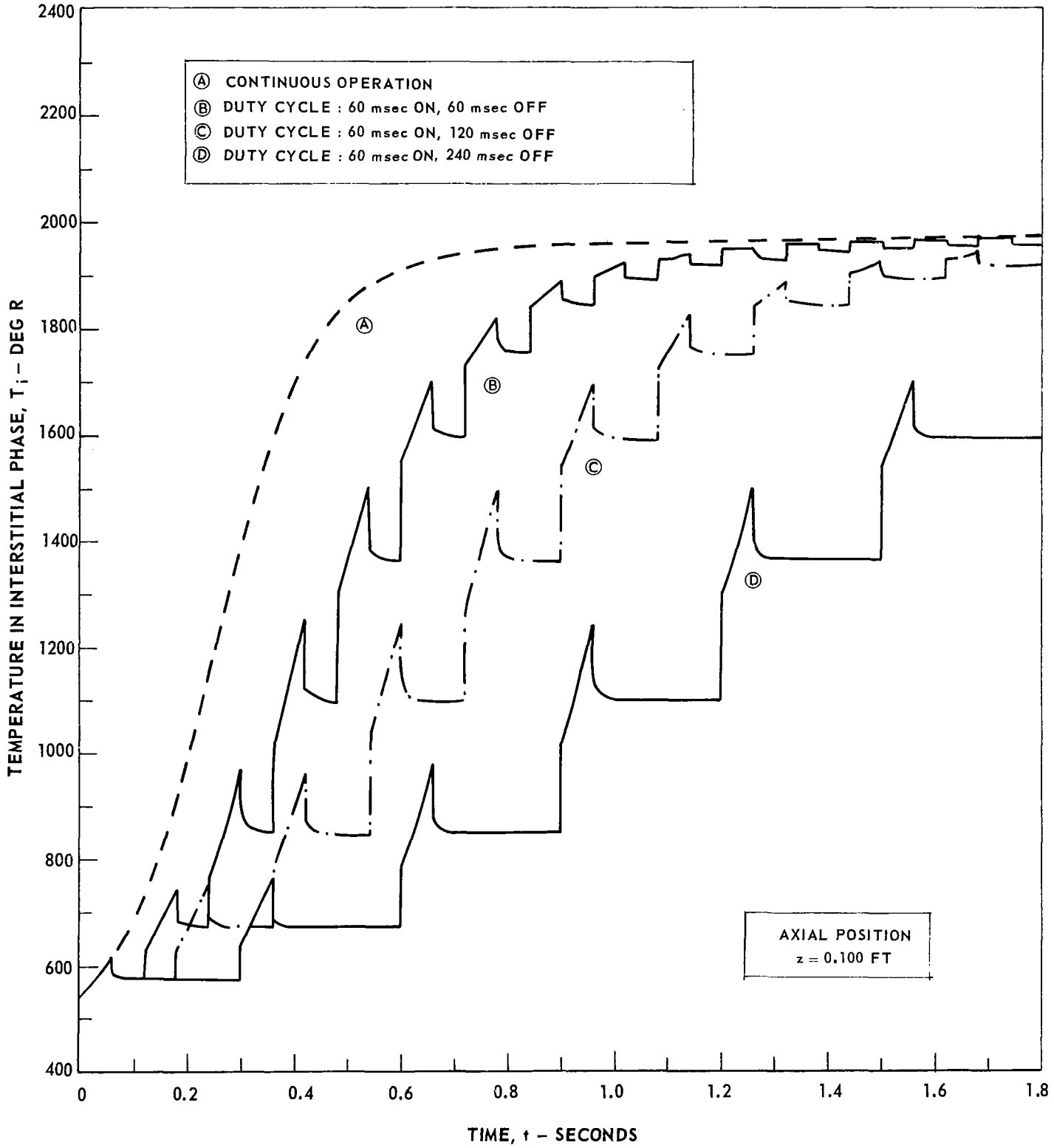

H910461-38

FIG. 39

TRANSIENT INTERSTITIAL TEMPERATURE PROFILE FOR A HIGH THRUST ENGINE

INJECTOR PRESSURE = 1405 PSIA
STEADY-STATE MASS FLOW RATE = 40.3 LB/FT^2 - SEC
CATALYST BED CONFIGURATION: ALL 25-30 MESH PARTICLES
SEE TEXT FOR ADDITIONAL REACTOR PARAMETERS

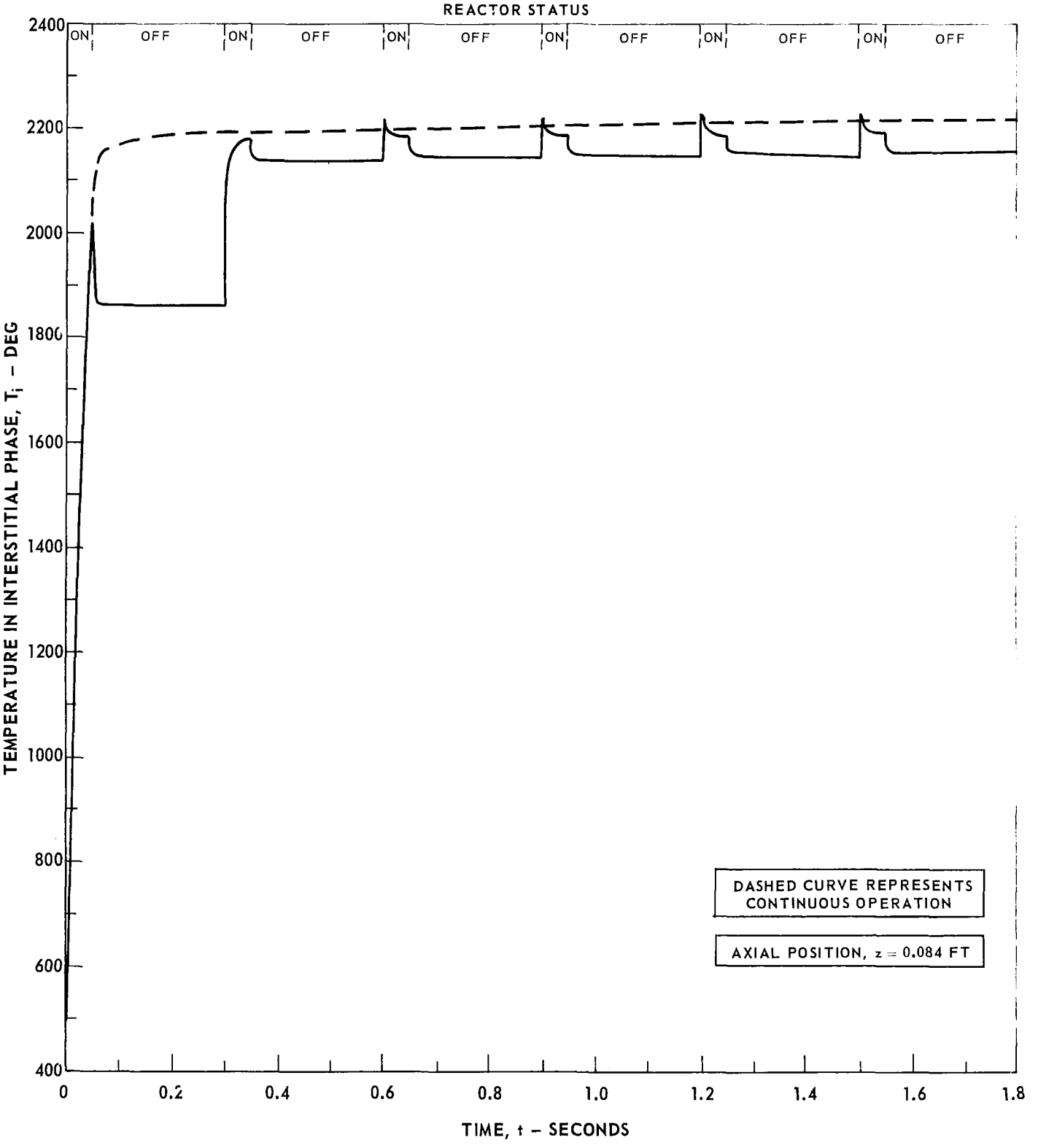

TRANSIENT PARTICLE TEMPERATURE PROFILE FOR A HIGH THRUST ENGINE

INJECTOR PRESSURE = 1405 PSIA
STEADY-STATE MASS FLOW RATE = 40.3 LB/FT^2 - SEC
CATALYST BED CONFIGURATION: ALL 25-30 MESH PARTICLES
SEE TEXT FOR ADDITIONAL REACTOR PARAMETERS

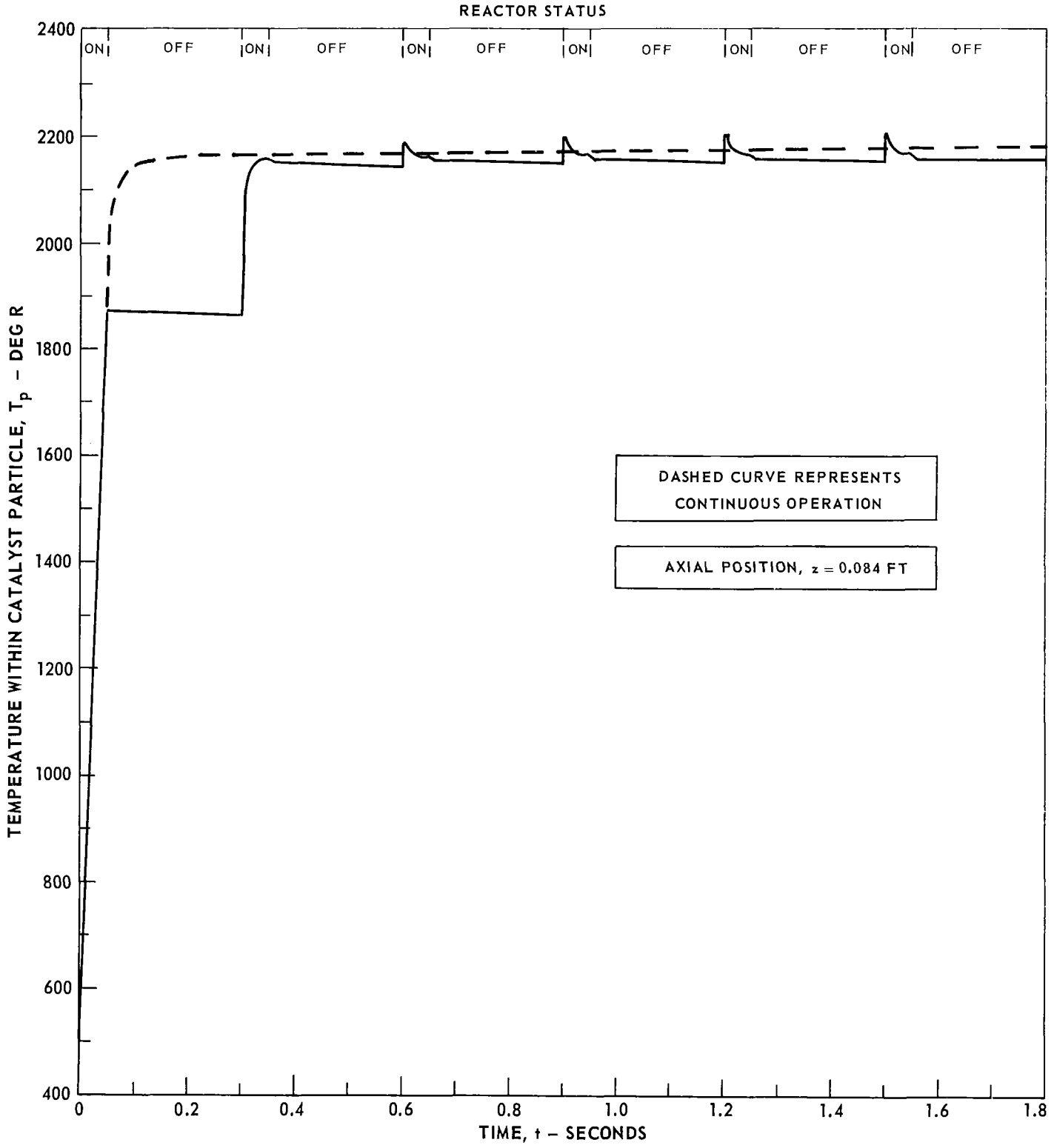

FIG. 41

TRANSIENT CHAMBER PRESSURE PROFILE FOR A HIGH THRUST ENGINE

INJECTOR PRESSURE = 1405 PSIA

STEADY-STATE MASS FLOW RATE = 40.3 LB/FT^2 - SEC

CATALYST BED CONFIGURATION: ALL 25-30 MESH PARTICLES

SEE TEXT FOR ADDITIONAL REACTOR PARAMETERS

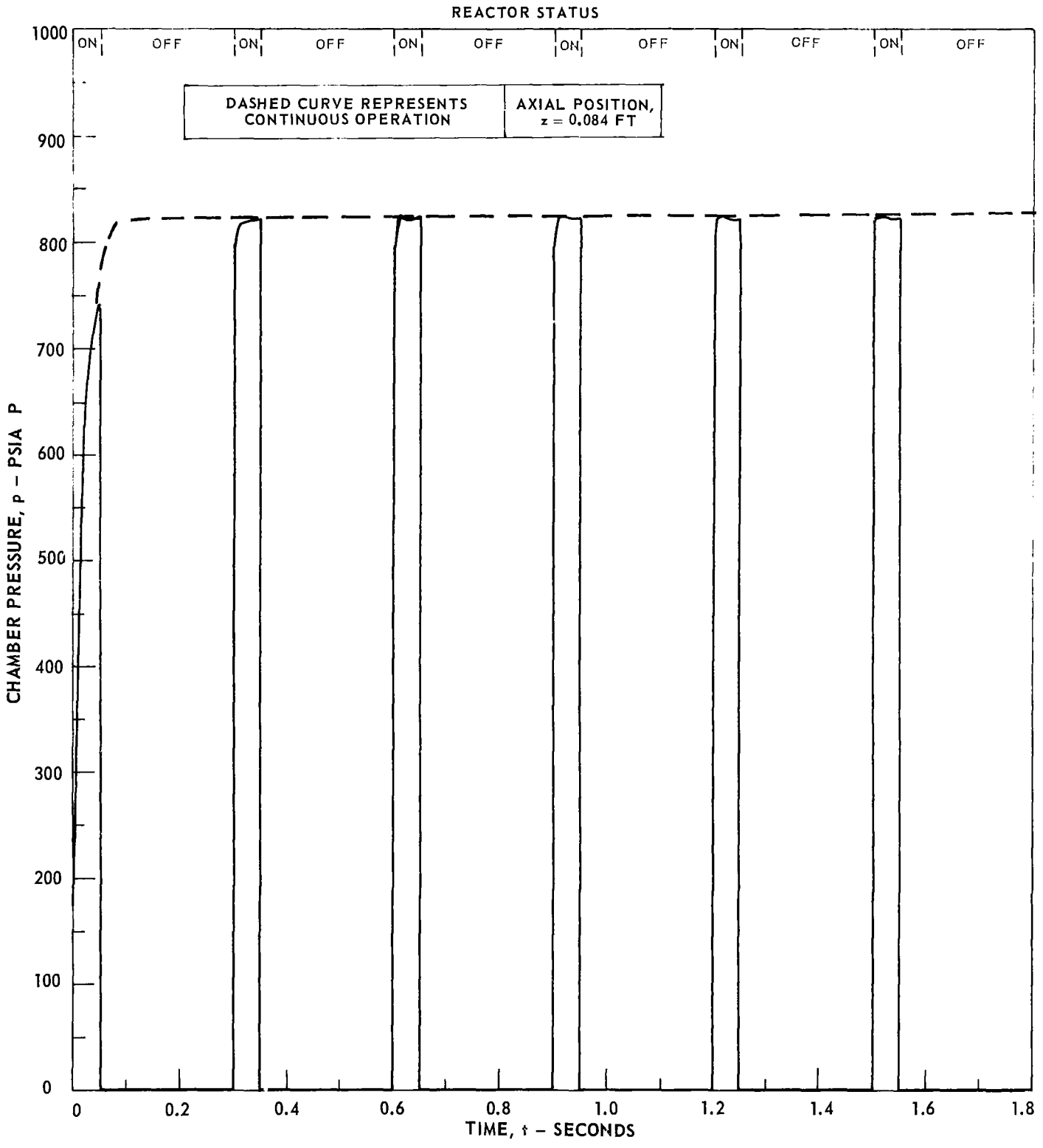

TRANSIENT PROFILE OF MOLE-FRACTION OF HYDRAZINE FOR A HIGH THRUST ENGINE

INJECTOR PRESSURE = 1405 PSIA

STEADY-STATE MASS FLOW RATE = 40.3 LB/FT^2 - SEC

CATALYST BED CONFIGURATION: ALL 25-30 MESH PARTICLES

SEE TEXT FOR ADDITIONAL REACTOR PARAMETERS

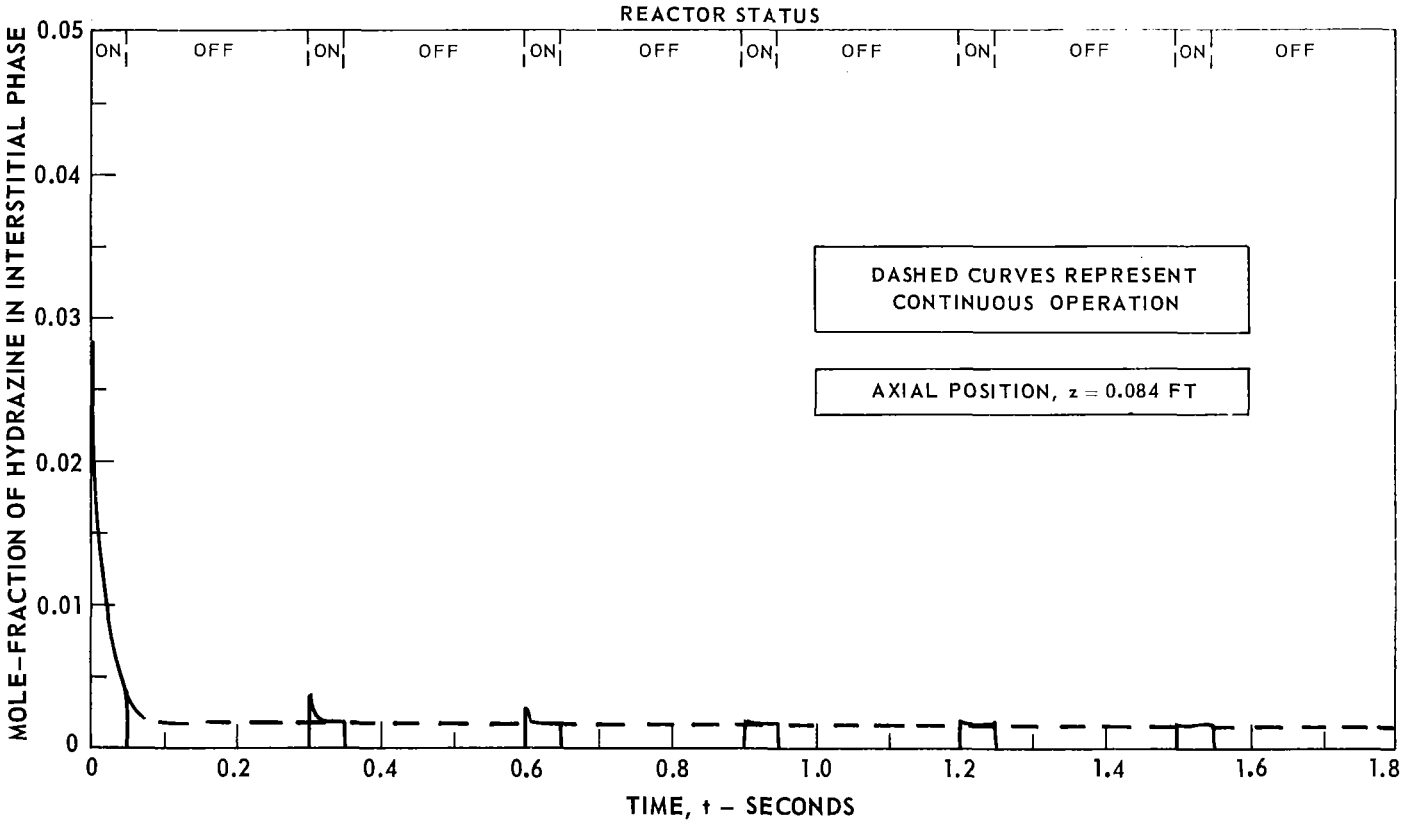

TRANSIENT PROFILE OF MOLE-FRACTION OF AMMONIA FOR A HIGH THRUST ENGINE

INJECTOR PRESSURE = 1405 PSIA
STEADY-STATE MASS FLOWRATE = 40.3 LB/FT^2 - SEC
CATALYST BED CONFIGURATION: ALL 25-30 MESH PARTICLES
SEE TEXT FOR ADDITIONAL REACTOR PARAMETERS

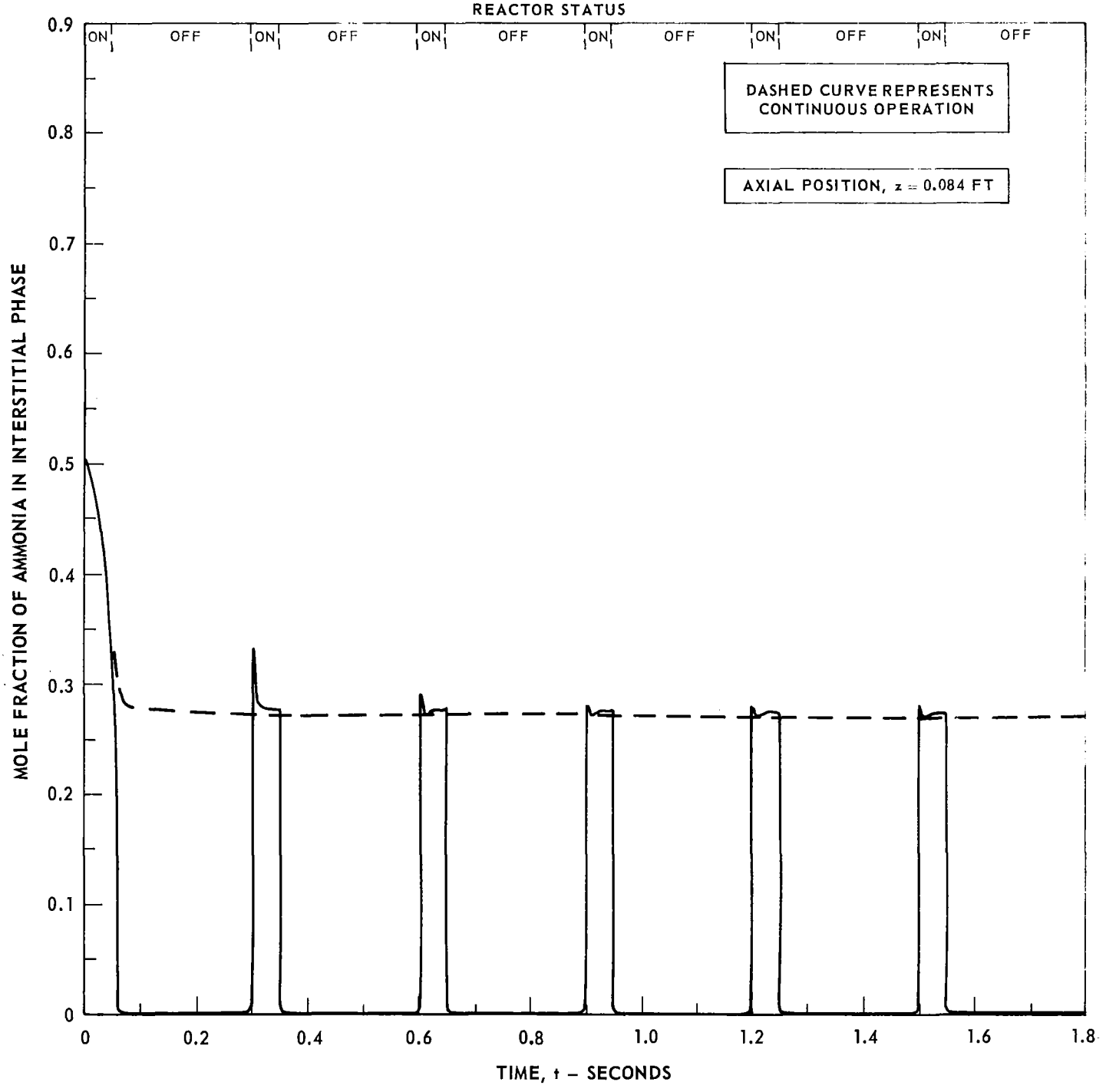

TRANSIENT PROFILE OF MOLE-FRACTION OF NITROGEN FOR A HIGH THRUST ENGINE

INJECTOR PRESSURE = 1405 PSIA

STEADY-STATE MASS FLOW = 40.3 LB/FT^2 - SEC

CATALYST BED CONFIGURATION : ALL 25-30 MESH PARTICLES

SEE TEXT FOR ADDITIONAL REACTOR PARAMETERS

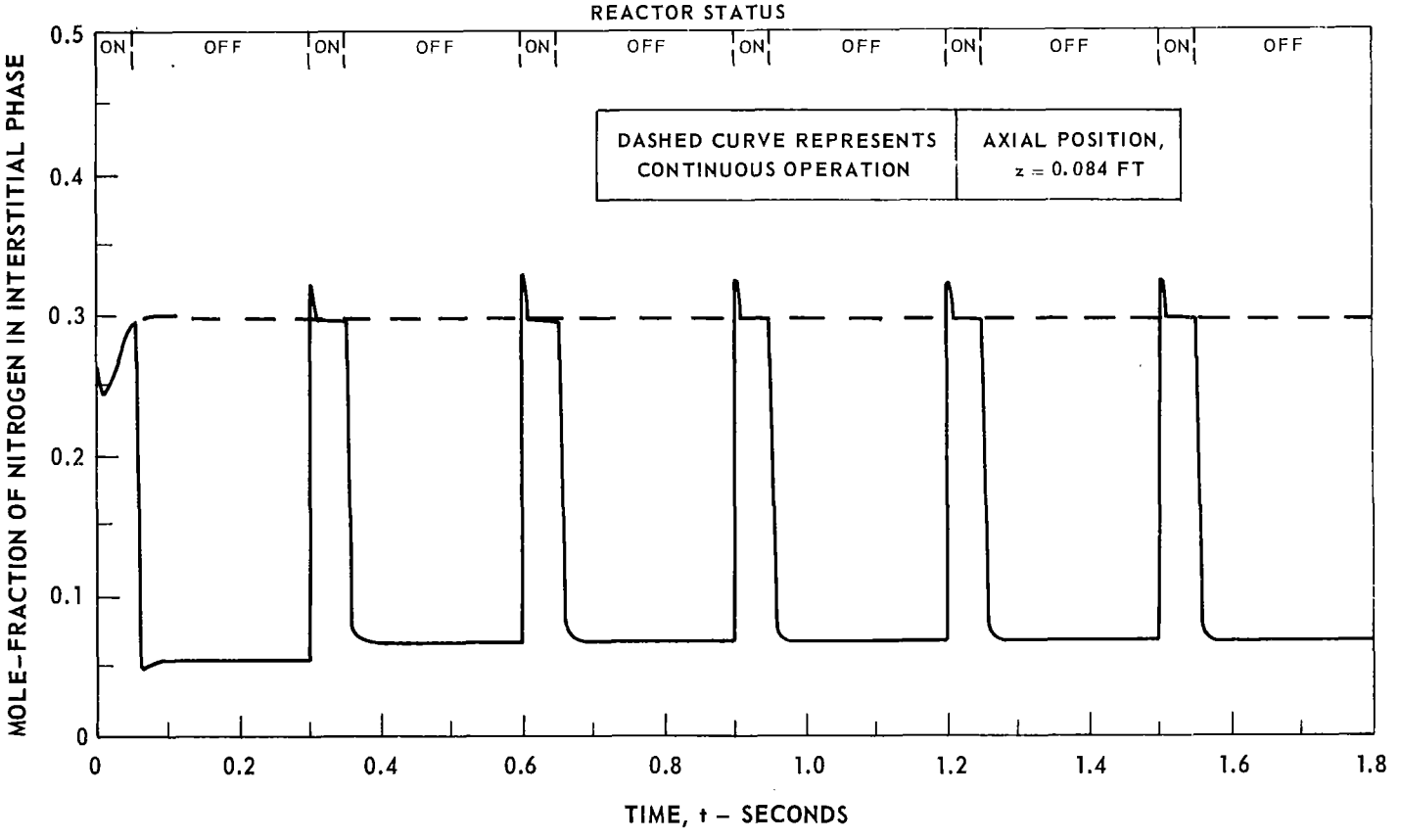

TRANSIENT PROFILE OF MOLE-FRACTION OF HYDROGEN FOR A HIGH THRUST ENGINE

INJECTOR PRESSURE = 1405 PSIA

STEADY-STATE MASS FLOW RATE = 40.3 LB/FT ^{2} – SEC

CATALYST BED CONFIGURATION: ALL 25–30 MESH PARTICLES

SEE TEXT FOR ADDITIONAL REACTOR PARAMETERS